5-2014

Augmenting Functional Adaptation: Does Obesity have a Systemic Effect on Bone Strength Properties in Humans?

Nicole Marie Reeves

University of Tennessee - Knoxville, nreeves@utk.edu

To the Graduate Council:

I am submitting herewith a dissertation written by Nicole Marie Reeves entitled "Augmenting Functional Adaptation: Does Obesity have a Systemic Effect on Bone Strength Properties in Humans?." I have examined the final electronic copy of this dissertation for form and content and recommend that it be accepted in partial fulfillment of the requirements for the degree of Doctor of Philosophy, with a major in Anthropology.

<div align="right">

Benjamin M. Auerbach, Major Professor
</div>

We have read this dissertation and recommend its acceptance:

Richard L. Jantz, Andrew Kramer, David R. Bassett

<div align="right">

Accepted for the Council:

Dixie L. Thompson

Vice Provost and Dean of the Graduate School
</div>

(Original signatures are on file with official student records.)

Augmenting Functional Adaptation: Does Obesity have a Systemic Effect on Bone

Strength Properties in Humans?

A Dissertation Presented for the

Doctor of Philosophy

Degree

The University of Tennessee, Knoxville

Nicole Marie Reeves

May 2014

ACKNOWLEDGEMENTS

This dissertation would not have been possible without the contributions and support of many people along the way. I would like to take the opportunity to recognize the following mentors, colleagues, friends, and family for their efforts on my behalf.

First, I would like to thank my committee members for their roles in shaping my graduate career, and ultimately this work. Many thanks to my advisor and committee chair, Dr. Ben Auerbach, who supported my vision for this project from its inception and always had excellent ideas for its improvement. His anatomy and biomechanics teachings also greatly influenced my research. I would also like to thank Dr. Andrew Kramer for his insightful comments and advice, which enhanced this research, as well as his unwavering support over the years. I will strive for a teaching style as effective as his. I extend my sincere gratitude to Dr. Richard Jantz for his encouragement of me and my project along the way. His statistical advice and courses on secular change and human variation have also significantly (pun intended) impacted my dissertation research. In addition, I sincerely thank Dr. David Bassett for applying his expertise to the review of my work. Furthermore, his enthusiasm and positivity will not be forgotten. The influence of each of my committee members on the development of my dissertation is clear, and I am exceedingly appreciative of their guidance.

There are many researchers and colleagues who were not on my committee that also had integral roles in making this project possible. I especially would like to thank Dr. Natalie Shirley for providing me with access to CT scans, teaching me various imaging software, and funding me with a research assistantship. None of this would have been feasible without her mentorship

ABSTRACT

This study considers the mechanical and neuroendocrine-metabolic effects of obesity on cortical bone and joint morphology throughout the human skeleton. Obesity has primarily been associated with changes in lower limb bone morphology, attributed to local mechanical responses; however, it is known that systemic metabolic shifts concomitant with obesity also influence bone turnover and cell signaling. Thus, the interaction of these mechanical and metabolic effects should be considered, rather than either factor in isolation.

The presented research addresses this interaction by examining skeletal data obtained the William M. Bass Donated Collection (University of Tennessee), a modern collection with documentation representing obese and non-obese individuals. Much of the collection has also undergone x-ray computer tomographic (CT) scanning, providing the means to assess bone morphologies beyond the external surface. The scans of 114 individuals are used here to test the hypothesis that obese individuals have increased cortical bone strength properties throughout the skeleton due to both mechanical and systemic effects, while the linear joint dimensions remain unaffected.

A total of 22 cross-sections from six skeletal elements (cranial vault, humerus, radius, femur, tibia, fibula), representing three mechanically disparate regions (cranial vault, upper limb, lower limb), and linear dimensions from three articulations (shoulder, hip, and knee) are examined for each individual. Results indicate that obese individuals exhibit larger cross-sectional geometric properties for the humerus, femur, tibia, and fibula relative to normal mass individuals, and the load bearing bones display the greatest magnitudes of difference. Furthermore, whole-diaphyses data indicate that variability in bone robusticity decreases along a

proximal-to-distal gradient. Equivocal cranial vault results require further investigation, although the present study suggests that there are minute, if any, macroscopic differences in cranial vault properties between obese and normal mass individuals. Articular dimensions are found to be constrained relative to the diaphyseal cross-sectional measures.

Both biomechanical and systemic stimuli are known to affect bone and adipose tissues in known capacities but are rarely examined together. The study presented here applies conclusions from the experimental literature to a human skeletal sample with known demographics, finding that both biomechanical and neuroendocrine-metabolic factors influence macroscopic bone morphology throughout the skeleton.

TABLE OF CONTENTS

LIST OF TABLES

LIST OF FIGURES

xii

CHAPTER 1

INTRODUCTION

This dissertation examines the potential interaction between metabolic and hormonal changes associated with obesity and the distribution of cortical bone throughout the human skeleton, typically modeled as being the product of mechanical loading. While it has been long established that bone responds to dynamic mechanical loads by changing the distribution and type of bone tissue present (e.g., see discussions in Pearson and Lieberman 2004; Ruff et al. 2006), it has only been in recent years that researchers have documented endocrinal changes associated with excess adipose tissue as influencing the skeleton (Karsenty 2006; 2011; see also Chapter 3). The excess body mass associated with obesity has the potential to affect the skeleton both mechanically (due to increased loading) as well as metabolically. For this reason, assessing the effects of obesity on the skeleton must involve disentangling the effects of these two sets of factors; this study is a first attempt to ascertain their influences by examining the skeleton systemically of obese and non-obese individuals.

Briefly, obesity is clinically characterized as a condition of excessive body fat. It is often associated with non-insulin dependent diabetes, cardiovascular diseases, cancer, and other co-morbidities (Ma et al. 2011). In adults, obesity is clinically classified by body mass index (BMI) the measure of weight adjusted for height, calculated as weight in kilograms divided by height (measured in meters) squared (see Chapter 6 for further discussion). It should be noted that this is not a direct measure of adiposity, though it is the defining characteristic of obesity and its related metabolic changes (see Chapter 4), as well as morbidities. Infrequently, some individuals

present with clinical normal weights (i.e., "healthy" BMIs as defined by the Centers for Disease

Control and Prevention) despite having a high percentage of body mass comprised of fat; these

normal weight obese individuals may present the same suite of morbidities and metabolic

changes associated with high-weight obesity (e.g., Romero-Corral et al. 2008); this is considered

further in Chapters 5 and 6. Obesity itself has multiple etiologies, which include increased

caloric intake, reduced physical activity, decreased sleep, increased stress, and genetic

predispositions, among other factors (Bell et al. 2005; Gangwisch et al. 2005; Weisner et al.

1998). Reduced physical activity continues to be implicated as a major factor in causing the

onset of weight gain that ultimately may lead to obesity.

Human body forms and skeletal responses to activity and diet have evolved for millions

of years to confer mechanical stability in relation to the strains encountered in regular activity

(Currey 2003; Shaw and Stock 2013). However, increased, sustained load bearing caused by the

high body masses associated with obesity were likely rare in hominid evolutionary history

(Wells 2006). As a species, our genes and developmental pathways have adapted for more active

lifestyles, which require the consumption and expenditure of many kilocalories. Transitioning

from highly active foragers, to semi-sedentary agriculturalists, and finally to highly sedentary

members of an industrialized society in a short evolutionary period of time (roughly 10,000

years; Ruff et al. 1993) suggests that the decrease in diaphyseal robusticity since the Pleistocene

(Ruff 1994) is a result of the steady decline in activity levels of our species over the same time

span. Ruff, among others, has argued that the technological transition of the past few millennia,

and especially the last century, has led to the adoption of a very different loading regime. In the

past few decades, technologies of convenience, coupled with the increased ease of access and

excess calories for consumption, has fueled an obesity pandemic; in the United States, up to a

third of the population is diagnostically obese, a trend that has emerged only in the last thirty

years (Flegal 2005; Flegal et al. 2010), accelerating in the last two decades (see Figure 1).

Further evidence suggests this increase is occurring globally (Dinsa et al. 2012; Pinhas-Hamiel

and Sabin 2013; Wells et al. 2012).
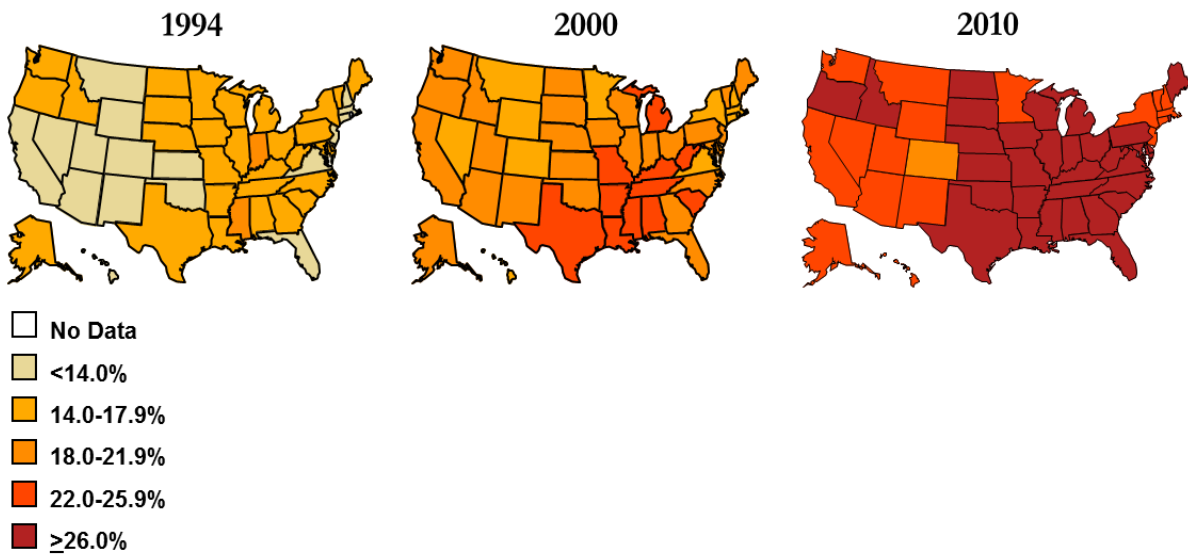
Figure 1. Obesity trends among US adults 1994, 2000, and 2010
Colors indicate the percentage of the adult population in each state that has been diagnosed as clinically obese. This figure is reproduced from (www.CDC.gov).

Interestingly, the propensity for humans to experience obesity itself may be a product of evolutionarily selective advantage (Prentice 2005a; Prentice et al. 2008), despite the many documented deleterious effects documented in the clinical literature (Ma et al. 2011). In the evolutionary recent past, energy stored in fat cells was essential to surviving times of famine. The modern environment where calories are abundant and rigorous physical exertion is not essential for obtaining them is diametrically opposed to the physiological adaptations meant to maintain energy homeostasis in the past. Health problems resulting from obesity may exceed the rate of technological and medical advancements, replacing tobacco as the primary health risk in developed societies (Gale et al. 2004). As the incidence of obesity has risen sharply in the past thirty years, so, too has the quantity of research focused on its etiology and comorbidities. Most of the research on obesity, however, has focused on understanding its etiology, as well as the direct and indirect effects of the diseases associated with it. Only a small portion of the total obesity-related research has considered the skeleton, and much of this centers on morbidities of the skeleton (e.g., osteoporosis, Zhao et al. 2007) in relation to obesity.

Previously, a few studies on the effects of obesity on the skeleton have been concerned with mechanical effects of increased mass on weight-bearing skeletal elements. One study, aimed at estimating body mass from femoral cross-sectional properties, found that cross-sections of the proximal femur were best for estimating body mass for both males and females (Moore 2008). Agostini and Ross (2011) also examined the effect of body mass on femoral diaphyseal shape (though the measurements were limited to external dimensions) and found a significant difference in mediolateral (ML) breadth. These studies have demonstrated significant differences in diaphyseal morphology at various cross-sections between BMI groups. Related to these findings, additional studies indicate that the ML forces associated with pelvic breadth

differentially affect the cross-sectional shape of the proximal femur (Ruff 2000; Ruff et al. 1991).

This dissertation adds to existing literature both by more thoroughly examining the mechanical effects of body mass throughout the skeletal elements, as well as approaching them systemically. The present study includes analysis of the femur, but expands beyond the lower limb. To better assess the varied effect of weight on the skeleton, the upper limb and cranial vault are also considered. As they experience different mechanical loading regimes, the three regions of the human skeleton (lower limb, upper limb, cranial vault) included in this study provide the opportunity to investigate variation with respect to mechanical as well as systemic effects of obesity.

The systemic approach to examining the effects of obesity on the skeleton taken in this dissertation is especially relevant given the recent breakthrough discovery that adipose tissues serve an endocrinological function in addition to energy storage (Zhang et al. 1994; Zhang et al. 1999). This function involves communication between the endocrine, immune, cardiovascular, musculoskeletal, and central nervous systems and partial regulation of development, metabolism, eating behavior, fat storage, bone maintenance, insulin sensitivity, hemostasis, blood pressure, immunity and inflammation (Eringa et al. 2012; Falcao-Pires et al. 2012). Previously unknown biological links between fat and bone, bone and pituitary gland, and bone and the hypothalamus have sparked interest in the role of these links in obesity pathogenesis.

As more current research uncovers signaling pathways related to bone maintenance and adipose tissues, the question of how obesity affects the human skeleton presents itself, especially in light of biomechanics. It is well established in biomechanics research that bone adheres to the principle of bone functional adaptation, wherein bone deposition occurs as a response to

5

localized strain (Currey 2003; Ruff et al. 2006). Numerous studies using animal models as well as human physical activity studies demonstrate that long bone diaphyses are particularly responsive to mechanical strains throughout life (Ferry et al. 2013; Forwood and Turner 1995; Greene et al. 2006; Shaw and Stock 2009b). Adapting to its mechanical environment, bone can change its size (amount of bone) and/or shape (the distribution of bone); this provides the stability necessary for the skeleton to support all forms of activity while resisting stresses produced by body mass and muscle forces. However, it is uncertain whether changes observed in the skeletons of obese individuals (as noted above) are adaptations to the increased mechanical loads experienced by these individuals alone; the endocrinal changes and other metabolic pathways affected by increased adipose tissue may mitigate the normal signaling that occurs in bone homeostasis, repair, and functional adaptation.

Thus, the skeletons of obese individuals may reflect both mechanical effects incurred with increased body mass as well as potential systemic metabolic changes on bone regulation. These effects cannot be isolated, but an understanding of how mechanical factors and metabolic factors shape the morphology and regulation of bone must be established. First, however, the normal cellular and tissue-level biology of both bone and fat must be established; this is discussed in the next chapter (Chapter 2). Chapter 3 summarizes mechanical effects on bone, especially of the limbs, while Chapter 4, building on Chapter 2, provides details about the metabolic factors that shape skeletal morphology. Despite the extensive background provided in these three chapters, the interaction of the effects of mechanics and metabolism on a systemic level remains largely unexplored (Eleazer 2013). In fact, most previous research has focused on the effects of these factors in isolation, despite the acknowledgement that bone properties are a product of the interactions between mechanical *and* metabolic stimuli (Pearson and Lieberman

2004; Ruff et al. 2006). Furthermore, multiple authors have explicitly stated that the interaction of these factors in humans is not well understood (Auerbach and Ruff 2004; Currey 2002; Rauch and Shoenau 2001; Skedros et al. 2007).

Therefore, though the localized responses to mechanical stimuli are relatively well established in the literature, the question of how these factors interact with the systemic metabolic and related factors emerges. The examination of this interaction in obese individuals presents a unique opportunity, as the effects of excess adipose tissue on bone homeostasis offer a window into an extreme case of both mechanical loads and physiological effects on normal metabolic pathways. Insights from ascertaining the differences in systemic bone morphology between obese and non-obese individuals, then, may highlight the relative impact these two groups of factors have on the skeleton.

To address this topic, the study presented here uses a unique human skeletal sample with which to analyze bone mass and shape properties for individuals of known age, sex, ancestry, height, and weight. The principal goal of this work is to assess and quantify the systemic effect of obesity on cortical bone mass and shape across the human skeleton (see Chapter 5 for the hypotheses tested by this project). In summary, though, this dissertation seeks to address the interaction between mechanical and metabolic factors by being the first to investigate whether obesity is associated with systemic skeletal changes in humans, detectable at the macroscopic level, on elements that experience different amounts of mechanical loading but, presumably, are affected by the same systemic metabolic effects. Specifically, the research conducted here will assess the relationship of body mass and BMI with measures of cortical bone strength properties throughout the skeleton (cranial vault, upper limb, lower limb), and with joint morphology both

in limbs that support body mass (e.g., the femur and tibia) and bones that do not (e.g., the humerus and radius).

CHAPTER 2

BONE AND FAT BIOLOGY

This dissertation focuses narrowly on specific functions of both bone and adipose tissue (fat), and is only able to examine their interactions from differences in patterns among individuals with and without excessive weight. Any differences observed between these groups imply interactions between factors associated with obesity and bone morphology, and thus may be argued to relate to the abnormal mechanics (i.e., high mechanical loads) and pathophysiology associated with high fat content in the body. To ascertain these potential effects, then, one must understand the relationship of bone to mechanics and physiology, the role of adipose tissue on these pathways, and the fundamental biology of normal bone and fat.

In this review, it is important to not be reductionist about the functions of bone or adipose tissue; both tissues are involved in a variety of actions within the body. The skeleton, for example, protects vital organs, provides the structural framework for mechanical movements, serves as a mineral reservoir, produces red blood cells, and regulates energy metabolism. Adipose tissues are also multi-functional, being involved in energy storage, appetite regulation, hormonal secretions, thermogenesis, blood pressure control, and bone mass maintenance. The pathways for many of these functions are linked and act together to affect the maintenance of (and alterations to) bone shape and size.

Cell Differentiation and Function

Both adipose and bone tissue consist of a combination of cells. A variety of genes and proteins control the differentiation of these cells from stem cells and other, generalized progenitor cell lines. In bone, these yield the basic multicellular unit (BMU), which are a team of cells that together create, remove, and directly contribute to bone tissue. In contrast, different populations of mesenchymal cells form types of adipose tissue, but specific fat tissue types are the product of single cellular lines (and not multiple cells, as in bone). Several systemic and local regulatory systems are involved in the signaling process between the cells of these tissues. These various cells, their derivations, and their contributions to their respective tissues are described in detail in this section.

Bone

Bone is highly organized and hierarchically structured (Nyman et al. 2005). At the macroscopic level, there are two types of bone, compact cortical bone and highly porous trabecular (spongy or cancellous) bone. The microstructure can be lamellar or non-lamellar, and at this level, bone can be directly deposited (primary mineralization) or it can replace existing bone (secondary mineralization). On the nanoscale, bone is comprised of collagen, mineral (hydroxyapatite), water, and non-collagenous proteins, in addition to embedded cells. Each of these levels contributes to the structure and strength of the human skeleton, and changes in organization at any level can result in bone strengthening or weakening (Reznikov et al. 2013; Vigliotti and Pasini 2013). Properties of bone and its arrangement in space, the size and shape of the bone, determine its effectiveness in load bearing (Currey 2002).

Many cells and proteins are responsible for bone growth and maintenance. Some of the cells include osteoblasts, osteoclasts, osteocytes, chondrocytes, and adipocytes; the first two cell types form the BMU. These cells are controlled by a number of factors and proteins. For example, bone morphogenetic proteins (BMPs) are growth factors involved in many embryonic and post natal developmental pathways, including the induction of bone formation (Gallagher and Sai 2010). Another set of proteins involved with development of bone are Wnts, which are a family of glycoproteins that trigger a succession of signals vital to embryonic development, as well as tissue regeneration throughout life (Monroe et al. 2012). These and other factors form interaction networks and feedback loops, which together regulate the abundance and distribution of bone cells.

As noted above, two cell types comprise the BMU—osteoclasts and osteoblasts—which create and remove bone in order to maintain homeostasis. Osteoclasts are multinucleated bone-resorbing cells that remove both mineral and organic content. Osteoclast precursors originate from the monocyte/macrophage lineage of hematopoietic stem cells located in bone marrow. The expression of RANKL, an osteocyte-derived bone matrix protein, is essential for osteoclast differentiation, function, and survival (Manolagas and Parfitt 2013; Tanaka et al. 2011; Tat et al. 2008). This is important because osteoclasts are generally short lived cells that must be continuously generated at the site of resorption to proceed with the process of bone matrix removal (O'Brien et al. 2013). Osteoblasts are derived from the same pool of multipotent mesenchymal stem cells (MSCs) as chondrocytes and adipocytes, and differentiation is regulated by several intracellular factors. Osteoblasts can be induced by BMP-2, which initiates signal cascades promoting osteoblast-specific genes (e.g. pro-osteogenic transcription factor Runx2; Darcy et al. 2012). An increase in expression of these genes favors osteoblast differentiation and

suppresses other cell differentiation (ie. adipocytes, chondrocytes; Sadie-Van Gijsen et al. 2013). Mature osteoblasts are single-nucleus, bone-forming cells that secrete the bone matrix, which subsequently mineralizes extracellularly (Tripuwabhrut et al. 2013).

The cells of the BMU are, effectively, temporary; osteoclasts die once their task is completed, and osteoblasts become embedded in the organic and mineral matrix of bone. Once embedded, these osteocytes make up 95% of bone cells (Krishnakanth et al. 2011). Osteocytes are located in spaces called lacunae, which are connected to each other by small spaces called canaliculi; together this network is called the lacuna-canalicular system (Klein-Nulend et al. 2013). Through this microscopic network, osteocytes can regulate bone resorption or formation in adjacent cells by signaling secretions, which affect osteoclast and osteoblast function. Osteocytes have been implicated in bone resorption by studies that demonstrated their role in the expression of RANKL, and therefore promoted osteoclast formation (Manolagas and Parfitt 2013). In addition, the discovery of sclerostin protein, a Wnt antagonist expressed primarily by osteocytes, led to the first evidence that osteocytes are directly involved in bone formation (O'Brien et al. 2013; Robling 2013; Robling et al. 2008). In addition to these localized functions, osteocytes can also have a systemic effect on calcium-phosphorous homeostasis by releasing other factors (fibroblast growth factor, dentin matrix protein, and PHEX; Durmaz et al. 2013; Welldon et al. 2013). The specific factors that cause osteocytes to release these various factors and proteins are still under investigation, though changes in hydrostatic pressure in the cellular extensions found in canaliculi—which results from mechanical loads—has been suggested to be one such factor (Robling et al. 2006; Turner et al. 2009). Further research is required for understanding the signaling pathways and transcriptional programs that regulate bone formation and resorption.

Fundamental to the formation of bone are chondrocytes (cartilage cells). The process of bone formation is discussed in more detail below, but, in short, most of the bone in the postcranial skeleton is initially comprised of cartilaginous anlages (rudimentary models), which then undergo primary ossification (Currey 2002). Chondrocytes comprise these anlages (in addition to proteins), and originate from mesenchymal cells. Like osteoblasts, chondrocytes are initially chondroblasts, which are the cells that create the protein (collagen and others) matrix that comprises cartilage; these chondroblasts become embedded in their matrix, where they become chondrocytes. In addition to osteogenesis, which is the product of ossification of cartilage models by osteoblasts, BMP signaling (especially BMP-4) is also involved in the proliferation of chondrocytes in growth cartilages (Mackie et al. 2008). In mature individuals, chondrocytes remain important in the formation and maintenance of cartilages, as well as in the healing of bone fractures.

Fat

Unlike bone, which is comprised of multiple cells, adipose tissue is mostly comprised of adipocytes, which are joined by a minority of other cells—mostly fibroblasts and immunological cells—in addition to vascular tissues to form the connective tissue (Lumeng 2013; Schaffler et al. 2007). This connective tissue does not have a hierarchical structure like bone, though it is confined to specific areas of the body. Adipose tissue performs a variety of functions, including storage, insulation, and hormonal production. As described below and in Chapter 4, much of the understanding of the cell types for adipose tissue, signaling pathways that create adipocytes, as well as the products produced by these cells, is still developing.

Adipocyte progenitors originate from the mesoderm and are derived from the same pool of pluripotent mesenchymal stem cells (MSCs) as myocytes (muscle cells), chondrocytes, and osteoblasts. To become a mature cell, the MSC must undergo a two-part process of determination and differentiation, wherein both local and systemic signals can determine cell fate (Reid 2010). Some of these signaling pathways involve bone morphogenetic proteins (BMP-2, BMP-4, BMP-7) and Wnt signaling proteins. Once the MSC has committed to the adipocyte lineage, the cell is called a pre-adipocyte (Algire et al. 2013). During differentiation, the pre-adipocyte undergoes several rounds of mitosis until maturation and exit from the cell cycle.

Adipose tissues have specific anatomy, plastic physiological functionality, and, as a multi-depot organ, are distributed in pockets throughout the body (Modica and Wolfrum 2013). In mammals, there two types of extra-medullar adipose tissues: white adipose tissue (WAT) and brown adipose tissue (BAT). Morphologically, these two types of fat differ in color due to differences in lipid droplet size stored, and the number of mitochondria in the cell. WAT stores triglycerides in a single large lipid droplet with few mitochondria, while BAT has many mitochondria and stores small droplets of triglycerides. In addition to their differences in morphology, the two types of adipose tissue function differently.

The WAT originate from mesenchymal Myf5-negative stem cells and is known to function in the storage of triglycerides for energy. Subcutaneous and visceral (intraperitoneal) fat depots are primarily made up of white adipocytes. In addition to their role in energy storage, white adipocytes are now known to serve an endocrine function, releasing various hormones (called adipokines) that contribute to energy homeostasis by regulating appetite, food intake, glucose disposal, and circadian rhythmicity (Algire et al. 2013; Lee et al. 2013; van der Spek et al. 2012). The specific function of WAT as an endocrine tissue is detailed further in Chapter 4.

Until recently, BAT was known primarily for its thermogenic properties with regards to heat production in children, especially newborns who lack muscle mass for shivering thermogenesis (Chechi et al. 2013). Only with recent advances in technology have the presence of BAT in adult humans been identified in the supraclavicular, suprarenal, paravertebral, and neck regions (Beranger et al. 2013). Current research demonstrates that BAT shares closer developmental origins with muscle cells than WAT. Characterized by myogenic Myf5-positive expression (Algire et al. 2013), brown adipocytes can be thought of as "adipomyocytes," or muscle cells that have developed the ability to accumulate lipids (Modica and Wolfrum 2013). Similar developmental origins explain the similarities in functions of the two types of cells, as well as the closer relationship of BAT to skeletal muscle than WAT. Both brown adipocytes and myocytes contain many mitochondria, have the ability to perform oxidative phosphorylation, and are capable of thermogenesis (Chechi et al. 2013; Virtanen et al. 2013). BAT generate heat through the expression of uncoupling protein 1 (UCP1), which uncouples respiration (oxidative phosphorylation) from ATP synthesis (Algire et al. 2013), resulting in heat production, and promoting energy expenditure. Furthermore, BAT is highly vascularized to ensure heat dissipation, and highly innervated by sympathetic nerve fibers to ensure regulation by the central nervous system (Chechi et al. 2013). Greater numbers of brown adipocytes have been shown to protect against weight gain, better regulate glucose homeostasis and insulin sensitivity, and correct hyperlipidemia (that is, an elevated lipid profile). Weight loss as a result of the increased energy expenditure associated with more brown adipocytes may be a potential therapy for human weight loss (Carey and Kingwell 2013; Kozak 2013).

In addition to WAT and BAT, a new type of fat cell has recently been identified. Although morphologically and functionally similar to brown adipocytes, "recruitable," "beige,"

or "brite" (brown in white) adipose cells seem to have distinct anatomic, developmental, and molecular properties. Brite cell precursors are still unknown, although they do not express myocyte-enriched genes and exhibit a distinctive molecular signature unlike BAT or WAT (Beranger et al. 2013). These findings may be indicative of a separate origin from other adipocytes. In some mouse models, the browning of white depots is associated with an improvement in metabolic phenotype and energy balance (Chechi et al. 2013), and resistance to diet-induced obesity (Lasar et al. 2013). The number of brown and brite adipocytes increases in response to extended cold exposure, undergoing thermogenesis upon stimulation (Barneda et al. 2013; Vosselman et al. 2013). The discovery that the amount of BAT is inversely correlated with body mass indices (BMI) (Saito 2013; Virtanen et al. 2013) further suggests that any conversion of WAT to BAT or brite, or the regeneration and/or activation of BAT, could be key in gaining control of energy metabolism in obese individuals (Algire et al. 2013).

Bone marrow fat, or yellow adipose tissue (YAT), comprises most of the medullary cavity of bone, and has been implicated in the systemic regulation of energy metabolism along with osteoblasts (Lecka-Czernik 2012). While the metabolic functions of WAT and BAT have been ascertained for energy storage and dissipation, respectively, the role of YAT has only recently been investigated. In the past, marrow fat was thought to serve as filler in a cavity no longer needed for hematopoiesis, although mature marrow adipocytes are now thought to be negative regulators of the hematopoietic micro-environment in bone (Lecka-Czernik 2012). Krings et al. (2012) discovered that the phenotype of YAT has characteristics of both WAT and BAT. Its origins and endocrine functions are similar to WAT, as it is differentiated from the same MSCs that can also become osteoblasts. This results in a reciprocal relationship between osteoblastogenesis and adipogenesis in bone marrow-derived MSCs, with factors stimulating one

process usually inhibiting the other (Sadie-Van Gijsen et al. 2013). Similar to WAT in some regards, YAT appears to be under similar transcriptional control as BAT (Krings et al. 2012). Bone marrow adipocytes have a yellow appearance due to a moderate amount of mitochondria (more than WAT and less than BAT).

There appears to be an inverse relationship between bone mass and YAT in bone. As bone mass decreases (and so the marrow cavity increases) with age, the amount of fat mass in the cavity increases (Lecka-Czernik 2012). It is also hypothesized that a decrease in the number BAT-type marrow adipocytes with aging results in deleterious changes in the marrow microenvironment with regards to bone remodeling. Systemic changes in energy metabolism, such as overnutrition and malnutrition, result in responses by WAT, BAT, brite, and YAT. Much research remains to be conducted with regard to the intricacies of these responses, but their general metabolic involvement is described in Chapter 4.

Regulation of Adipose Tissue

The regulation of the amounts of adipose tissue present throughout the body depends on a number of factors, including the presence of certain hormones, physical activity, diet and nutrition, and genetic predispositions, as well as the age of the individual (Alemany 2013; Bohler et al. 2010; Bredella et al. 2011; Eringa et al. 2012; Kozak 2013; Poulos et al. 2010). These are considered in some more detail in Chapter 4. However, it should be noted here that no single factor—high fat content diets, reduced physical activity, or increased leptin levels (see Chapter 4)—may be attributed to increases in the amount of adipose tissues. In fact, as reviewed above, the presence of some types of adipose tissue (e.g., BAT) may influence the amount of other types

(e.g., WAT). Therefore, any discussion of the regulation of amounts and types of adipose tissue must take all of these factors into consideration. A full discussion of these relationships is beyond the parameters of this dissertation, however, as the quantities of types of adipose tissues among the study subjects is not known.

Bone Development and Maintenance

The cellular components of bone described above work together to build the skeleton, first by ossifying precursor tissues, and then refining, modifying, and expanding the distribution of the ossified tissue to form final bone shape and size. Despite the varying sizes and shapes of bones comprising the human skeleton, all bones are formed by one of two processes: endochondral or intramembranous ossification. Bones of the axial and appendicular skeleton are generally formed by endochrondral ossification, while most bones of the cranium are formed by intramembranous ossification. This section briefly details these processes, and also discusses the processes of bone modification during growth and upon maturity.

Limb bone development

Both the upper and lower limbs are comprised of homologous structures in four segments: an articular girdle with the axial skeleton, a proximal element (stylopod), a pair of intermediate elements (zeugopod), and a distal limb section comprised of multiple elements (the autopod). Genetic control of the formation of these involves a network of proteins, morphogens, and other factors, including HOX genes, sonic hedgehog (SHH), BMPs, fibroblast growth factors (FGFs), and Wnts (Lu et al. 2013; Monroe et al. 2012; Provot et al. 2013; Wesseling-Perry and

18

Juppner 2013). Limb formation occurs between embryonic weeks four to eight, with the upper

limbs forming slightly ahead of the lower limbs. Outgrowths of limb buds, which then

differentiate into the four limb segments, are mediated by the factors listed above; these factors

determine the anatomical planes of the limb, the length of the limb, and the specific morphology

of the bone elements. The cartilaginous precursors of the limb bones appear around week six.

Endochondral ossification is a complex process by which the embryonic cartilaginous

anlage of most bones contributes to longitudinal growth, and is gradually replaced by bone

(Mackie et al. 2008). In general, this process consists of a temporary structure (the anlage) that is

gradually replaced over time by a stronger and better-adapted structure (ossified tissue), able to

meet the mechanical and systemic demands of the adult body. More specifically, the

cartilaginous model is formed as mesenchymal cells (derived from lateral plate mesoderm)

condense and differentiate into chondrocytes (Lu et al. 2013). Once the anlage has been formed,

blood vessels, osteoclasts, osteoblasts, and bone marrow cells invade it. These cells invade the

center of the forming element first, forming the primary center of ossification; after birth, these

cells then invade each end (epiphysis) of a developing long bone, creating the secondary centers

of ossification. It is thought that the intrusion of blood vessels into the chondral anlage induces

the ossification process, perhaps by introducing the mesenchymal cells that become osteoblasts

(Carter et al. 2004; Chim et al. 2013; Cole et al. 2013). In a process called coupling, osteoblasts

replace hypertrophic chondrocytes and ossification spreads from the primary center toward the

epiphyses, while osteoclasts break down previously formed bone and allow for modeling and

remodeling of the growing bone (see below).

Between the primary and secondary ossification centers, a layer of cartilage, called the

epiphyseal cartilage plate or growth plate, remains throughout development (Macsai et al. 2011;

Nilsson et al. 2005). Within the developing bone are several distinct layers of chondrocytes, which are oriented in columns along the long axis of the bone. At the epiphyses are rounded, resting chondrocytes; towards the diaphysis (bone shaft) is a layer of flattened proliferating chondrocytes, then a prehypertrophic layer, followed by a layer of enlarged, hypertrophic chondrocytes (Felber et al. 2011). Osteoblasts then replace the hypertrophic chondrocytes, and the centers of ossification gradually replace the remaining cartilage model, until skeletal maturity when the model is completely replaced with bone, even at the growth plate (Villemure and Stokes 2009).

Synovial joint development

Synovial joints connect the long bones of the appendicular skeleton (as well as some other joints in the body). They are characterized as having an enclosed capsule that surrounds the bony articulation, and this capsule produces synovial fluid, which greatly reduces friction between the bony elements as their articulations move (Currey 2002). During development, synovial cavities form as the mesenchymal zone between two cartilaginous bone models differentiates into fibroblastic tissue, which is undifferentiated connective tissue. This zone is then further differentiated into three regions: two cartilaginous layers in contact with the adjacent cartilage bone models (one at each end), with dense connective tissue between. As bones ossify, part of these cartilaginous layers overlying the developing articulation will also mineralize, but the cartilage largely remains unmineralized and will line the bony articular surface. The dense connective tissue between the two forming long bones gives rise to the internal joint elements (e.g. menisci, joint capsule, synovial cavity) through a series of programmed cell death sequences (Carter et al. 2004; Eckstein et al. 2002). In utero movement and genetic coding both

shape the specific structures of the articulations and the internal joint tissues (Carter and Beaupré 2001).

Cranial vault development

The cranial vault and face are formed by intramembranous ossification (the cranial base is formed endochondrally). Intramembranous ossification occurs when bone is formed directly from mesenchymal cells, derived from neural crest cells and mesoderm, without a prior cartilaginous model. In this developmental pathway, osteoblasts differentiate directly from the mesenchyme and deposit osteoid, which subsequently ossifies. Like the bones of the limbs, though, this initial ossified tissue is modified by the BMU through modeling and remodeling.

Modeling and remodeling

Osteoclasts and osteoblasts augment the structure of developing bone, as well as replace existing bone; these processes are termed "modeling" and "remodeling." This addition and removal of bone is performed to maintain bone strength in response to mechanical loading, as well as to deposit and remove nutrients stored within bone, namely phosphorous and calcium. The process of maintaining adequate mechanical resistance to loading is generally termed bone functional adaptation, which is covered in more detail in Chapter 3.

Bone modeling is defined as an asymmetry in the action of osteoblasts and osteoclasts; osteoblasts lay down bone without prior osteoclast activity. This system of bone growth is controlled through aforementioned signaling by osteocytes, which sense mechanical strains and recruit osteoclasts or osteoblasts as needed (Klein-Nulend et al. 2013). This process is important for bone growth, increasing bone mass, and maintaining bone strength (that is, resistance to

failure). While some modeling occurs after bones fully ossify (e.g., subperiosteal expansion in

aging adults; Ruff and Hayes 1982), bone modeling defines the period of primary growth, which

is the period of growth from conception to maturity, marked in the skeleton by the final

ossification of all of the bones. Bone size and shape change considerably during this period, both

in the external shape of the bone and in the internal distribution of bone. Through this process,

bone has the ability to adapt to its mechanical environment (Chapter 3); the daily stresses

(amount of loads experienced) incurred by the skeleton inevitably result in microcracks and

defects, which must be repaired (Burr et al. 1998; Reilly and Currey 2000). New bone may be

added to better reinforce planes under higher mechanical stresses. Strength properties of a bone

can be optimized by modifying its spatial distribution, rather than simply increasing mass.

Specifically, periosteal apposition along the bone perimeter, concurrent with endosteal

resorption, shifts the thickening cortex outward from the neutral axis of the bone, resulting in an

increase in strength (that is, resistance to bending; see Chapter 3).

The process of remodeling is also important during bone growth by optimizing the

developing structure of bone in relation to mechanical loads. In contrast to modeling, remodeling

involves the symmetric replacement of bone; osteoclastic activity signals for and is directly

followed by osteoblastic activity. Also unlike modeling, remodeling is a continuous process that

occurs throughout the lifetime of a vertebrate (Pivonka et al. 2008). While it is not typified as the

alteration of gross bone shape, remodeling can change the density, geometry, and structure of the

bone to reinforce or remove bone where necessary (Krishnakanth et al. 2011). The very act of

replacing existing bone alters the microscopic mechanical transmission of forces through bone,

as well as the signaling mechanism for initiating bone remodeling (as new osteoblasts get

embedded as osteocytes into the bone). In a normal state of bone maintenance, bone resorption

and formation occur at approximately the same rates (Henriksen et al. 2009). However, in certain disease states, bone resorption occurs at a greater rate than it is replaced, resulting in osteoporosis and similar disorders (Teitelbaum and Ross 2003).

The differences between modeling and remodeling have noteworthy consequences for interpreting at what period of an individual's life changes could have occurred within bones, especially in the shape and distribution of cortical bone in the diaphyses of long bones. Bone adaptation occurs in response to various stimuli (Chapters 3 and 4), and is not necessarily uniform throughout the bone. Two important examples demonstrate: 1) the periosteal margin is more responsive to mechanical loading prior to mid-adolescence and the endosteal margin is more responsive after this time period; and 2) diaphyseal cross-sections have a different pattern of growth than articulations or maximum bone lengths, which are more ontogenetically constrained (Lieberman et al. 2001; Ruff et al. 1994; see also Chapter 3).

Independence and Variability in Skeletal Dimensions

Growth of the skeleton requires developmental control to maintain proper shape and size, both with respect to articulating bones and to the functional needs of the individual. That is, bones of the skeleton are interdependent, and so are expected to be regulated to conform as they form and ossify. Thus, the amount of variability possible in the size and shape of bones relative to each other within an individual would be specific to certain dimensions; a lack of conformity among mechanically related structures would lead to functional impairment. It is important to establish the mechanisms for these restrictions, as correlations between some bony dimensions may be due to underlying developmental or functional constraints (Lazenby et al. 2008b;

23

Lieberman et al. 2001). Moreover, differences in the levels of these limitations will have consequences for predicting what bone dimensions will be more likely to change in response to the mechanical or metabolic shifts relating to obesity.

These differing magnitudes of phenotypic variances are measured by degrees of canalization, developmental stability, and morphological integration (Hallgrimsson et al. 2003; Hallgrímsson et al. 2002). Canalization refers to the tendency of a genotype to follow the same trajectory under different developmental and environmental influences, or the inhibition of phenotypic variation among individuals (Wagner et al. 1997). Developmental stability is related to canalization, as it is the minimization of developmental instability; that is, developmentally stable phenotypes reflect a tendency of a genotype to follow the same trajectory under the same developmental and environmental influences. Phenotypes that show correlated variation, either due to shared developmental processes or shared functions with other structures, are classified as morphologically integrated (Hallgrímsson et al. 2002).

It is difficult to determine how dimensions relate to these states (canalization, stability and integration), and the measurement of these states is beyond the scope if this study. However, it is important to understand that integration of some morphologies will have implications for the interpretation of morphological changes associated with obesity, as well as for setting up the hypotheses for this study. For instance, the dimensions of two skeletal elements may be developmentally coordinated because the same developmental processes control them, but they may experience different amounts of developmental stability depending on ontogenetic factors. The dimensions may appear to be less correlated or independent. Skeletal dimensions that are functionally or developmentally integrated would be considered developmentally stable and canalized if they have low variability and high correlations, regardless of the developmental or

24

environmental factors present. Therefore, it is not possible to tell whether two dimensions are morphologically integrated or independent by their correlation alone. Yet, if dimensions show related patterns of difference in obese compared with non-obese individuals, but those dimensions are not modeled as being developmentally or functionally integrated, then this would argue for similar environmental effects (i.e., those associated with obesity) as influencing their correlated difference.

This logic is especially applicable to the dimensions of the limbs. Limbs can be thought of as comprised of a hierarchy of modules that are functionally or developmentally integrated (Lieberman et al. 2001; Young et al. 2010). Each of these modules is a semi-independent, tightly integrated subunit of the whole, and may be separately affected by influencing factors (Klingenberg 2008; Mitteroecker and Bookstein 2008). Epiphyses, for instance, must conform between functionally related limb bones, but they are also the product of coordinated development (Carter and Beaupré 2001); the similarity of articulations would be more important than their integration with either bone lengths or diaphyseal dimensions. When viewed this way, the developmental pathways responsible for bone lengths are semi-independent from those for articulation breadths or diaphyseal measurements, and may be more canalized due to mechanical functional constraints (Auerbach and Ruff 2006; Lieberman et al. 2001; Reeves et al. in review). For example, it is important that an individual display little asymmetry in lower limb lengths so as not to interfere with successful locomotion. Diaphyseal breadths are shown to be the most plastic of limb bone measures (Auerbach and Ruff 2006), likely due to the need for modeling and remodeling of these areas to effectively withstand various loading patterns (resisting axial and various bending and torsional strains).

The cranium is also a complexly integrated structure, as it is also composed of many semi-independent yet connected modules (Ackermann 2009; Cheverud 1982; Mitteroecker and Bookstein 2008). More specifically, there are three embryologically separate units of the cranium: the basicranium (cranial base), neurocranium (cranial vault), and splanchnocranium (facial skeleton). As indicated, the cranial base is formed by endochrondral ossification, while the vault and face are formed through intramembranous ossification. These differences in development and germ layer derivatives may contribute to the differences in response of these regions to both endogenous and exogenous factors, as parts of the cranium are more canalized, while others are more plastic. The more canalized traits would be more conserved over time and among a population, signifying that these types of traits (or suite of traits) would be reliable indicators of population affinity. Following this logic, Hollo et al. (2010) examined the neurocranium and facial skeleton and determined that the latter region was more plastic than the neurocranium. As the neurocranium is the only one of the three cranial regions examined in this study, this is important to take into account; the calvaria may be more buffered against the effects of environmental perturbation than other parts of the cranium. Yet, from this perspective, any differences between obese and non-obese individuals in the sample, which was culled from the same general population, would strongly indicate obesity or its effects as a major contributing factor.

Bone-Fat Interactions and Experimental Models

Taking the independent biology of bone and adipose tissue into account, it is important to ascertain the effect each has on the other. Animal models have often been employed to examine

the relationship between obesity, genes, endocrine pathways, and various bone diseases (see West and York 1998 for a review). Using experimental models, the subjects have known genetic and environmental backgrounds, which make controlling for experimental factors of interest more successful.

For example, Lieberman (1996) conducted one such study using sheep and armadillos to try and isolate the specific effects of physical activity on bone. Other factors known to affect bone robusticity were controlled for by using genetically identical specimens fed the same diet and subjected to the same living environment. The samples were separated into exercised and control groups. When later analyzing the skeletons of these laboratory animals, any differences noted could be explained by the physical activity. As expected, the exercised group presented significantly stronger bone properties than those for the control group. Another experimental study of interest varied diet and physical activity, comparing four groups of mice: a high-fat diet group (HF), high-fat diet + running group (HFR), control diet group (C), control diet + running group (CR). Ma et al. (2011) conclude that both the HF and HFR groups became obese, with femora that demonstrated greater strength properties at the whole bone, as well as micro-structural level. Adaptations to physical activity on the control diet (the CR group) revealed improvements primarily in trabecular structure.

Mice have by far become the most commonly preferred animal models for bone research, in part because of their short reproductive periods, small size and ease of care, as well as the widespread availability of the entire mouse genome (Yang et al. 2013). Genetically engineered mouse strains have been bred for several decades now, resulting in a variety of genetic knockout mice. Observing the effects on development, anatomy, and physiology after removing particular genes has led to advances in understanding the complex interactions of various structures,

including: adipocytes (Caluwaerts et al. 2007; Hamrick et al. 2005; Schaffler et al. 2007), leptin (Ducy et al. 2000; Hamrick et al. 2005; Xie et al. 2013), estrogen (Järvinen et al. 2003; Sniekers et al. 2009), and insulin (Bellido and Hill Gallant 2014; Caluwaerts et al. 2007; Yamanouchi et al. 2004) to name only a few. These experimental studies have been used to direct clinical studies of humans, and have resulted in many recent discoveries.

Many investigations into the effects of obesity on the body involve dietary-induced obesity (DIO) (Cheverud et al. 2011; Cheverud et al. 1999; Ma et al. 2011; West et al. 1992). For otherwise endocrinologically and metabolically normal rats, Brahmabhatt et al. (1998) discovered that an ad libitum supply of a junk food diet results in increased cortical areas and anteroposterior (AP) and mediolateral (ML) outer diameters for the femora of DIO murines. Ma et al. (2011) also discovered an increase in bone strength in DIO mice, as a result of endosteal resorption and periosteal expansion. In a sample of white rabbits, Brunner et al. (2012) report that dietary fat, regardless of animal weight, alters chondrocyte function and could be a risk factor for the development of osteoarthritis.

One disadvantage to experimental models remains: while many animals may be similar in some ways to humans, no singular animal model can accurately simulate the characteristics of humans. For example, the differential effects of increased loads on limb bones due to overall increased weight cannot be determined in murine models as they are quadrupedal, and any attempt to isolate bones from loading (e.g., induced paralysis) in mice would potentially conflate influential factors. In addition, the difference in scale between mice and humans likely affects the manner in which their bones respond to mechanical loading (Carson et al. 2012), and the accumulation of adipose tissue in murine bone differs from that of humans with regards to age and skeletal location (Krings et al. 2012).

Despite some limitations to experimental models, the ability to control potential influencing factors has led to many advances in understanding how bone functionally adapts to mechanic and metabolic stimuli. Chapter 3 will consider the knowledge gleaned from experimental and observational studies for understanding the mechanical effects on bone. Chapter 4 presents a more complete review of the interactions of endocrinal functions of adipose tissue with the formation and maintenance of bone.

Chapter Summary

Experimental models have paved the way for ever expanding discoveries in bone and fat research and the connection and communication between these two tissues. Skeletal homeostasis involves a complex signaling system involving many factors and pathways. Osteocytes play a key role in mechanotransduction, sensing external loads and transmitting the information to osteoblasts (that mediate bone deposition) or osteoclasts (that mediate bone resorption) to maintain the anatomy, architecture, and strength properties of the bone. These signals are triggered by various stimuli and can affect the bone locally or systemically, as well as differentially. Long bones, as well as the cranium, are comprised of various modules that are semi-independent yet functionally integrated, resulting in differential responses to influencing factors. The following two chapters will further detail some of the stimuli known to affect bone size and shape.

CHAPTER 3

MECHANICAL EFFECTS ON BONE

In the previous chapter, the tissue biology of bone and its basic physiology were reviewed. As noted, most of the activity of the basic multicellular unit, modeling, and remodeling are controlled by biochemical signaling molecules, genes, and other factors, many of which are discussed in more detail in Chapter 4. However, the mechanical forces encountered by bones, or their absence, are an essential component of the activities of these cellular networks. It is the reaction to its mechanical environment that results in the shaping and distribution of bone. As this dissertation is centrally focused on variation in the shape and distribution of bone, a background in the mechanical mechanisms that generate that form is necessary for context. This chapter reviews that mechanism as well as the methods researchers use to measure the physical properties of bones in order to understand these biomechanical forces.

Bone functional adaptation

It has been widely demonstrated and accepted that bone adapts to the mechanical environment encountered throughout life (Currey 2002; Martin et al. 1998). The model of "bone functional adaptation" recognizes that skeletal morphologies change over the course of an organism's lifetime, in response to the mechanical environment (Carter and Orr 1992; Ruff et al. 2006). Bone is a dynamic structure (as described in Chapter 2); it responds to various mechanical loads through signaling mechanisms that will result in osteoblast activation and subsequently, bone deposition. The exact signaling pathway is still under investigation (e.g., Turner et al.

2009), although studies have identified osteocytes as the pivotal cells, regulating bone mass and structure for efficient load bearing (Burr et al. 2002; Klein-Nulend et al. 2013; Pavalko et al. 2003).

In general, strains that occur with *dynamic* activity (rather than static loading) drive bone adaptation, and the result is that higher or more frequent strains will illicit increased bone deposition as a localized response (Robling et al. 2006). In this way, bone is able to adapt functionally to its loading regime, laying down bone where it is needed (where the loading strains induce a signal). The frequency of loading influences the response of bone, in addition to the amount of force placed on an element. Studies on model animals have shown that the signaling pathway becomes quiescent when loading frequencies and stresses are high (Hsieh and Turner 2001; Warden and Turner 2004). Nonetheless, bone is "error driven," meaning that bone apposition is especially adapted to unusual bouts of loading, or strains over the normally incurred threshold (Turner 2002). Bone tissue, therefore, adapts to minimize metabolic cost while also reducing the risk of fracture due to inadequate bone strength or cumulative microdamage.

High levels of activity and greater variation in the amount of strain experienced by a bone will yield the greatest changes in bone size and shape. Strains result from forces incurred from the effects of gravity, body mass, reaction forces of substrates, and, importantly, muscle (Burr 1997; Robling 2010). Changes in response to these forces more commonly occur in the distribution of cortical bone in long bone diaphysis, and are not evident in the outer dimensions of articular surfaces (i.e., epiphyses; Auerbach and Ruff 2006; Lieberman et al. 2003; Reeves et al. in review). The reason for this difference within elements seems to be due to differences in canalization or developmental stability of the traits. Trabecular bone structure within epiphyses has been shown to change with loading, however, despite the apparent constraint in the shape

change of the external dimensions of articulations (Lazenby et al. 2008b). Notwithstanding the adaptive nature of cancellous bone at articulations, researchers still regard diaphyseal shape and size to be the best method for investigating the functional adaptation of bone to mechanical stimuli.

It is important to note that the morphological changes to the distribution of cortical bone in the diaphysis, and therefore changes in bone shape, are age-dependent (Ruff et al. 1994). Developing diaphyses demonstrate greater sensitivity to mechanical loading. This means that the bony response to the activities and loading patterns encountered at a young age have a large impact on the bone size and shape prior to skeletal maturity, when the ability to adapt becomes restricted. In a longitudinal study that examined children as they grew from middle and late childhood (5-11 years), Janz et al. (2007) concluded that physical activity is an important contributor to bone strength prior to adolescence; childhood physical activity is key to reaching optimal bone strength. The periosteal envelope is more responsive to mechanical factors prior to mid-adolescence, while the endosteal envelope is more responsive after this period (Ruff et al. 1993; Ruff et al. 1994); as noted in Chapter 2 and below, the apposition of new bone periosteally will increase strength in bending and torsion without the need for thicker bone, a mechanical resistance that is diminished in adding bone endosteally. New cortical bone deposition along the diaphysis is only effective until early adulthood when bone resorption begins to outpace bone deposition, the extreme of which is osteoporosis. The responsiveness of the diaphysis is important, as body mass may change vastly throughout adulthood, which will effect skeletal dimensions to maintain skeletal support. One of the assumptions made here is that load bearing diaphyseal cross-section properties, while influenced by the growth period, will be more highly

correlated with current body mass rather than mass at skeletal maturity or at any other point in an individual's lifetime (Ruff et al. 1991).

Engineering beam theory and cross-sectional geometry

Beam Theory

The limb bones of the body act as mechanical levers and cantilevers, moved at pivots (i.e., joints) by muscle action (Currey 2002; Ruff and Hayes 1983). In the case of the long bones, they both appear and act essentially as hollow, cylindrical beams in these levers. Therefore, beam theory—the mechanical model used to describe the resistance of structures to loading— may be applied to describe the mechanical properties of bone shape.

Beams are typically subjected to a variety of mechanical loading conditions; loading can be defined as the application of a force to an object. The five fundamental loading conditions, in addition to the unloaded condition, are pictured in Figure 2 and include compression, tension, shear, bending, and torsion. Compression involves forces that press the material together, shortening and widening the structure. Tension, the opposite of compression, is the condition where two ends of a plane are pulled apart, resulting in elongation and narrowing of the beam. Compressive and tensile forces act perpendicular (normal) to the surface of the structure, while shear forces act parallel to the surface, causing lateral displacement within a beam (Figure 2). These first three loading conditions (compression, tension, and shear) represent the primary modes of loading, as bending and torsion are a combination of the former. Bending results from loads applied in a manner causing the structure to curve; one side of the beam experiences maximum compression while the opposite side experiences maximum tension. Both compression

and tension decrease toward the central plane of the beam; the center, where the beam neither experiences compression nor tension, is called the neutral plane (or, in three dimensions, the neutral axis). As stated, shear forces cause lateral displacement within a beam; these displacements occur perpendicular to the axis of rotation during torsion. With respect to human long bones modeled as beams, most experience some torsion when loaded, rather than pure uniplanar bending (Butcher et al. 2011). In addition to the mode of loading, frequency of the forces incurred can affect the structure. Static loading is characterized by a constant force applied to the beam, while dynamic (cyclic) loading is distinguished by fluctuations in the loading regime.
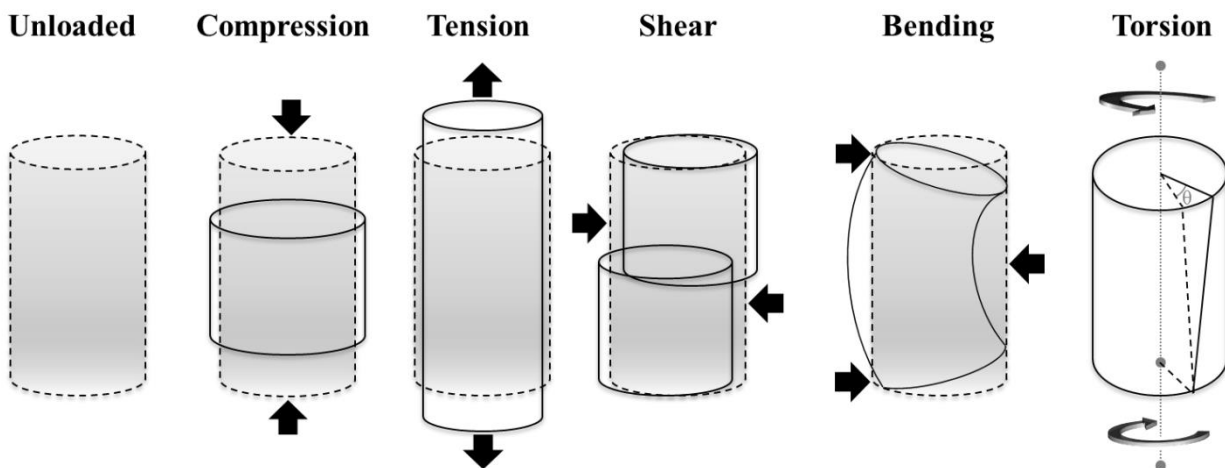
Figure 2. Modes of mechanical loading
The dashed line and grey-coloration indicate the initial geometry of the beam, as in the unloaded condition. The solid line contour represents the beam after the forces indicated by bold black arrows are applied. The dotted grey line in the torsion schematic indicates the axis of rotation, and θ represents the twisting angle.

The effects of forces applied to a structure are measured as stress (the amount of force applied to an area) and strain (the amount of deformation that occurs due to the force). Stress and strain properties may be consistent for specific materials, and so their ratio (Young's modulus) reflects the mechanical properties for a material under loading. Ultimately, the resistance of a beam to failure depends on the Young's modulus of its material composition; the amount of stress necessary to cause the beam to deform and break (that is, the ultimate stress at failure) is the strength of the beam under a specific load (e.g., compressive strength, tensile strength, torsional strength, etc.). The way a beam is loaded largely affects its mechanical properties.

Mechanical properties of bone may only be reliably established by experimental loading of the bone to the point of failure. Ascertaining these properties, however, depends on a number of variables; whether the element is wet or dry, is embedded in soft tissues or isolated, and is loaded as would typically be experienced *in vivo* all have significant effects on the outcome measurements of strength (Currey et al. 2009). In addition, the methods are inherently destructive and not replicable with the same sample. Therefore, researchers instead rely on knowledge of material properties and the shape and size of the beam in cross-section to estimate strength and resistance to loading (Ruff and Hayes 1982; Ruff and Leo 1986).

Cross-sectional Geometry

Cross-sections are typically obtained through radiographic methods, such as computed tomography (CT) scans, or through casts of the outer contour followed by a variety of methods to estimate the size, shape and location of the medullary cavity (Macintosh et al. 2013; O'Neill and Ruff 2004). Typically, the diaphyseal cross-sections are taken at mechanically relevant points, chosen by their location along the diaphysis, determined as a percentage of bone

35

maximum length when measured parallel to the longitudinal axis of the diaphysis (Ruff 2002a).

For example, length of the femur is defined as the average distal projection of the femoral

condyles to the superior surface of the femoral neck, and maximum length for the humerus

would be from the lateral lip of the trochlea to the humeral head (Ruff 2008b). In the past,

midshaft (50%) measurements of long bones have been preferentially compared, as the midpoint

of a beam (long bone) would incur (and therefore need to resist) the greatest bending and

torsional forces at this location. However, dynamically loaded bone functionally responds to

modes of loading incurred throughout the diaphysis, and does not necessarily maintain the same

size and shape properties throughout the element (Lieberman et al. 2003). More specifically,

research indicates that different parts of the diaphysis are adapted to resist different loads. Ruff et

al. (2003a; 1993) have found that the proximal femur is more resistant to loads incurred from

body mass due to body breadth, while the middle and distal femur more accurately reflect

activity patterns.

These diaphyseal cross-sections, which are two-dimensional images, are measured for a

series of properties that reflect the geometry and distribution of cortical bone (Table 1). A

schematic representing the cross-section of a hollow cylinder (an idealized condition of bone) is

presented in Figure 3. Because most bone cross-sections are not exactly cylindrical, the calculus

can be more complicated but is based on the same premise. Total area (TA) of the cross-section

establishes the size of the bone, is a general measure of robusticity for a bone, and is proportional

to the resistance of a bone to axial loads. Cortical area (CA), the amount of the total area of the

cross-section comprised of cortical bone, is another measurement of bone strength in axial

compression. Resistance to bending in bones (i.e., rigidity) is measured by examining the

distribution of bone relative to the neutral plane around which the bone is subjected to bending.

This second moment of area (also called second moment of inertia or area moment of inertia) is ascertained using calculus to quantify the distribution of cortical bone (in the case of this study), and is affected more by bone distributed farther away from the axis of bending than an overall increase in bone area. The larger the value of the second moment of area (I), the more rigid the beam is in relation to a reference plane that is a proxy for the neutral plane (Pearson and Lieberman 2004), the x or y axes, I_x or I_y, respectively. These reference planes typically correspond with anatomical planes (e.g., mediolateral, I_y or anteroposterior, I_x); greater values for second moments of area in a specific direction (AP or ML) will show the direction in which the bone incurs the highest strains and has adapted to withstand those loads. The maximum (I_{max}) and minimum (I_{min}) second moments of area can also be calculated, and they estimate the maximum and minimum diaphyseal bending strengths, respectively. The polar second moment of area (also called polar second moment or moment of area about the z axis) measures a beam's ability to resist torsion. Larger values for the polar second moment of area (J) indicate more rigidity when the beam is placed under torsional forces; the beam is stronger against twisting. Furthermore, the polar second moment is equal to any two perpendicular planes of second moments ($J = I_x + I_y$ or $J = I_{max} + I_{min}$), and may be the most relevant indicator of a bones' mechanical performance (Ruff et al. 1993).

In addition to the cross-sectional strength indicated by the polar second moment of area, the section modulus of a cross-section provides additional information about torsional strength. "Strength" in this context refers to a bone's resistance to failure or deformation when subjected to these directional forces (i.e., bending about a neutral plane and torsion about a neutral axis). The section modulus (Z_x and Z_y) reflect values proportional to the bone strength in the x-axis or y-axis (again, often corresponding with anatomical planes), and are essentially calculated as the

Table 1. Cross-sectional properties for quantifying bone mass, shape, and strength

Measurement Type	Measurement	Description
Cross-sectional properties of bone mass[1]	Total subperiosteal area (TA)	Area within periosteal surface
	Medullary area (MA)	Area within medullary cavity
	Cortical area (CA)	Correlate of compressive strength
Cross-sectional properties of bone shape	%Cortical area (%CA)	Amount of cortical bone relative to total area of the cross-section; (CA/TA) x 100
	Shape (circularity) index, max-min	I_{MAX}/I_{MIN}; estimate of distribution of cortical bone in relation to the principal axes
Cross-sectional properties of bending and torsional strength[2]	Maximum second moment of area (I_{MAX})	Maximum bending rigidity
	Minimum second moment of area (I_{MIN})	Minimum bending rigidity
	Polar second moment of area (J)	Sum of any perpendicular second moments of area, correlate of torsional strength ($I_{MAX} + I_{MIN}$)
	Maximum section modulus (Z_{MAX})	Maximum bending strength
	Minimum section modulus (Z_{MIN})	Minimum bending strength
	Polar section modulus (Z_p)	Torsional and twice average bending strength (J /moment arm)

[1] Should be size-standardized by body mass or a proxy (following Ruff et al. 1991; Ruff 2000).
[2] Second moments of area (I and J) and section moduli (Z) should be size-standardized by the product of body mass and bone length (Ruff, 2008).

moment of area (I) divided by the length of the outer edge of a bone from the neutral axis

(centroid) on that given axis (Ruff and Hayes 1983). The polar section modulus, Z_p, reflects the

strength of a bone cross-section in torsional loading and is the calculation of J scaled to the

circumference of the diaphysis. Two cross-sections can have the same cortical area (mass),

although one as a greater external diameter. The cross-section with the larger diameter will have

considerably higher polar moments of area and polar section modulus; for this reason, cortical

area relative to total cross-section area (%CA) can be a useful measure.
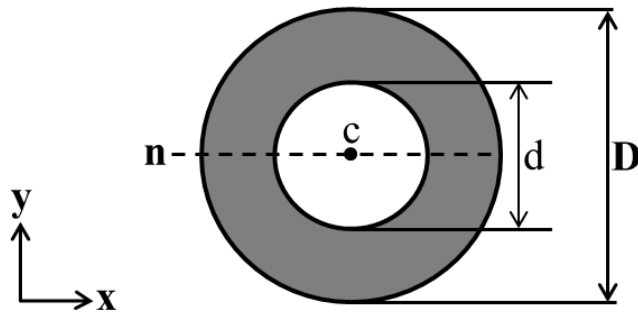
$$TA = \frac{\pi\ (D^2)}{4}$$

$$CA = \frac{\pi\ (D^2 - d^2)}{4}$$

$$J = \frac{\pi\ (D^4 - d^4)}{64}$$

$$Z_P = \frac{J}{0.5D}$$

Figure 3. Cross-sectional properties of bone modeled as idealized hollow cylinder
Abbreviations: c, centroid; D, diameter of outer circle; d, diameter of inner circle; n, neutral axis; TA, total area; CA, cortical area (gray area); J, polar second moment of area; Z_p, polar section modulus

The cross-section shape index (I_{max}/I_{min}), or circularity index, has implications for interpretations of mobility. An index close to 0 would be representative of a circular shaped cross-section, while a much lower or much higher index indicates elongation of the bone.

Unlike the limbs, where biomechanical researchers have focused analyses for the last thirty years, the role of mechanical stimuli on the maintenance of cortical bone in the cranial vault is not well understood. As the calvaria of the cranium experiences minimal loading, the bone is not expected to remodel under the same circumstances that affect the limb bones. Strains are known to be very low in regions not involved in masticatory or nuchal musculature (Peterson and Dechow 2003). For these reasons, portions of the cranial vault that do not include areas of muscle attachment (namely from the temporalis muscle) are examined as bones with minimal mechanical influence.

Human biomechanical studies

Mechanics of bone under known stereotypical loading behaviors

The calculation of cross-sectional geometry (CSG) as described in the preceding section is based on beam theory and the geometry of mechanics. However, the interpretation of variation in these properties in relation to known activity for a given limb segment, for example, requires either experimental data (e.g., Torrance et al. 1994) or observational evidence gathered from individuals with known stereotyped (i.e., repetitious) behaviors. Studies of living humans, then, have provided further insight about the patterns of cross-sectional strength properties associated with particular habitual physical activities. These findings are best demonstrated by studies of high proficiency athletes relative to control (that is, relatively inactive) groups. Some of these studies are summarized here.

A variety of studies have examined general differences in bone properties for specific bones known to be loaded in stereotypical activities. Most of these papers have looked at variation in bone mineral content or bone mineral density in limb elements known to be loaded in athletic activities (e.g., Heinonen et al. 1995; McCulloch et al. 1992; Seeman and Martin 1989). While these types of studies are numerous, as are experimental studies using animal models, relatively few have calculated differences in cross-sectional geometry from humans with known activity patterns, in part owing to the difficulty of obtaining radiographic data from living subjects (Shaw 2008). Yet, these studies provide useful baseline evidence for differences in how bones respond to high frequency and/or intensity of loading; for instance, in a sample of elite young gymnasts, both radial and femoral CSG properties were greater in the athletes versus a control group of non-gymnasts (Dowthwaite et al. 2012).

Studies of competitive athletes also demonstrate particular geometric changes to bone shape with activity. As noted in the previous section, greater bending strength in a specific direction indicates the plane in which the bone incurs the highest bending strains. For example, comparing tibial mid-diaphyseal shape, varsity cross-country runners presented a greater anteroposterior bending strength relative to field hockey players; while the latter had overall greater CSG properties, it did not occur in a dominant plane of loading (Shaw and Stock 2009b). These findings correspond with the unidirectional locomotor patterns of varsity cross-country runners versus the greater abundance of multidirectional loads in field hockey players. An important general finding of this study, though, was that high-mobility activities generally increased CSG properties compared with non-athletes. Moreover, all of the subjects in Shaw and Stock's (2009b) study had started engaging in these activities at young ages, during or before adolescence, and therefore the activities were encountered during primary growth. These results are further reflected in a study of young elite rhythmic gymnasts, adult ex-gymnasts, and a control group, wherein both the active gymnasts and retired gymnasts—who had all started training as juveniles—preserved increased vertebral strength properties over non-athletes (Dowthwaite et al. 2011). The idea that mechanical adaptations acquired during growth confer strength advantages into adulthood is supported by this study.

In addition to comparisons of CSG between groups, contrasts of these properties within individuals have brought significant insight into the different magnitudes of responses that parts of bones (e.g., epiphyses versus diaphyses) or bones within a functional unit (e.g., a limb) have in response to side-biased activities. Investigations of directional asymmetry examine the effects of activity on bone morphology when comparing right and left side elements, where significant differences between sides indicate different loading (and therefore use). These studies are

especially valuable over intergroup comparisons, as asymmetry studies provide researchers with the ability to analyze effects of differential activity levels and patterns because genetics, hormones, climate, nutrition, and subsistence are controlled for within an individual (Auerbach and Ruff 2006).

Because the upper limb in humans is decoupled from the preferred form of locomotion (bipedalism), one of the most widely recognized examples of directional asymmetry in humans is the demonstrable lateralized preference for use of the right upper limb. Tying specific handedness to asymmetric differences in bone, however, is difficult, as fine motor tasks often associated with lateralization will not affect the CSG of arm or forearm bones; only gross motor tasks would likely have an effect (Auerbach and Raxter 2008). Nevertheless, asymmetries in the human upper limb consistently show a right side bias for humans (see Auerbach and Ruff 2006 for a review; Lazenby et al. 2008b). In particular, the dominant side is often associated with greater strength properties and dexterity (Shaw 2011), which are reflected in the diaphyseal CSG of the metacarpals, the forearm bones, and the humerus.

Furthermore, these studies of directional bilateral asymmetry have been important for demonstrating that regions within limb bones show different levels of variability (again, since other endogenous and exogenous factors are accounted for within an individual). When comparing three types of bone measurements, long bone lengths, articular dimensions, and diaphyseal breadths, there is a consistent ranking in the amount of asymmetry between sides. Long bone lengths demonstrate the least variable measurement between sides, followed by articular dimensions, and diaphyseal breadths being the most variable (Auerbach and Raxter 2008; Auerbach and Ruff 2006). In fact, this pattern may be widespread among primates (Reeves et al. in review), indicating that these three locations are under different degrees of canalization,

likely to minimize functional restrictions. These findings suggest that the diaphyses adapt to increases in load bearing with increases in cortical bone structure. While articular sizes are relatively more canalized, with respect to adaptation of their linear dimensions (and likely surface areas), it has been shown that the underlying trabecular structure adapts substantially to the mechanical stimuli (Lazenby et al. 2008a).

Again, studies of athletes with highly stereotyped lateralized behaviors have illuminated these patterns. Studies of racquet sports players show that the dominant upper limb displays significantly greater measures for CSG properties like *I* and section moduli than non-athlete control groups. Higher humeral and ulnar cortical strengths were found in dominant upper limbs of cricketers (Weiss 2003) and racquet-ball players (Kontulainen et al. 2003), relative to non-dominant upper limbs. When comparing these results with those of participants engaged in bilateral upper limb activities, such as swimmers and rowers, the upper limbs show increased CSG properties relative to control groups, but no significant asymmetry (Shaw and Stock 2009a).

Living subjects studies versus past human studies

The results of investigations into the functional adaptation of bones to particular stimuli in living subjects allow biological anthropologists to extrapolate and reconstruct human behaviors in the past based on observed bone morphology (Bridges 1995; Ruff 1994; Ruff 2008a; Weiss 2003). The CSG of long bone diaphyses has been used to draw inferences about mobility, body mass, subsistence strategies, habitual behaviors, and combinations of these characteristics among human groups (Shaw and Stock 2009b; Stock and Pfeiffer 2001; Wescott 2006). In general, these and other researchers argue that increased bone strength is indicated by

greater CSG properties, and have associated this exclusively with differences in physical activity. Dietary differences, though, have only been taken into account with regard to variation in the effects of specific subsistence activities, such as grinding (Bridges et al. 2000) or use of specific tools like spears (e.g., Shaw et al. 2012). It has not been shown if differences in nutrition, other than extreme nutritional stress (e.g., the Kulubnarti; van Gerven et al. 1985), can influence the variation in bone CSG properties observed in past human populations.

In some cases, studies of the skeletons of past human groups reveal patterns not evident in living human groups. This is especially true for trends in changes to bone CSG properties over human evolutionary time. For example, Ruff et al. (1993) showed that diaphyseal strength in modern humans has substantially decreased compared to archaic *Homo*, while articular dimensions were not significantly greater. Shaw and Stock (2013) also show that the variation in tibial cross-section properties for modern competitive athletes and Holocene foragers are consistent with known or inferred activity. These findings indicate that studies of modern human physical activity can be applied to the fossil record to infer behavior and activity levels of the past. Lieberman (1996) investigates why modern humans have thinner bones and skulls than archaic humans, suggesting that higher levels of sustained exercise relative to body mass could be the cause. The trend has been for modern humans to become less robust (more gracile) than in the past. Obesity may be reversing this trend.

Biomechanics of obese mobility

Body mass is a significant source of mechanical loads on the skeleton (Ruff 2000; Shaw 2010). Though body mass has a stronger association with loading in the lower limbs (except for crawling infants), it may be difficult to parse out whether greater CSG properties occur as a

result of systemic metabolic effects instead of increase in bone resistance to higher loads incurred with increased body mass, both overall and within limbs. Presumably, obese individuals will not be engaged in high activity levels, though it is not known in this study (see Chapter 6) whether individuals were highly active prior to becoming obese, and therefore their bones retain morphology that formed earlier in life in association with more active lifestyles. Extrapolating from the findings of the experimental models and exercise studies, it is hypothesized that while both an obese individual and highly active individual should demonstrate relatively thicker diaphyseal cortices in the load-bearing long bones, the bone shape of the highly active individual would be expected to be elongated in a particular direction (unless the individual was a rugby or field hockey player), as a result of bone functional adaptation to habitual activity in a particular plane. Ambulatory obese individuals might be expected to present with a more circular distribution of the cortex (Moore 2008), as the primary response to loading would be in axial compression; cortical areas may be similar, but perhaps bending and torsional rigidity and strength are not as great due to less dynamic movement.

The largest loads on bones, and therefore the largest bone stresses, come from muscle action during movement (Martin and Burr 1989; but see Shaw 2010). As obesity increases body mass, lever-arm effects increase the forces necessary to move the body (Frost 1997). It takes more muscle strength to move an obese individual than one of non-obese body mass. Therefore, obese individuals should present with increased bone strength properties in bones resisting body mass (i.e., the lower limb) and, to a lesser magnitude, non-body mass bearing bones (i.e., the upper limb), relative to individuals of normal body mass who are not known to engage in rigorous physical activity. In all cases, both body mass and muscle activity will have influences on the CSG properties of the lower limb.

The femur and tibia are often the primary focus of load bearing studies (see studies listed above), as the fibula is generally not considered to be a load-bearing element. Experimental studies have argued that the fibula may experience between 7% and 30% of the bending load found in the tibia (Goh et al. 1992; Skraba 1982), and so it has minimal mechanical relevance. However, a study by Marchi and Shaw (2011) argued that variation in fibular robusticity among human groups does relate to different mobility patterns in past groups. Thus, the role of the fibula is likely minor, but still may be diagnostic with respect to loading behaviors. The fibula is included in the present study to ascertain two possibilities. First, it could be that the fibula experiences an increase in loading as a result of biomechanical compromises in obese individuals; this is based on indications from the work by Marchi and Shaw. On the other hand, the fibula could remain minimally weight bearing and, therefore, it would serve as an additional bone not known to be significantly loaded by body weight (e.g. more like the humerus or radius).

There is a well-established association of musculoskeletal disorders with obesity, especially osteoarthritis (OA), and their effect is especially present on articulations. Obesity has long been known to be correlated with morphological changes in joints, and it is the most predictive risk factor for osteoarthritis, after age (Runhaar et al. 2011). OA is the most common type of arthritis, affecting millions, most commonly in the weight bearing joints such as the spine, hips, knees, and feet. While the exact reason for onset (correlated with age) of OA in non-obese individuals is unknown, it has been hypothesized that too large and too frequent strains placed upon the joint surfaces causes them to deteriorate more quickly (Vignon et al. 2006). This is especially important given the information reviewed above concerning the normal lack of plasticity in external articular shape and dimensions in response to mechanical loading (Auerbach and Ruff 2006; Lieberman et al. 2001).

Changes in joint morphology associated with obesity and OA are typically regarded as pathological responses to increased compressive loads (Eckstein et al. 2002; Frost 1997; Lim and Doherty 2011; Pereira et al. 2011). When viewed this way, osteoarthritis is a disease of mechanics, whereby a combination of anatomy (e.g., malalignment, trauma, or joint instability) and excess loading cause damage to the joint (Felson 2013). As a result of excessive mechanical demands, the joint capsule degrades, thinning the cartilage cushion between bones, and narrowing the joint space. All of these changes in joint morphology are painful for an individual, and mobility is often reduced. In the case of obesity, the load bearing joints are compromised due to the increased load on the joints themselves, and weight loss by engaging in physical activity is usually prescribed for treatment (Bennell and Hinman 2011; Messier 2010). Individual joint alignment and mobility should also be considered; if individuals with OA succumb to the pain and reduce their mobility, the lack of mechanical loading should inhibit functional adaptation; without dynamic loading bone cannot functionally adapt, regardless of body mass. An additional concern would be that obese individuals could further increase the energy imbalance, if the joints were so painful as to inhibit preference for physical activity as a weight loss prescription. Excessive mechanical stresses are a risk factor for OA, while at the same time exercise is a protective factor usually recommended for the OA patient (Vignon et al. 2006).

While increased joint dimensions would accommodate greater resistance to increased axial compressive forces, it remains unclear whether human joints can functionally adapt to excessive loading after skeletal maturity. In especially severe cases, the joints become particularly compromised, and the inflammation at the site likely localizes a signal for bone apposition responses, resulting in extra bony deposition in the form of osteophytes or bone spurs. Therefore, it will be important in this study to quantify joint size in both high load-bearing

regions (e.g., the knee) and lower load-bearing regions (e.g., the shoulder) of obese and normal weight individuals, in order to assess in what ways joint size relates to greater body mass.

Scaling

In order to identify significant differences in bone morphology, such as the ones in the studies mentioned, it is necessary to control for the effects of body size and shape (Ruff 2000). This is because differences observed between groups attributed to variation in non-scaled cross-sectional geometric properties may spuriously lead to conclusions about differences in activity, when the real differences were related to differences in bone lengths and/or body masses, as lever length and loading mass have significant effects on CSG properties. In some past research (e.g., Bridges 2000), the tendency has been to standardize these measures by bone length alone, as bone lengths are equal to lever arms. However, this only accounts for the length of the beam under loads; in order to appropriately interpret CSG measurements, body mass must be accounted for as well, as it may significantly vary among groups and thus erroneously contribute to differences in CSG properties attributed to usage variation.

In this study, the individuals sampled have associated anthropometric data, which includes reported body masses. A question emerges, however, about *which* body mass should be used as a scaling factor. Actual masses are more likely an accurate proxy for the mass the individual had close to death than for years prior; for some individuals, a non-obese body mass may have been present during most of life. Without medical records, this cannot be ascertained, and so an alternative form of estimating "lean" body mass must be used. Femoral head diameter, which has a mechanical relationship with body mass, is commonly used to predict living body masses by linear regression (Ruff 2002b; Ruff et al. 1991; Ruff et al. 1997). As shown by Ruff

(2007), femoral head size likely does not change in concert with actual body mass during ontogeny, even though it matches body mass at the end of femoral growth (i.e., around age 18); thus, the mass predicted from femoral head size may be an "ideal" or "programmed" body mass. As femoral head size is considered especially stable despite changes in mechanical loads (Lieberman et al. 2001), even though an examination of articular size differences is part of this study, it may be used as an estimator. Further consideration of the use of femoral head estimated body masses over recorded body masses may be found in the Methods (Chapter 6). An alternative would follow Ruff (1994) suggestion that bi-iliac breadth may be used to accurately estimate body mass in conjunction with stature (the "morphometric" body mass estimation method; Auerbach and Ruff 2004; Ruff et al. 1997). As this method requires both rearticulating and measuring the pelves, in addition to acquiring reliable statures, it is not favored in this study. Furthermore, in an investigation as to which standardization methods perform best, Stock and Shaw (2007) recommend standardization of CSG properties to bone length and a proxy for body mass (both femoral head and bi-iliac breadth estimation perform well).

Dimensions that must resist loading due to mass should account for both mass and lever arm length; it is less certain whether bones not directly experiencing body mass loading should also incorporate body mass as a scaling factor. However, current consensus among researchers (Ruff 2000; Stock and Shaw 2007) is that cross-sectional areas (CA, TA) in both the upper and lower limb should be standardized by body mass, while moments of area for both limbs should be standardized by the product of body mass and maximum bone length (representing the moment arm). Once the differences in body size and shape have been taken into account, then the measures of CSG can effectively be compared within and between groups.

Chapter Summary

Skeletal morphology changes over the lifespan of an organism, responding to maintain functional integrity within and between elements. Functional adaptation of bone occurs with respect to the mechanical loading regimes encountered. Dynamic loading of bone results in localized cellular responses that induce bone deposition, while prolonged unloading signals for bone resorption. When engineering beam theory is applied to long bones, diaphyseal cross-sectional geometric properties can be calculated, providing a means of quantifying bone strength with respect to various modes of mechanical loading (Figure 2). Experimental data and studies of living humans engaged in habitual, stereotyped (sometimes lateralized) behaviors (i.e., competitive athletes), have provided a strong basis for interpreting human behavior from skeletal remains. Body mass is also known to be a significant source of mechanical loads on the skeleton, as is evidenced especially in the morphology of the bones bearing most of the load (i.e., femur and tibia). Chapter 4 will explain another set of stimuli known to affect bone morphology.

CHAPTER 4

NEUROENDOCRINE-METABOLIC STIMULI OF FAT AND BONE

The focus of this study is on the mechanical properties of bone throughout the skeleton, as reflected in the cross-sectional geometry of the diaphysis and size of articulations, and as reviewed in Chapters 2 and 3, bone mass is regulated through remodeling, a balanced two-part process beginning with osteoclastic bone resorption followed by osteoblastic bone formation. Yet, as also noted in Chapter 2, this process responds to and is mediated by a number of factors, including activity, estrogens, androgens, vitamins (namely B_{12}, C and D), growth factors, and various systemic hormones. Chapter 3 considered the effects of activity on bones—mostly of the appendicular skeleton—in the absence of these other factors. Given their importance, both in normal bone remodeling and function as well as a result of abnormal physiology (e.g., the effects of obesity), more detailed consideration must be given to the non-mechanical factors that shape bone.

The influences of these factors occur at different scales, but may generally divided into mechanical and metabolic variables. Mechanical loading (see Chapter 3) has been shown to influence changes in CSG properties locally, meaning that specific tasks will affect the bones that experience loading to perform that activity. However, neuroendocrine-metabolic stimuli have been associated with systemic changes in bone mass (Harada and Rodan 2003; Lee et al. 2007a; Reinehr and Roth 2010) and the normal ossification of skeletal elements (Brickley and Ives 2008; Smith et al. 2010). Most of this research has only emerged since the 1990s, and thus continues to be a focus for new studies and discoveries; it is a rapidly changing field. A

fundamental concept that consistently and fundamentally underlies this research is that bone is threshold-driven (Forwood and Turner 1995). This idea has its roots in the Utah Paradigm, or mechanostat hypothesis, which was the fundamental paradigm that bone responds to varying activity thresholds for deactivation and activation of bone remodeling or modeling—that is, the basis for bone functional adaptation (Frost 2000).

Given the increase of expression of some neuroendocrine-metabolic factors (see below), it may be that these likewise cross a threshold between normal body mass and obesity, which in turn affects the size and shape of bones both as a result of and independent of mechanical loading. Recent research, for example, has shown that exercise induces the release of hormones (such as growth hormone, GH) throughout the body. The circulation of this hormone may interact with the signaling mechanism involved in bone functional adaptation. Lieberman (1996), in fact unintentionally demonstrated this experimentally by exercising genetically identical armadillos and sheep on treadmills. While there was an expected increase in cortical thickness in the load bearing bones of the limbs, there was also an increase in cranial vault thickness. The cranial vault was not subjected to differential loading in his study, and as it does not support body mass, its changes may be associated with the hormonal changes (such as increased GH) associated with the exercise. Likewise, other hormones such as leptin and estrogen have been implicated in skeletal bone regulation. Levels of these hormones vary as a result of adipose tissues and/or body mass and contribute to greater CSG properties in the skeleton in regions beyond the load-bearing anatomy. This chapter considers these factors further, especially in light of the aims of this study (see Chapter 5).

Endocrine and Systemic Signaling

Aptly named from the Greek "endo" meaning inside and "crinis" for secretion, the endocrine system is responsible for releasing various hormones, which then function as chemical mediators, communicating with tissues throughout the body. This system is composed of glands (e.g., pituitary, hypothalamus, thyroid), which are activated by the nervous system or other chemical factors (e.g., adipokines), and which produce and secrete particular hormones into the bloodstream to maintain normal functioning of metabolism, growth and development, tissue function, sleep, and mood (Lee et al. 2007b; Valassi et al. 2008). These hormones interact directly with cells in target organs and tissues, locally or systemically, or affect the production and release of other chemicals. In this manner, the central nervous and endocrine systems communicate with tissues throughout the body to maintain homeostasis.

Prior to the finding of endocrinal systemic regulators that affect the control of bone remodeling, researchers regarded only local cell-cell interactions through autocrine or paracrine mechanisms as the primary means for achieving bone remodeling (Ducy et al. 2000). The autocrine system involves local signaling in which a cell secretes a hormone that binds to receptors on the same cell to change cellular functions, while paracrine signaling is characterized by cell signaling in which the target cell is near the signal-releasing cell, altering the behavior or differentiation of those cells (Kim and Moustaid-Moussa 2000). The paracrine and autocrine systems at most affect adjacent cells. In contrast, the endocrine system releases hormones that target cells throughout the body, resulting in a systemic response. Hormones can also serve multiple functions at different levels of expression, with unique roles and responses in both the endocrine and paracrine systems, for example. It is difficult to disentangle the interaction of signals from all of the systems of the body, as cardiovascular, musculoskeletal, nervous, and

immune systems all communicate with each other via hormones, and are collectively tied to the chemical signaling of the endocrine system. Until recently, perhaps the most overlooked signaling, though, comes from adipose tissue.

Types of Adipose Tissue

As reviewed in Chapter 2, there are two major types of fat found in humans: white adipose tissue (WAT) and brown adipose tissue (BAT). The latter has long been considered restricted in its expression to infancy and childhood, though more recent studies (see Chapter 2) have shown that it persists in adults. Both tissue types store energy in the form of fat droplets, and both have thermogenic physiological properties, though these differ in their proportions; WAT stores more fat, while BAT is the originator for non-shivering thermogenesis. As indicated in Chapter 2, both also serve endocrine functions, though the biochemical products and adult physiological function of BAT are still under active investigation (Cannon and Nedergaard 2003; Villarroya et al. 2013). Thus, though BAT likely plays a role in the development of obesity, almost all research has focused on WAT and its endocrinal role.

Adipose Tissue as an Endocrine Organ

As adipose tissue has long been studied for energy storage and thermoregulation properties, the investigation of it as an endocrine organ is in its infancy (Dubern and Clement 2012; Galic et al. 2010; Harwood 2012; Poulos et al. 2010). While the research regarding the function of adipose tissue as an endocrine organ is still not completely understood, research consistently shows that adipocytes sense, regulate, and distribute systemic signals in an effort to maintain energy equilibrium in the body (Vazquez-Vela et al. 2008). Secretion of adipocyte-

derived hormones, adipokines (also referred to as adipocytokines), result in regulation of normal development, metabolism, eating behavior, fat storage, insulin sensitivity, hemostasis, blood pressure, immunity and inflammation (Eringa et al. 2012; Falcao-Pires et al. 2012). Among these chemical factors are leptin, adiponectin, PAI-1, and MCP-1, which collectively affect weight loss and weight gain, as well as associated physiology (e.g., inflammation and appetite). In addition to the endocrine system, this regulation of energy occurs through the paracrine and autocrine systems, wherein communication occurs between adipocytes and other cells found in the brain, liver, musculoskeletal tissues, and pancreas (Harwood 2012; Kim and Moustaid-Moussa 2000; Lee et al. 2007a). White adipocytes are known to secrete adipokines and other proteins for interaction with peripheral tissues and systems (Carlton et al. 2012; Lumeng 2013; Vazquez-Vela et al. 2008).

The focus of this study is on the hormonal interactions with and functions of adipocytes on cells of the musculoskeletal system. Adipose tissue is widely dispersed throughout the body, found both surrounding bone and within marrow cavities, and also is highly vascularized. Thus, it has far reaching physiological effects on bone, both as an endocrine organ and through paracrine mechanisms.

Hormonal Regulation of Bone Cells

As indicated above, the link between the skeleton and energy metabolism is a recent finding (Ducy et al. 2000; Reinehr and Roth 2010). Importantly, many of the homeostatic functions of the endocrine system also directly or indirectly affect skeletal cell regulation, repair, and remodeling. Experimental and clinical research demonstrate a relationship between various hormones and the maintenance of overall bone mass (Bellido and Hill Gallant 2014; Devlin

2011; Thomas et al. 2001; Wang et al. 2011; Wiren et al. 2008), through a series of cell signaling pathways (Antuna-Puente et al. 2008; Lago et al. 2009; Leal Vde and Mafra 2013; Raucci et al. 2013; Zhuang et al. 2009). These are discussed in more detail below, especially in relation to obesity. Table 2 highlights and explains the role(s) of selected hormones known to affect bone cells.

Adipokines

As briefly touched upon above, energy maintenance is essential for the survival of all animal species because, in the absence of energy reserves, an organism faces death. Adaptations for storing energy as fat are especially essential for species survival in times of famine. In the past, humans more often encountered starvation as the main pathological condition with respect to energy imbalance (Prentice 2005b). However, in the past several decades, obesity is increasingly becoming the primary pathological response, resulting from the abundance of calories (but not necessarily adequate nutrition) available in modern industrialized countries (Dinsa et al. 2012; Kanter and Caballero 2012; Wells et al. 2012). As the incidence of obesity has risen, so too has research to understand the myriad functions of adipokines.

The sole function of adipose tissue was believed to be energy storage, until the discovery of the obese gene and its product, *leptin,* in the mid-1990s (Galic et al. 2010; Lago et al. 2009). This discovery was the first to indicate a signaling molecule (leptin) could be produced by adipocytes, functioning in a negative feedback loop, from production in adipose tissue to the satiety center in the hypothalamus (the arcuate nucleus), to regulate food intake, body adiposity, and energy stores (Zhang et al. 1999). Further research on this hormone has indicated that once secreted into systemic circulation, leptin functions as a regulator of energy utilization & storage,

Table 2. Hormones and their known effect(s) on bone cells

Hormone	Produced by tissue or organ	Effect(s) on bone cells	Net effect on bone deposition
Calcitonin	Thyroid C cells	Up-regulates osteoblasts	Increase
		Down-regulates osteoclasts	
Cortisol	Adrenal cortex	Down-regulates osteoblasts	Decrease
		Down-regulates chondrocytes	
		Up-regulates osteoclasts	
Estrogen	Ovaries, testes, brain, adipose tissue, bone, liver, adrenal glands, breasts, placenta	Up-regulates osteoblasts	Increase
		Up-regulates chondrocytes at moderate levels	
		Down-regulates osteoclasts	
		Down-regulates chondrocytes at high levels	Decrease
Growth hormone	Anterior pituitary gland	Up-regulates osteoblasts	Increase
		Up-regulates chondrocytes	
		Up-regulates osteoclasts	Decrease
Insulin-like growth factor-1	Liver	Up-regulates osteoblasts	Increase
		Up-regulates chondrocytes	
Insulin	Pancreas	Up-regulates osteoblasts	Increase
		Up-regulates chondrocytes	
Leptin	Primarily: WAT Also: BAT, YAT, stomach, placenta, skeletal muscle, brain (pituitary gland)	Up-regulates osteoblasts at normal levels	Increase
		Down-regulates bone formation through hypothalamic relay	Decrease
Osteocalcin	Osteoblasts	Up-regulates osteoblasts	Increase
		Up-regulates chondrocytes	
Parathyroid hormone	Parathyroid glands	Up-regulates osteoclasts	Decrease
Testosterone	Testes, Ovaries, Adrenal gland	Up-regulates osteoblasts at moderate levels	Increase
		Up-regulates chondrocytes at moderate levels	
Thyroid hormone	Thryoid gland	Up-regulates osteoblasts at normal levels	Increase
		Up-regulates chondrocytes at normal levels	
		Up-regulates osteoclasts at high levels	Decrease
Vitamin D	Skin, dietary intake	Up-regulates osteoblasts at moderate levels	Increase
		Up-regulates chondrocyte division	

endocrine pathways, bone metabolism, and thermoregulation (Lago et al. 2008; Zhang et al. 1999). Circulating leptin levels serve as a physiological indicator of the energy reserves available to the body, because it is proportional to adipose tissue mass (the energy balance of adipocytes) (Lago et al. 2008). Curiously, individuals with leptin deficiency present with the obese phenotype, although obese individuals have high serum leptin concentrations (Fuqua and Rogol 2013). This finding is suggestive of a leptin concentration threshold, whereby at a sustained high serum concentration, leptin ceases to function properly (leptin resistance). Thus, in obese individuals, the complex regulation of feeding behavior (satiety) and body mass is disrupted (Xie et al. 2013).

Leptin is also a major regulator of bone turnover (Reid et al. 2006), although its specific role(s) in bone remodeling remain controversial; differences in research design, subject selection, and methods between studies have led to contradictory results. Generally, *in vitro* studies suggest that leptin, at normal serum levels, induces osteoblast differentiation (and suppresses adipocyte differentiation), whereas *in vivo* studies indicate leptin signaling is largely mediated by the sympathetic nervous system, resulting in suppression of bone formation and elevation of resorption activity (see Motyl and Rosen 2012 for review). The effects of leptin on bone are complex and differ dependent upon varying serum levels, temporal changes therein, and the interactions with other systemic factors. To the latter point, leptin indirectly affects bone through several pathways.

In addition to its endocrine function, leptin has been shown to play an important role in immune and inflammatory responses, indicating dual functionality as a cytokine and bridging the neuroendocrine and immune systems (Lago et al. 2008). Obesity itself is often referred to as an inflammatory condition, and leptin is generally considered key in the role of

inflammatory/immune response. For inflammatory conditions generally believed to be a result of senescence and degeneration, such as rheumatoid arthritis or osteoarthritis (OA), mechanical factors are thought to be the driving force for the morphological changes (Aspden 2011); however, deletion of leptin or leptin-receptor genes in mice models result in obese phenotypes without an increase in incidence of OA (Griffin et al. 2009). This has important implications when taking into account the mechanical effects of loading and locomotion that would be associated with high body weight; as discussed in Chapter 3, obese individuals select a low velocity gait and maintain similar joint forces to normal weight individuals (Silvernail et al. 2013), and avid rock climbers subjected to extremely high mechanical strains lacked OA in the joints of the fingers (Sylvester et al. 2006). Taken together, these results support the idea that excessive loading is not the only or most important means by which obesity affects pathological skeletal changes (Aspden 2008). The systemic effects of hormones like leptin in the bloodstream could be causing the bony response in autoimmune inflammatory conditions such as OA, rather than or in combination with loading. To this point, adipokines (especially adiponectin) are involved in other obesity-induced inflammatory responses including type II diabetes and atherosclerosis (Kang et al. 2007).

While leptin affects many functions throughout the body, the expression of the adipokine also varies dependent upon several factors including food intake, other circulating hormones, inflammatory mediators, and energy status. For example, leptin levels are positively correlated with insulin levels (Capurso and Capurso 2012; Fulzele and Clemens 2012; Reinehr and Roth 2010) and BMI (Lago et al. 2008), while inversely related with cortisol (glucocorticoid) levels (Henneicke et al. 2011). Interestingly, serum leptin levels also seem to be sexually dimorphic in expression, even after adjusting for BMI (Blum et al. 1997). In general, leptin is inhibited by

testosterone, and increased by ovarian sex steroids (Leder 2010; Michalakis et al. 2013; Wiren et al. 2012).

Gonadal Hormones

Estrogen is also a key hormone for bone mass maintenance in both males and females. Direct estrogen effects on osteocytes, osteoclasts, and osteoblasts result in inhibited bone remodeling, decreased bone resorption, and maintenance of bone formation, respectively (Khosla et al. 2012). Additionally, estrogen can regulate skeletal mechanosensitivity via the estrogen receptor alpha, which serves as mechanosensor in osteoblasts (Devlin 2011). This functionality links the mechanical and systemic factors that affect bone, and could be a source for future investigations of interaction effects.

For females, the importance of estrogen to skeletal homeostasis is best demonstrated by the significant age-related bone loss after menopause (Eastell 2005; Riggs et al. 2002). Aging females experience two phases of bone loss: an initial accelerated phase at the onset of menopause, followed by an extended slow phase of bone resorption (Järvinen et al. 2003). Habitual loading, in the form of exercise, is limited in its ability to maintain or restore bone in postmenopausal women (Wallace and Cumming 2000), resulting in high incidences of osteoporosis in this population (Beck et al. 1992; Riggs et al. 2002). Obesity, though, may attenuate the pattern of osteoporosis in aging females because greater adipose tissue is associated with increased estrogen circulation (Nelson and Bulun 2001). An inverse relationship between obesity and osteoporosis has long suggested a link between the skeleton and energy metabolism, because the inducement of bone resorption by gonadal failure is prevented by the obese phenotype (Karsenty 2006; Reinehr and Roth 2010).

60

Estrogen is also the main bone regulating hormone in males; however, while females experience two phases of bone resorption with advancing age, males only experience resorption similar to the slow phase in females (Riggs et al. 2002). For males, the additional action of testosterone promotes periosteal expansion, and so in part accounts for the larger size and thicker cortices of the male skeleton (Pacifici 2010), especially into advancing years. However, members of both sexes exhibit subperiosteal expansion with increasing age (Ruff and Hayes 1982). While it is clear that estrogen is imperative to bone formation and homeostasis, the mechanisms are still under investigation.

Growth Hormones

Produced in the pituitary gland, growth hormone (GH) plays a prominent role in the growth and development of the skeleton, as well as the maintenance of bone mass, lean body mass, and bone density (Yamanouchi et al. 2004). Children with high GH levels exhibit excessive and rapid growth resulting in gigantism (Mackie et al. 2008). There are also close relationships between GH and estrogens, evidenced by the increase in both hormones at puberty, resulting in a growth spurt, secondary sex characteristics, and epiphyseal fusion (Bolamperti et al. 2013; Soucek et al. 2011). As with estrogen, the secretion of GH declines with age, adding to the reduced bone mass characteristic of postmenopausal females and, to a far lesser extent, older males. In the liver, GH stimulates production of insulin-like growth factor-1 (IGF-1), which then regulates GH production through a negative feedback loop with the hypothalamus (Yakar and Adamo 2012). IGF-1 functions in autocrine, paracrine, and endocrine capacities, and together GH and IGF-1 regulate longitudinal bone growth through the chondrocytes at the growth plate (Nilsson et al. 2005).

Both of these hormones also are involved in the obesity phenotype. In clinical studies, human subjects showed decreased propensities to become obese with the administration of GH (Berryman et al. 2013); therefore, higher serum concentrations of growth hormone inhibit the increase in adipose tissue, both directly (by reducing the addition of extracellular tissues within WAT) and indirectly (by increasing muscle mass and decreased organ fat deposition). Suppressing IGF-1 expression, likewise, will affect the feedback loop it has with GH, and so its overexpression in the liver has the potential to increase the risk of developing obesity, despite the direct effect of IGF-1 on fat oxidation. Therefore, both of these hormones have important roles in the development of healthy musculoskeletal systems, while also suppressing the development of excessive adipose tissue.

Other Hormones

Thyroid hormones function to regulate metabolism, and are involved in skeletal development, acquisition of peak bone mass, as well as bone maintenance and function, both at the initiation and duration of the bone remodeling cycle. Systemic thyroid levels are maintained by a hypothalamus – anterior pituitary – thyroid signaling loop, in synergy with GH, and have different actions before and after maturity. Wojcicka et al. (2013) demonstrated that thyroid hormones exert anabolic actions during skeletal growth and development, but mediate catabolic responses in adult bone, which result in increased bone resorption and net bone loss.

As a calcium and phosphorous reservoir, the skeleton functions to regulate calcium homeostasis. At low serum calcium levels, parathyroid hormone (PTH) signals for the release of calcium stored in the skeleton by increasing osteoclastic bone resorption (Heaney 2003). When serum levels are high, bone takes up calcium stores; any excess is excreted from the body.

Interestingly, PTH is also one of the only FDA-approved treatments for osteoporosis (Pettway et al. 2008). When given PTH continuously, bone resorption increases; however, with intermittent anabolic dosing, osteoblast activity is stimulated, creating new bone and improving the structure of existing bone (Bellido et al. 2013; Chandra et al. 2013; Wojcicka et al. 2013; Yang et al. 2013). Calcitonin, produced by the thyroid gland, is the antagonist to PTH and functions to inhibit osteoclastic resorption and enhance ostoblastic bone formation (Reid et al. 2006; Sisask et al. 2013).

Active vitamin D is also involved in this process, as it primarily functions to mediate calcium levels when dietary calcium levels are normal or low, and does so by enhancing intestinal calcium uptake (Lieben and Carmeliet 2013). Most commonly, the endocrine activity of vitamin D [hormone $1,25(OH)_2D_3$] has been recognized as necessary for the maintenance of healthy skeletal tissue through actions on the intestine and kidney (Anderson et al. 2011). Recently, a direct osteoblastic/osteocytic role for vitamin D has been introduced, though a thorough understanding is still enigmatic. Under the new model, hydroxylation of dietary vitamin D [converting dietary vitamin D, $25(OH)D_3$, into $1,25(OH)_2D_3$] occurs locally within osteoblasts and osteocytes, playing a role in osteoblast differentiation and mineralization, as well as in the regulation of osteoclastogenesis and osteoclast activity (Anderson et al. 2013). These findings have implications for vitamin D supplementation, as a dose sufficient for normalizing (increasing) serum levels and enhancing intestinal calcium and phosphate absorption, may not reach the skeleton, preventing fractures. Anderson et al. (2013) propose future studies focus on adequate supply of $25(OH)D_3$ to bone specifically (rather than focusing on circulating levels). In addition, there are likely interactions between vitamin D and PTH, as both have been implicated in production and inflammation, though this research is ongoing.

63

Glucocorticoids, like cortisol, are produced by the adrenal cortex and are released in response to signaling from the hypothalamus to pituitary gland, vascular system, and finally, adrenal gland; this system is termed the hypothalamus-pituitary-adrenal (HPA) axis, and is important for response to physiologic stress (Rose and Herzig 2013). Stressors activating the HPA axis can be physical (i.e. physical activity) or psychological, resulting in increased cortisol production and activation of the sympathetic nervous system (Fuqua and Rogol 2013). In times of stress, non-essential physiological processes (e.g. ovarian cycle) are suppressed to allocate glucose reserves for core functioning, and glucose levels are raised further by mobilizing stored energy reserves (Hillman et al. 2012). Cortisol also reduces bone formation; when exposed to these hormones in excess or for extended periods of time, bone resorption is accelerated, bone deposition is inhibited, and bone fragility increases (Bellido and Hill Gallant 2014).

As reviewed above, both bone and adipose tissues exhibit related endocrine functions. Just as adipocytes produce leptin, which play a large role in this system, osteocalcin is the bone cell-derived counterpart (Korostishevsky et al. 2012). Furthermore, osteocalcin is produced by osteoblasts and has been found to function in stimulating insulin expression (as well as adiponectin secretion from adipocytes) and decreasing plasma glucose, resulting in improved insulin sensitivity and energy expenditure (Aoki et al. 2011). Once synthesized by osteoblasts, most osteocalcin is incorporated into the bone matrix, but small amounts are released into circulation and are considered a marker of bone formation (García-Martín et al. 2013).

Chapter Summary

Although the general neuroendocrine-metabolic effects of obesity have been identified for the body, no study has yet demonstrated their manifestation, and therefore their effect,

throughout the skeleton, especially at the scale of individual elements and local impacts on their mechanical properties. The common feedback loops between hormones and other factors associated with both adipose tissue formation and bone maintenance, though, argues that there is the potential for obesity to affect the skeleton through up-regulation and down-regulation of the substances reviewed above. The identification of a systemic, partial regulation of bone resorption by adipose tissue suggests a similar mechanism may control bone formation. To this point, many of the hormones listed in Table 2 increase bone deposition by up-regulating (increasing activity) osteoblasts and chondrocytes, or down-regulating (decreasing activity) osteoclasts. These recent discoveries are the basis for the hypotheses set forth in this work, suggesting a systemic effect of obesity on the skeleton resulting from neuroendocrine-metabolic factors.

CHAPTER 5

HYPOTHESES AND RESEARCH AIMS

In light of the background information provided in the prior chapters, the main aim of this study is to investigate whether there are macroscopic differences in bone morphology as a result of obesity, and whether these differences are systemic or region-dependent. To address this question, six skeletal elements (cranial vault, humerus, radius, femur, tibia, fibula) and three joints (shoulder, hip, knee), experiencing varying biomechanical loading regimes are examined. Skeletal elements experiencing the highest levels of mechanical loading are expected to functionally adapt more than those not directly involved in bearing body weight. The first set of hypotheses below address the relationship between excessive body mass and systemic bone deposition. This has not been tested on a human model. The second set of hypotheses establishes the relationship between excessive body mass and articular morphology. It is currently unclear whether degenerative changes are a reaction to increased compressive loads, and whether these changes affect linear dimensions.

Obese individuals present an excellent comparative group to use in assessing these mechanical differences in relation to a known metabolic condition. Skeletal properties are obtained from modern (late 20th Century and early 21st Century) individuals from the William M. Bass Donated Collection, University of Tennessee. The skeletal measurements were then compared within and between individuals identified as obese and those of normal mass. Normal weight obesity (Oliveros et al. 2013; Romero-Corral et al. 2008) could be hidden in this sample, as the percent of total body mass comprised of adipose tissue was not known for individuals.

This caveat is discussed further in Chapter 6 (Methods), but the general criterion used for the categorization of individuals was BMI.

Researchers usually examine *either* mechanical loading or metabolic stimuli in isolation, a tendency reflected in research on the effects of excessive body mass on the skeleton (Aspden 2011). Anthropological studies of obesity and bone morphology have focused only on weight bearing bones of the lower limb and spine (Agostini and Ross 2011; Moore 2008), and therefore only consider the effects from mechanical factors. Yet, as reviewed in the preceding chapters and synthesized in Figure 4, a nascent literature suggests that neuroendocrine-metabolic stimuli associated with bone and adipose tissues also affect bone mass systemically (Frost 1997; Harada and Rodan 2003; Lee et al. 2007a). In contrast, greater mechanical loads increase bone mass and distribution locally, within the skeletal element being loaded, and primarily in the plane of loading (Shaw and Stock 2009a; Shaw and Stock 2009b; Stock and Pfeiffer 2001; Stock and Pfeiffer 2004). Proper interpretation of the effect of either factor (mechanical or neuroendocrine-metabolic stimuli), then, is dependent on the relative influence of each upon the bone properties of interest (Kimmel 1993). Therefore, the relative influence of these factors should be identifiable within individuals by comparing skeletal elements undergoing differing mechanical demands.
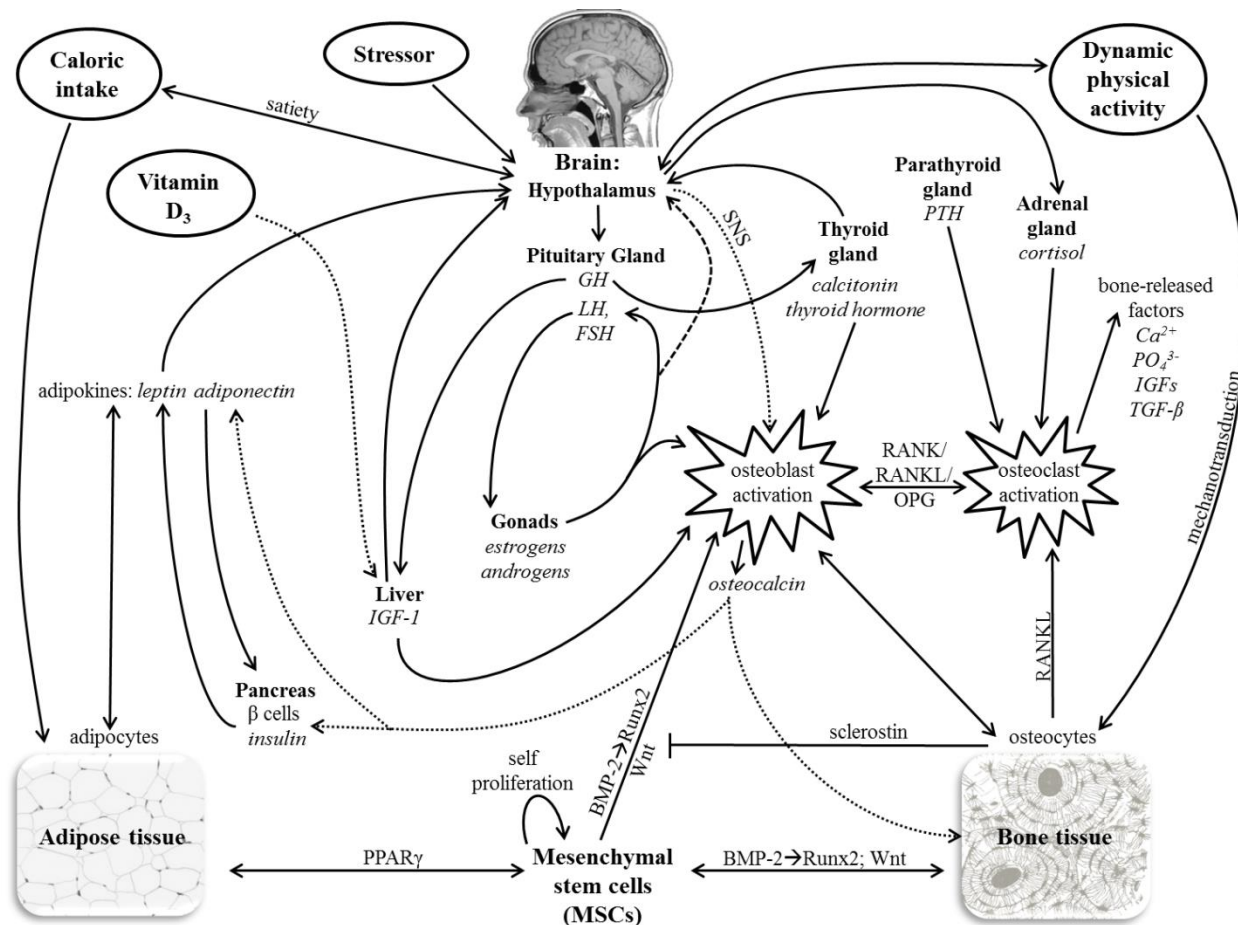
Figure 4. Endogenous (e.g. neuroendocrine-metabolic) and exogenous (e.g. mechanical) factors known to influence bone and/or adipose tissues

A selection of tissues, factors, and their effects on bone and fat are pictured; this list is not exhaustive. Solid, dotted, and dashed lines do not signify differences, but are meant to aid in readability of the figure. Exogenous factors are circled, tissues and organs are bolded, and the specific hormones they produce are italicized. Arrows indicate the directionality of effect (though not specifically the direction of regulation, i.e. up-regulation or down-regulation of the factor), and text along a line indicates a mechanism or factor by which a process/effect is carried out.

Abbreviations: BMP, bone morphogenetic protein; Ca^{2+}, calcium ion; FSH, follicle-stimulating hormone; GH, growth hormone; IGF, insulin-like growth factor; LH, luteinizing hormone; MSC, mesenchymal stem cell; OPG, osteoprotegerin; PO_4^{3-}, phosphate ion; PPARγ, peroxisome proliferator-activated receptor gamma; PTH, parathyroid hormone; RANK, receptor activator of nuclear factor-kappa-β; RANKL, receptor activator of nuclear factor-kappa-β ligand; Runx, runt-related transcription factor; SNS, sympathetic nervous system; TGF-β, transforming growth factor-β; Wnt, wingless-type

68

Hypothesis Set 1: Obesity and systemic bone deposition

Individuals characterized as obese by their BMI will demonstrate systemic increases in bone strength properties relative to individuals with normal body masses. These differences in bone mass and strength would be indicated by a positive relationship between body mass and measures of CSG properties. It is expected that obese individuals exhibit higher cortical strength properties in all skeletal elements (cranial vault, humerus, radius, femur, tibia, fibula) relative to normal mass individuals.

It is also projected that bones experiencing different loading regimes will demonstrate different magnitudes of differences, as some will be more influenced by mechanical loads than others. Bones under the highest loads due to supporting body mass (femora and tibiae) are expected to exhibit the greatest CSG measurements relative to size, with obese individuals presenting with the largest CSG values. Upper limb bones and the fibula are expected to exhibit greater strength properties for individuals of high mass as well, although the magnitude of difference is expected to be less than that for the femur or tibia. While the upper limb would be subject to increased mechanical loading as a result of increased fat mass in the upper limbs, it should not be affected to the same magnitude as the lower limb. It is possible that the fibula bears a greater share of body mass loading in obese individuals, which is why it is included in this study as well.

Cranial cross-sectional properties are hypothesized to exhibit the least difference between groups, although larger values are still predicted for obese individuals if there are macroscopically detectable differences between BMI categories. Adipose and bone tissues are linked by many pathways (Chapter 3 & Chapter 4), which function to provide the skeleton with the bone mass appropriate for the mass of adipose tissue it carries (Reid 2010). If systemic

differences were discovered, the effect in the cranium would be due primarily to effects of neuroendocrine-metabolic stimuli rather than mechanics.

Logic for these hypotheses

Bones comprising the lower limbs are subjected to the highest loads due to their function in weight bearing (support of body mass) and role in locomotion (Ruff 2003b; Ruff 2003c). In active, high body weight obese individuals, these bones would be expected to incur greater loads as a result of high body mass when compared to normal weight individuals. The cross-sectional cortical areas of the femur and tibia would be expected to be highly correlated with body mass, while the upper limbs would be expected to have more independence (i.e., lower correlations).

The upper limbs are not subjected to the strains associated with bipedal locomotion, but are loaded during gross manipulative tasks (Sumner and Andriacchi 1996). Greater muscle and fat mass distribution in the upper limbs of obese individuals may suggest that the cross-sections of these bones would also demonstrate thicker cortices relative to individuals of lesser mass, although the magnitude is expected to be less than that shown for the lower limbs. However, it is possible that the magnitude of differences between the two study groups in cross-sectional geometric properties occur for both the upper limb and the lower limb; this may indicate that these differences are not due to mechanical loading behavior alone.

The cranial vault is also examined here, serving as a bone that is not expected to mechanically adapt to increased body mass. The cessation of the growth of the neurocranium is earlier than the splanchnocranium and postcranial bones, leading researchers to assume less influence by environmental effects in the cranial vault (Hollo et al. 2010). However, if the neuroendocrine-metabolic system regulating bone formation is affected by the effects of obesity,

as potentially indicated in Chapter 4, then this effect would be expected to occur systemically, including in the cortical bone of the cranial vault.

Hypothesis Set 2: Obesity and articular morphology

Previous research indicates that articular measurements are less variable than diaphyseal measurements, but more variable than maximum lengths (Auerbach and Ruff 2006; Reeves et al. in review). It is hypothesized here that articular dimensions of obese individuals will not differ when compared to individuals of lower body mass due to the apparent constraints to mechanical adaptation that occur in the external articular dimensions after maturity. The lack of differences in linear articular measurements is expected when osteophytic or other pathological bony growths are not included in the measurement; however, it is hypothesized that obese individuals will demonstrate higher incidences of osteoarthritis and osteophytosis in all joints, relative to individuals of normal mass due to the pathological response in these areas.

Chapter Summary

Taken together, it is hypothesized that for obese individuals 1) there is an increase in cortical bone mass and strength properties, but 2) no differences in joint size throughout the skeleton, relative to those of normal mass. If the first set of hypotheses is supported, then the metabolic effects of obesity may *augment* skeletal responses to mechanical loading. Furthermore, non-rejection of these hypotheses suggests that there are detectable systemic changes in the skeleton associated with obesity, and that these changes are not solely due to

mechanical adaptation. If the second set of hypotheses is upheld, it would support previous research indicating that articular dimensions are more constrained than those of the diaphysis.

If the hypotheses are not supported, the results still have important implications. Rejection of the first set of hypotheses would indicate that macroscopic changes in the skeleton as a result of obesity are due almost entirely to compensation of the skeleton to increased mechanical forces. That is, results that reject this set of hypotheses will, at best, rule out clinically established metabolic effects on bone due to obesity as an overriding or influential factor over mechanical effects on bone in humans, at the macroscopic level. If the second set of hypotheses is not upheld, two interpretations could be considered; either articular dimensions are adaptable after skeletal maturity (contrary to previous findings), or the sample examined represents individuals who were obese during primary growth, resulting in adaptation of larger articular dimensions.

CHAPTER 6

MATERIALS AND METHODS

This chapter describes the sample used to assess the hypotheses detailed in Chapter 5, the cross-sectional geometric property data and measurements obtained from the sample, and the methods for analyzing those data. The skeletal sample used in this study is introduced first with descriptions of the sex distribution, representation of body mass, demographic profile, and general context for the sample. Methods for obtaining cross-sectional data from these skeletons are then described, followed by a description of the dimensions (introduced in Chapter 3) obtained and their analysis. Data collection and analytical limitations are considered throughout.

Human Skeletal Sample

Sample Source

An experimental study of living humans would be ideal for observing the effect of obesity on tissues throughout the body. However, it is impractical to seek age- and sex-matched human subjects from within one population and ask them to voluntarily subject themselves to unnecessary radiation, the only method by which to assess bone mechanical properties *in vivo*. Additionally, acquiring clinical datasets taken from individuals of known health status was not practical for this study, as the variety of sampling areas necessary for the same individual (crania, upper limb, and lower limb) made data collection unfeasible.

This study instead used the skeletal remains of humans who died within the last forty years and donated their bodies for scientific study. As this sample is not an experimental one, it

is not possible to account for variation in most factors (reviewed in the preceding chapters) that would affect bone, such as physical activity habits, a history of athleticism, genetic variation, or metabolic disorders. Some of these factors, though, are partially accounted for through making comparisons within individuals among elements, as well as data from bones that experience different loading regimes.

The sample of skeletons used in this study was taken from the William M. Bass Donated Collection, curated at the University of Tennessee (UT). This collection of over 1000 skeletons consists of individuals who were born in the 20th century, and provides an opportunity to study individuals of known age-at-death, sex, height, and weight. Most important to this study, the Bass Donated Collection is unique among existing skeletal samples for the large number of documented overweight and obese individuals it contains, encompassing approximately 45% of the total collection (23% overweight and 22% obese)[1]. Since 2000, individuals who donated their remains completed an associated biological questionnaire aimed at gaining more demographic information about the individual (e.g., occupational, athletic, and medical histories).

Selection Criteria and Final Sample

In order to be included in the study, individuals needed to meet certain criteria. Minimally, the individuals used in this study had recorded weight at death and stature at death, known age-at-death and sex, an intact humerus, radius, femur, tibia, and fibula from at least one

---

[1] Percentages are based on individuals of known height and weight at death in the William M. Bass Donated Collection, current as of September 2012.

side, as well as an intact neurocranium. Preference was given to individuals with both right and left long bones, and a biological questionnaire submitted at the time of donation to the Bass Collection. The individuals used in the study have no documented conditions that are known to confound the bony properties of interest. For example, when questionnaires were available (filled out by the individual in life, or family members after death), indicators related to occupation, athleticism, medical history, pathologies, and the like were subjectively evaluated. Individuals with any such confounding factors (e.g. chronic illness, lifetime of manual labor, competitive level of athleticism, etc.) in their biological questionnaire were not included in this study. It is possible that individuals did not report these confounding factors in the questionnaires, and so it is acknowledged that this missing information may have allowed individuals, who would have been excluded had the information been reported, to be included nonetheless.

Once the total available sample was reduced by the criteria explained above, individuals were sorted into categories based on body mass index (BMI). BMI is the measure of weight adjusted for height, and calculated as weight in kg divided by height in m^2. BMI has gained favor for use in clinical studies as a proxy for fat mass, as it is an easy measurement to obtain non-invasively and without skinfold data. The BMI classifications for adults, as outlined by the Center for Disease Control and Prevention (CDC) are listed in Table 3. BMI is an imperfect method for categorizing individuals as obese; these categories are used in this study even though BMI is only a *proxy* for actual fat mass. This is because alternative data for measuring percent body fat were not obtained from individuals when they completed a questionnaire, as well as because, even if individuals self-reported their body mass status, it would undoubtedly be based on clinically-assessed BMI; moreover, skinfold data were not obtained from cadavers prior to inhumation at the Forensic Anthropology Center.

75

It is possible that, using BMI as a categorizing criterion, this study will include non-obese individuals in the obese category, and obese individuals in the normal weight category. For example, an individual with a large amount of muscle mass relative to body fat (e.g., a body builder) could fall into the obese category due to her or his greater mass for height, despite the fact that the greater mass is due to muscle, rather than fat. Likewise, as noted briefly in Chapter 5, in normal weight obesity, individuals have high fat content (i.e., more than 30% body mass) despite BMIs within the "normal" range. These individuals will have the metabolic and hormonal changes associated with obese phenotypes (i.e., they are clinically obese); they will be subject to the same metabolic and hormonal changes as individuals with body mass indices greater than 30 that result from excess fat (Romero-Corral et al. 2008). Individuals who are either "obese" due to high muscle mass, or are normal weight obese are less common than high-percentage body fat and mass obesity, however, and so this study assumes that the BMI categories adequately represent the degree of adiposity. In addition, there are some indications that BMI is influenced by age and sex (Gallagher et al. 1996), and is variable as a means of characterizing the obesity phenotype among humans of different ancestries (Muller et al. 2010).

Thus, while BMI is not an accurate indicator of fat mass in the case of every individual, it is a useful tool when used for studies at the population level. Despite its limitations to precisely reflect fat mass for some individuals, BMI is still the current standard used in clinical studies (Heymsfield et al. 2007), and will be the criterion in this study to designate classes of weight groups among humans. Hereafter, the terms normal, overweight, and obese refer specifically to the corresponding BMI ranges outlined by the CDC (Table 3).

Using the selection criteria, and selecting a sample that is balanced between BMI categories, the total sample selected for this study is comprised of 114 adults (70 males and 44

females). Half of the male sample ($n = 35$) is of normal mass, and the other half is obese. As the overall number of females available for analysis is much fewer than that for males, 22 females fall into the normal mass category and 22 are obese. As noted above, sex, age, height, and weight at death are known for all of the included individuals, and the sample is limited to self-reported European American ancestry ("whites"). Age-at-death categories were used in some analyses for this study, and Table 4 presents the number of individuals in each BMI category by age group and sex.

Table 3. CDC defined categories for BMI

BMI	CDC category
< 18.5	underweight
18.5 – 24.9	normal
25.0 – 29.9	overweight
≥ 30.0	obese

Table 4. Age and sex of the sample by BMI category

Age category (yrs)	Sex	BMI category (N)		Total N	Mean age (yrs)
		Normal	Obese		
31 – 50	Male	15	15	30	43.1
	Female	6	5	12	46.8
> 50	Male	20	20	40	58.0
	Female	16	17	42	64.1
Pooled	Male	35	35	70	51.6
	Female	22	22	44	60.2

Scanning Procedure for Obtaining Radiographic Data

X-ray Computed Tomography (CT) scan technology is regularly used in anthropological mechanical studies of bone cross-sectional properties (e.g., Ruff and Leo 1986; Shaw and Stock 2009b). It is a non-destructive technique for visualizing the internal features within solid objects, and as technology continues to advance, is becoming less expensive and more practical as an analytic tool in the field. Skeletal elements no longer need to be physically sectioned to acquire information about the internal, three-dimensional geometries of the bone. Each scan results in a sequence of images (stored in DICOM image files) that are available for digital segmentation and the creation of three-dimensional models; this sequence of radiographic image slices is stored as a stack in the DICOM files. Typical digital images are two-dimensional and composed of pixels (picture elements), whereas a CT slice image is three-dimensional and composed of *voxels* (volume elements). The scan of a single skeleton may contain upwards to a stack of 2000 slices, stored at the same voxel resolution.

Since 2005, over 600 individuals in the William M. Bass Donated Collection have been CT scanned in collaboration with the Center for Musculoskeletal Research and the UT Department of Biomedical Engineering. The scans used in this study were acquired from a high-resolution GE Lightspeed 16 slice computed tomography scanner, using 0.625-millimeter cubic voxels; each image slice, therefore, has a resolution at 0.625 millimeters. Each skeleton was stereotypically positioned in foam board boxes built specifically for these scanning purposes (Figure 5). The placement of each bone in the same relative location for each scan made subsequent image processing (like segmentation) more manageable. Foam board was chosen because it does not interfere with the imaging of the skeleton (as the foam is radiolucent). The two foam boxes, comprising the entire skeleton were physically stacked; the box containing the

78

cranium (see Figure 5) was longer to allow enough room for the crania to extend beyond the length of the second box, which contained most of the postcrania and was placed on top. The two stacked boxes were entered headfirst into the GE Lightspeed CT scanner.

Figure 5. The placement of skeletal remains in boxes for CT scanning

The resulting DICOM files were processed using digital image manipulation software in order to obtain measurements. ImageJ (http://rsbweb.nih.gov/ij/) was chosen over other visualization software (e.g., Avizo, Amira, Osirix) for this project due to its widespread availability as freeware, and because many freely available plugins have been developed to process images based upon specific research questions of users worldwide. Furthermore, ImageJ supports image stacks saved in the DICOM format, and allows for display, editing, analyzing,

processing, and saving of these images. Exceptional computing power is required to open a stack as large as the full DICOM sequence, so often the full stack was cropped into smaller, more manageable sequences. The specific process for obtaining cross-sectional geometric properties and other measurements from the bones is described in the next section.

Measurements

As noted above and in Chapter 5, five limb bones and the cranial vault were evaluated for cortical bone properties. Both proximal and distal segments of the upper and lower limbs were examined, as differences in mechanical effects have been demonstrated within the limb. This was reviewed in Chapter 3; proximal elements (humerus and femur) have greater variability in diaphyseal robusticity than their more distal counterparts (Stock 2006; Stock and Pfeiffer 2001). Furthermore, several locations along the long bone diaphyses of each element were investigated, as there are also demonstrated differences within a single element (e.g., differences in the sources of mechanical effects on the diaphysis of the femur; Ruff and Hayes, 1983). Articular surface measurements were also investigated because of their functional role at the joints, but relatively lesser ability to adapt in external dimensions to mechanical stresses after maturity (Auerbach and Ruff 2006; Reeves et al. in review). Finally, a novel measurement of cranial vault thickness is central to this study, due to the unique functionality of the vault, which does not include body weight bearing.

For this project, each full stack (including the entire skeleton) was manually cropped in ImageJ, creating five smaller stacks consisting of the following elements: 1) cranium; 2) right and left humeri; 3) right and left radii; 4) left lower limb; and 5) right lower limb. These stacks were then thresholded, which is the simplest form of segmentation, wherein a grayscale image is

processed by digitally isolating the pixels of a specific object (in this case, the bone of interest) from the background. In this process, the grayscale image data is binarized (changed into two states—bone or air); details of this process are explained below. The result of this process allows for a three dimensional reconstruction of the bone to be separated from the background. These isolated, digital visualizations of each element were then aligned, virtually measured, and virtually sliced to isolate the bone sections to be evaluated for cross-sectional geometry.

Diaphyseal Measurements

There are many different thresholding methods available to binarize grayscale images. The Fiji plugin for ImageJ has the option to test sixteen different algorithms[2] simultaneously to determine which best visualizes the data to meet the interests of the researcher. Following this process, the Maximum Entropy method (Kapur et al. 1985) was selected for the long bones, as it was visually determined to be the most effective method for differentiating the intensity of cortical bone, which is more radiopaque (white), from trabecular bone (light grey) and the medullary cavity (black). In a more exhaustive, objective survey, consisting of 40 algorithms, the Maximum Entropy method was ranked second in overall performance for non-destructive image thresholding (Sezgin and Sankur 2004). The thresholding of each of the four extracted stacks representing the postcranium (humeri, radii, left lower limb, right lower limb) for each individual

---

[2] Default (a variation of the IsoData method), Huang, Intermodes, IsoData, Li, MaxEntropy, Mean, MinError(I), Minimum, Moments, Otsu, Percentile, RenyiEntropy, Shanbag, Triangle, Yen methods were all tested. See ImageJ User Guide (http://rsbweb.nih.gov/ij/) for details on each of these thresholding methods.

were processed each as entire stacks, not just a single slices of the stacks, in order to apply the same criteria for extraction to the entire stack histogram.

At this point each bone (left and right sides of humerus, radius, femur, tibia, and fibula), was segmented and saved as a binary stack for future CSG analysis using BoneJ (Doube et al. 2010). A freeware plugin for ImageJ, BoneJ, is a three-dimensional visualization and analysis software package, designed specifically for skeletal analyses. Optional output from BoneJ, when analyzing whole bones, includes fitting ellipsoid or sphere models to bone, identifying three-dimensional moments, the angle of femoral necks relative to shafts, and slice geometry. While the current study is focused on evaluating shape data for cortical bone, it should also be noted that BoneJ has features for analyzing trabecular structure and particles. These types of data are generally from micro-CT scans. Currently, the higher resolution of micro-CT scans can only be achieved for smaller objects (smaller bones or segments of bone). Thus, the scans used in this study did not allow for analyses at the microscopic level.

In mechanical studies, all bones must be oriented in a stereotypical manner to allow comparability of results among individuals (Ruff and Hayes 1983). This is performed so that sections of bones are reliably acquired at homologous locations along the length of the bone, despite individual variation. Typically, when bone is physically oriented, this is accomplished by ascertaining homologous landmarks from metric measurements, which, in turn, are used to orient the element in three dimensions. The goal of this process is to keep the diaphysis of the bone oriented completely perpendicular to a neutral axis that runs the long length of the element. Adherence to this strict alignment minimizes errors that would result if slices were obtained at non-perpendicular planes (that is, if they were skewed), which would distort the values obtained for cross-sectional properties in one or more anatomical planes (Ruff and Hayes 1983).

82

Thus, once each individual bone was segmented, it was virtually oriented prior to cross-sectional analysis. This process was also achieved using the BoneJ plugin. The "Align result" option in the software created a new stack (heretofore referred to as the aligned stack) with the bone centered and rotated so that the principal axes were parallel to the x, y, and z axes of the image stack. Figure 6 presents a single cross-section from the raw DICOM file, the segmented file, and the aligned orientation (x and y axes pictured, bone has been aligned along the z-axis). These were determined based on the shape of the bone, and in many ways are more reliable than manual alignment, as they are not dependent on the accurate measurement of alignment landmarks from linear osteometric dimensions.

CSG properties were computed on the aligned stacks for each bone. BoneJ has the computational power to provide CSG data for every slice. For this analysis, several locations within the aligned and processed stack, representing percentages of maximum bone lengths were extracted. The locations of the sections of interest are listed and depicted by bone element in Table 5; five locations were sampled on the lower limb bones (80, 65, 50, 35, and 20% of maximum bone length; Figure 7), and three sample locations were collected from the upper limb bones (65, 50, and 35%). These percentages were measured from the distal end. At each of the specified locations, the entire suite of CSG output produced by the "Slice Geometry" option in BoneJ was acquired. Table 6 lists and defines the CSG properties used in subsequent analyses (See Chapter 3 for review). Additionally, in order to obtain a measure of total cross-sectional area (TA), the medullary cavity of each slice under analysis was virtually filled (using the "Fill Holes" option in the software) and the "Slice Geometry" procedure was run again.
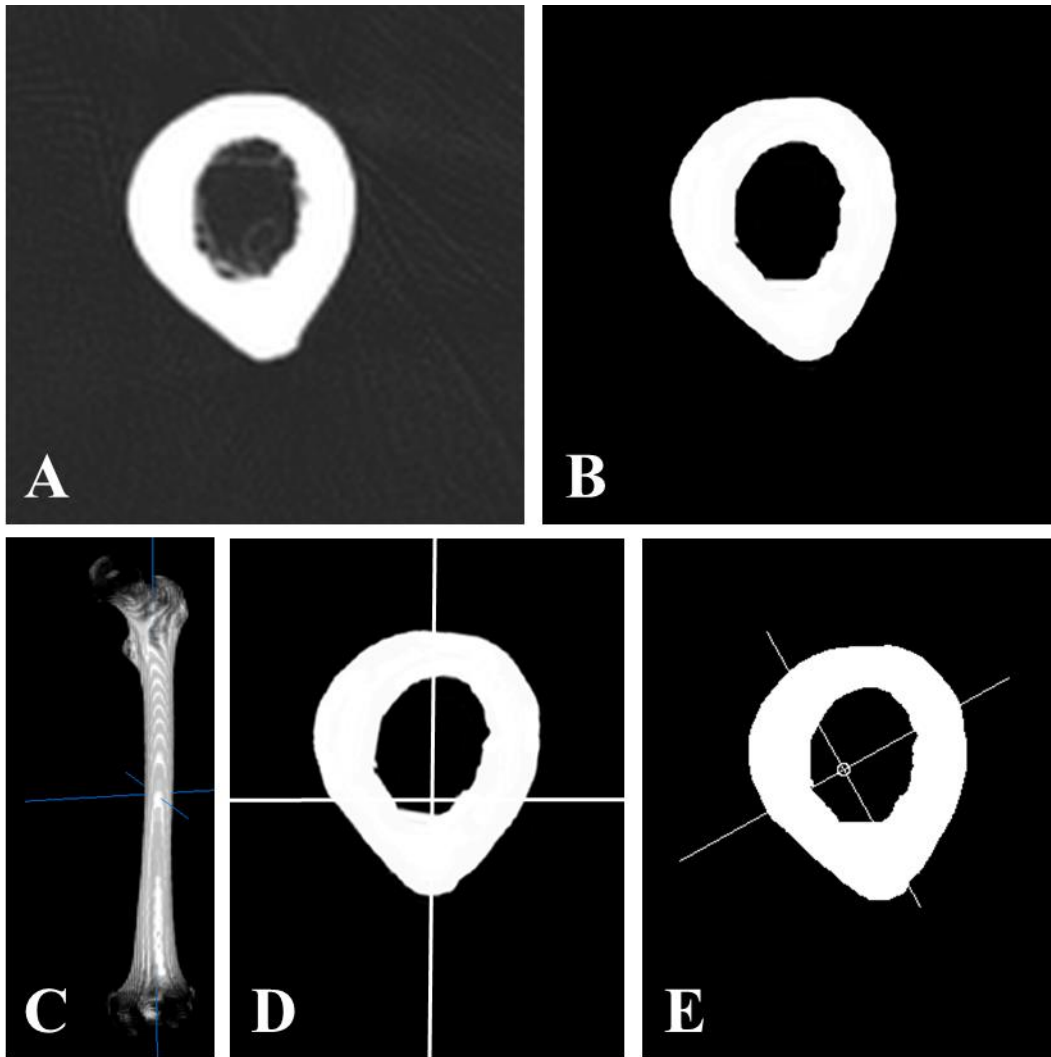
Figure 6. Stages of image processing and alignment for a midshaft femur cross-section
Panel A depicts a cross-section from a raw DICOM image file; B represents the same cross-section after binarizing (thresholding); Panel C shows a slightly oblique view of the whole bone diaphysis after alignment with the principal axes; D shows the same midshaft cross-section from panels A and B after alignment; Panel E shows the same cross-section after acquiring cross-sectional geometric properties, and pictures the centroid (center of cortical area) and major and minor principal axes for the cross-section (about which the second moments of area and section modulus are calculated).

Table 5. Long bone diaphyseal sampling locations used for cross-sectional property analyses

Bone element	Measurement[1]	Visual representation[2]
Humerus	65%	
	Midshaft	
	35%	
Radius	65%	
	Midshaft	
	35%	
Femur	80%	
	65%	
	Midshaft	
	35%	
	20%	
Tibia	80%	
	65%	
	Midshaft	
	35%	
	20%	
Fibula	80%	
	65%	
	Midshaft	
	35%	
	20%	

[1]Percentages measured from distal end of the element.
[2]Bones are not to scale and percentages are approximated.
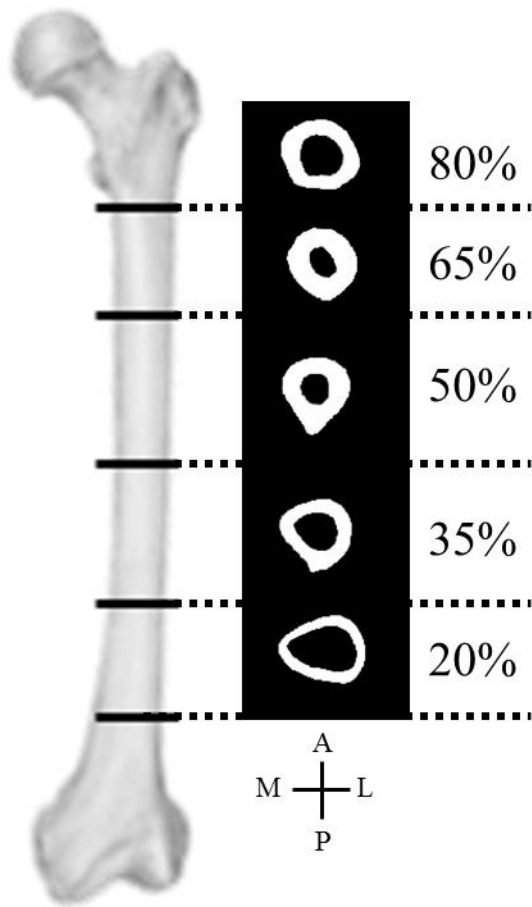
Figure 7. Example of cross-sections sampled for the femur

Table 6. Cross-sectional properties used for analysis

Bone	Measurement Type	Measurement	Description
humerus, radius, femur, tibia, fibula	Cross-sectional properties of bone mass[1]	Total subperiosteal area (TA)	Area within periosteal surface
		Cortical area (CA)	Correlate of compressive strength
	Cross-sectional properties of bone shape[2]	%Cortical area (%CA)	(CA/TA) x 100
		Shape (circularity) index	I_{MAX} / I_{MIN}; values near to 0 indicate more circular cross-section; high values indicate AP elongation; negative values indicate ML elongation
	Cross-sectional properties of bone strength[3]	Polar second moment of area (J)	Sum of any perpendicular second moments of area, correlate of torsional strength ($I_{MAX} + I_{MIN}$)
		Polar section modulus (Z_p)	Torsional and twice average bending strength (J / moment arm)
cranial vault arc	Cross-sectional properties of bone mass and shape[2]	Total subperiosteal area (TA)	Area within the periosteum, including the inner & outer table & diploë
		Cortical area (CA) – inner & outer table	Correlate of compressive strength
		%Cortical area (%CA)	(CA/TA) x 100
		Mean 2D thickness	Mean 2-dimensional (caliper) thickness across the arc
		Maximum 2D thickness	Maximum 2-dimensional (caliper) thickness across the arc

[1] Size standardized by body mass (following Ruff et al. 1991; Ruff 2000).
[2] Unstandardized
[3] Size standardized by the product of body mass and bone length (Ruff, 2008).

Articular measurements

Linear articular measurements of the shoulder, elbow, hip, and knee were examined to address Hypothesis Set 2 (see Chapter 5). The articular measurements are listed in Table 7. These dimensions, as well as bone maximum lengths, were previously obtained by direct measurement of bones using sliding calipers and an osteometric board, respectively. These data were recorded and retrieved for individuals comprising the current sample from the Forensic Databank. A subset of these dimensions was compared against virtual linear measurements taken from the three-dimensional renderings of the bone surfaces within ImageJ. The error between the databank measurements and those obtained from the CT scans was, on average, less than 1%.

Table 7. Articular dimensions representing the shoulder, hip, and knee

Measurement	Description (Martin 1928 number)
Humerus head diameter	The superoinferior length of the humeral head, measured between the margins of the anatomical neck. (Martin Humerus #10)
Femoral head anteroposterior diameter	The anteroposterior diameter of the femoral head, measured with an orientation perpendicular to the long axis of the femoral diaphysis, with the femur held vertically. (Martin Femur #19)
Tibia Plateau Mediolateral (Bicondylar) Breadth	The mediolateral breadth of the tibial plateau, including the medial and lateral cortical projections of the condyles beyond the articular surfaces. This measurement is taken with the axis of the measurement passing through the visually-determined anteroposterior midpoint of the condyles. (Martin Tibia #3)

Cranial Measurements

No convention has been established for collecting cranial vault thickness measurements from CT data. As they are joints and therefore have different properties than the cortical bone of the vault, cranial sutures between bones of the vault are especially problematic, affecting the

accuracy and consistency of measurements of cortical thickness. Additionally, the locations of sutures relative to homologous cranial landmarks (e.g., the arc from glabella to opisthacranion) are not the same among individuals, and therefore obtaining cross-sections at the same location relative to these landmarks may only be homologous among some individuals. On a practical scale, sutures can be difficult to visualize in three-dimensional CT scan renderings in some cases, making their avoidance difficult. For these reasons, this study used a novel method to acquire a homologous cranial bone cross-section, considering the cross-section of an arc rather than a single point along the arc.

The short stack containing the cranium was opened with ImageJ. The cranium was then segmented using the "Minimum" thresholding method in ImageJ. The only observable difference between this method and the Maximum Entropy method was the ability of the algorithm to differentiate diploë from the cortical tables; total vault thicknesses remained the same. The Minimum method was chosen because it generally did not include the gray values of the diploe (unless particularly dense). Choosing this method provides a way to distinguish the cortical area from total area, in this case including diploic trabeculae in the total area but not in the cortical area CSG property calculations.

Once the cranium was segmented, it also required rotation and alignment. Achieving consistent orientation for the crania required variable processing steps, dependent upon the placement of the cranium during scanning. First, the cranium was aligned and cropped along the transverse plane through cranial maximum length (CML), as pictured in Figure 8. This point was used as analogous to the measurement from glabella to opisthacranion (GOL), although that terminology is not used here because the software determined CML based on the geometry of the calvaria. The CML plane could be determined by the "Moments of Inertia" component of BoneJ,

although it was not programmed for that purpose. For this reason, the plane designated by BoneJ that corresponded with the CML plane could sometimes be located off center (not midline). In these cases, it was necessary to download TransformJ, a package of plugins for ImageJ that allows for manual geometrical image transformation and manipulation (Meijering et al. 2001). The TransformJ package was used on 16 crania in order to ensure that the CML occurred along the transverse plane. Once aligned along a transverse plane at CML, each stack was cropped superior to the CML plane, only preserving the cranial vault (Figure 8). Next, a coronal plane perpendicular to the first was located at half of cranial maximum length (50% CML), and the most superior (cranial) 50% of this slice comprised the arc analyzed for all crania. Figure 9 provides a visual representation of the coronal slice of interest with the CML plane and superior 50% plane marked; the point referred to as C is located at 50% of the cranial maximum length at the intersection of the transverse (CML), midsagittal and coronal planes.

Once the arc of interest was extracted, cortical and total areas were acquired, using the same algorithms as those for the diaphyses. Bone geometric properties were obtained both for the bone retaining the diploë, as well as, for total area, the diploë filled in virtually. In this study, the main dimensions of interest for the cranium were the cross-sectional area (cortical area, and total area when the holes are filled), max/min Feret (caliper) widths, and max/mean two-dimensional and three-dimensional thickness of the bone.
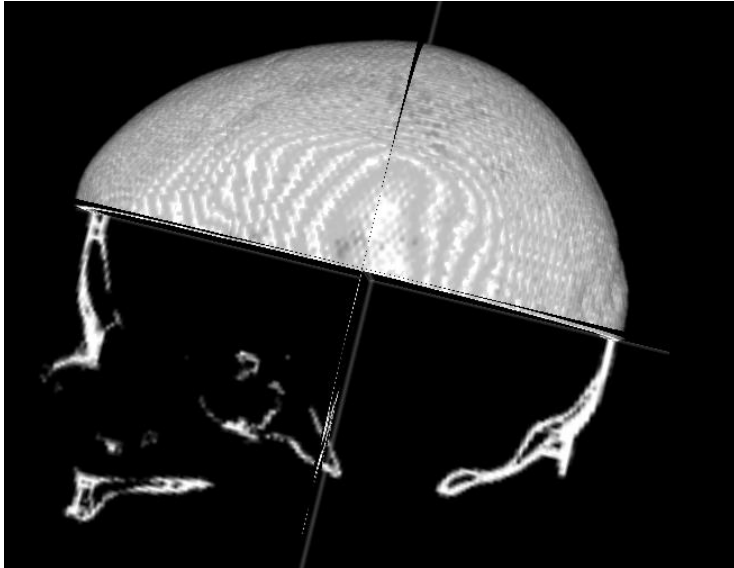
Figure 8. Visualization of cranial vault superior to the section through cranial maximum length (CML)
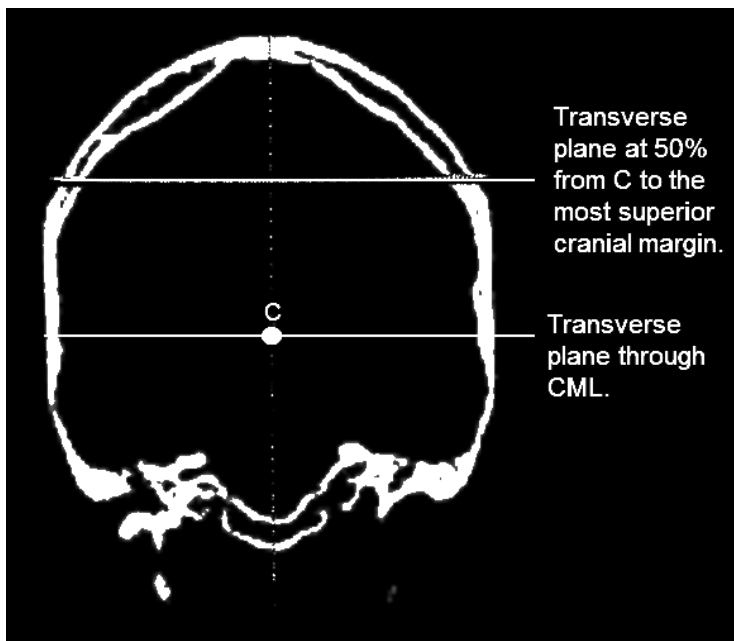
Figure 9. Coronal slice of interest with the transverse planes labeled

Measurement Error

The humeri and femora for $n = 30$ male individuals were completely resegmented and processed to account for measurement error. In addition, $n = 16$ male crania were resegemented to verify reproducibility of the cranial orientation and subsequent measurements. Table 8 presents errors for the cross-section areas of the midshaft humerus and femur, as well as the cranial vault.

Table 8. Measurement errors for humerus, femur, and cranial vault cross-section areas

Bone	Cross-section	Cross-sectional property	Normal BMI group		Obese BMI group	
			n	% measurement error	*n*	% measurement error
Humerus	50%	CA	15	2.59	15	2.64
Femur	50%		15	0.75	15	0.81
Cranial vault	coronal slice		8	1.97	8	2.03
Humerus	50%	TA	15	1.78	15	1.82
Femur	50%		15	0.99	15	1.24
Cranial vault	coronal slice		8	0.86	8	0.83

Measurement Standardization

Appropriate interpretation and comparison of CSG properties depends on accurate size standardization. Where appropriate, cross-sectional properties were size-standardized by estimated body mass, or the product of maximum bone length and estimated body mass, depending upon the measurement (Ruff 2000; Stock and Shaw 2007). As argued in Chapter 3, femoral head size has been thought to be independent of the effects of adult obesity (and

potentially high body masses encountered during primary growth), and so femoral head size remains constant between obese and non-obese individuals. Body mass estimates from femoral head size were chosen for standardizing CSGs so as not to conflate the factor of interest, namely the effect of obesity on the bone structure (see Chapter 7 for statistical results).

In some cases, more than one standardization procedure was used to assess differences in interpretation of CSG. Generally, cortical and total areas (CA and TA) were standardized by estimated body mass; second moments of area (I), the polar second moment of area (J), and section moduli (Z) were standardized by the product of bone maximum length and estimated body mass. The articular measurements were size standardized by stature rather than bone length, following Auerbach and Sylvester (2011), in order to avoid assumptions about allometric effects of scaling factors.

Cranial measurements were not standardized. Because %CA is a ratio variable, it does not need standardizing. The other cranial variables considered in this study represent the 2D maximum and mean thicknesses along the arc of interest, which, while they are gross measurements, they are not subject to the same types of confounding mechanical influences as the limb bones (assuming intracranial pressure is normal).

Analytical methods

All statistical procedures were carried out using IBM SPSS Statistics version 21, with an alpha level of 0.05. Statistical tests were performed on a subset of slices for the left side bones, represented as percentages from the distal margin of the bone (Table 5), heretofore referred to simply as cross-sections. Differences between males and females were assessed at the midshaft

femur as a preliminary step to determine whether or not there was reason to pool the groups or treat them separately.

Cross-sectional areas included in the analysis include total cortical area (CA), total area (TA), and percent cortical area (%CA = CA/TA *100). Cross-sectional geometric properties presented are the polar second moment of area (J = Imax + Imin), the polar section modulus (Zp), and a measure of cross-section circularity (Imax/Imin). The six variables chosen for analysis (CA, TA, %CA, Imax/Imin, J, and Zp) are related to, or are a combination of, various other CSG variables, as explained. In an effort to maximize statistical power, these variables were chosen based on their representation of the larger set of variables listed in Table 1.

The raw data were checked for normality of distribution at each cross-section, for each sex. To explore possible differences in CSGs with respect to BMI category, age, bone, and cross-section location, several multivariate analysis of variance (MANOVA) tests were used. This method was chosen over a series of univariate ANOVAs to reduce the probability of making a Type I error; in this case, the probability of rejecting the null hypothesis when it is actually true. The overall (omnibus) test protects against inflated error probability. Additionally, a series of MANOVAs were chosen over ANOVA to see whether a combination of the CSGs produced a significant main effect, which would mean that the CSGs are more meaningful when taken together than considered separately. Finally, MANOVA tests also take into account intercorrelations among the CSG measurements, which could be an issue as cross-sectional properties are functionally correlated.

First, sex and age effects are addressed. Next, MANOVA tests were conducted for each long bone to assess whether BMI category has an effect on the CSG properties (CA, TA, %CA, I_{max}/I_{min}, J; Z_p was analyzed separately due to its autocorrelation with J). In cases where

94

significant multivariate main effects for BMI category were obtained, post hoc tests were conducted to determine which variables contributed to the overall multivariate significance. From these results, trends and significant patterns could be discerned regarding how obesity differentially affects bones of the upper and lower limb, as well as the differential effects within a single bone (i.e. proximal and distal differences). A repeated measures design was also used to examine within-subjects effects, accounting for the CSG measures at different cross-section locations within the diaphysis of each individual.

Two-factor ANOVA tests were used to examine whether or not there were significant differences in articular and cranial dimensions among BMI categories and age groups. Humeral head diameter, femoral head diameter, and tibial plateau breadth were examined, representing joints of the shoulder, hip, and knee, respectively. A multivariate ANOVA test was also performed for BMI categories, with CA, TA, %CA of the cranium, as well as mean and maximum 2D thickness as dependent variables.

CHAPTER 7

RESULTS

This chapter presents the statistical results for the analyses described in Chapter 6. Cross-sectional properties are presented first, reporting MANOVA results for both within and between bone comparisons with respect to obese and normal BMI categories. Statistics for CA, TA, %CA, I_{max}/I_{min}, J, and Z_p are presented within the chapter. Linear articular dimensions were analyzed with 2-factor ANOVA tests, with BMI category and age category as factors. Finally, the cranium is analyzed with a series of ANOVA tests. Discussion of the results presented here is reserved for Chapter 8.

Cross-sectional Geometric Properties

This section presents the results of analyses comparing the subset of CSG properties described in Chapter 5, and listed above. First, the issue of proper standardization is sorted out, followed by an investigation into whether or not males and females should be examined together or separately. Once these issues have been addressed, CSG properties are compared between BMI categories for within and between bone differences.

Preliminary Exploration of the Data

As indicated previously in Table 6, proper standardization of all CSG properties requires the consideration of body mass. In anthropological studies, observed body mass is often not available, which has led to the development of many techniques for estimating body mass (e.g.

estimations from the femoral head, or from a combination of stature and bi-iliac breadth). In this study, observed body mass is a known variable, although in the case of obese individuals, it could be problematic for size standardization. Paired sample t-tests were used to compare body mass estimated from femoral head diameter with recorded body mass. Results of these pairwise comparisons are presented in Table 9. The mean body masses estimated from the femoral head are not significantly different between the two BMI groups ($p > 0.05$), for males or females; however, recorded body masses are significantly different from estimated body mass for the obese groups ($p < 0.05$). These results suggest that standardization of cross-sectional measurements by observed body mass would be tautological, as it would be standardizing by an effect of interest, namely obesity. That is, standardizing the bone cross-sectional measurements by the recorded, excess masses in obese individuals is likely to mask the increase in cortical bone concomitant with obesity; if obesity leads to increased cortical bone, then scaling this increase with recorded mass would fail to demonstrate the higher cortical areas, even if these two properties are not isometric. For these reasons, estimated body mass is used to standardize the CSGs in this study.

Correlations between age and raw BMI were assessed with a bivariate Pearson's correlation between these two variables. The results for males, females, and the pooled sample are presented in Table 10, which shows individuals' BMIs are independent of age; older individuals neither had higher nor lower masses for their statures. Thus, this indicates that BMI and age can be treated separately in the subsequent analysis.

Table 9. Estimated body mass vs. recorded body mass

Sex	BMI category	Body mass estimated from femoral head		Recorded body mass	
		Mean	Standard deviation	Mean	Standard deviation
Male	Normal BMI group	69.07	5.27	68.36	7.70
	Obese BMI group	**69.87***	5.62	**127.04***	27.91
Female	Normal BMI group	59.57	3.42	56.84	1.41
	Obese BMI group	**61.38***	4.45	**109.75***	29.84

*Significant difference between the estimated and recorded body masses for obese individuals, $p < 0.05$.

Table 10. Pearson's correlations for BMI and Age

Sex	Variable	Correlations	BMI	Age
Males N = 70	BMI	Pearson correlation	1	0.104
		Sig. (2-tailed)		0.394
	Age	Pearson correlation	0.104	1
		Sig. (2-tailed)	0.394	
Females N = 44	BMI	Pearson correlation	1	-0.062
		Sig. (2-tailed)		0.658
	Age	Pearson correlation	-0.062	1
		Sig. (2-tailed)	0.658	
Pooled sample N = 114	BMI	Pearson correlation	1	0.006
		Sig. (2-tailed)		0.946
	Age	Pearson correlation	0.006	1
		Sig. (2-tailed)	0.946	

An initial MANOVA was performed in an effort to determine whether or not the sexes should be pooled or analyzed separately in the remaining analyses. The left side midshaft femur (50%) CSG properties were input as dependent variables (as these have previously been shown to be sexually dimorphic in other studies; Moore 2013; Sigurdsson et al. 2006), with sex and BMI category (normal or obese) as fixed effects. Results of the MANOVA revealed significant main effects for sex and BMI category, while the interaction effect was not significant. For the sex effect, Wilks' lambda test of overall differences among groups was significant ($\lambda = 0.508$, $F = 24.912$, $p < 0.05$). The multivariate significance of sex as a main effect at this particular bone location (left femur 50%) indicates that males and females should be treated as separate groups. For the remaining cross-section analyses, males and females are analyzed separately.

Cross-sectional Properties Between Groups and Within Elements

Each long bone was examined with respect to six cross-sectional properties at each bone location within the diaphysis. Summary statistics are presented by sex, bone, BMI category, and CSG property (CA, TA, %CA, I_{max}/I_{min}, J, and Z_p) in Table 11, reporting means, standard deviations, and mean differences between groups. When there are differences between the BMI groups, the individuals from the obese category generally have greater mean values for most cross-sectional geometric properties; one exception is for shape index (I_{max}/I_{min}), where the normal group often has greater values (indicating AP elongation) than the obese group. Additionally, Table 11 presents univariate significance (p values) for each cross-section location and corresponding CSG value considered separately in a series of one-way ANOVA tests; these are subject to Type I error, and are included only for comparison with the MANOVA and repeated measures ANOVA results that follow.

Table 11. Means and standard deviations (sd), and difference between means (Normal – Obese) of cross-sectional geometry properties by BMI category.

a. **Male Humerus**

Cross-section location	Cross-sectional property																
	Cortical Area (CA)						Total Area (TA)						%CA = CA/TA *100					
	Normal		Obese		Mean	Univar.	Normal		Obese		Mean	Univar.	Normal		Obese		Mean	Univar.
	mean	sd	mean	sd	Difference	Sig.	mean	sd	mean	sd	Difference	Sig.	mean	sd	mean	sd	Difference	Sig.
65%	3.83	0.63	4.09	0.59	-0.26	0.082	5.22	0.87	5.33	0.72	-0.11	0.579	73.98	8.29	77.17	7.83	-3.19	0.115
50%	3.99	0.63	4.29	0.53	-0.30	**0.038**	5.46	0.80	5.72	0.66	-0.26	0.173	73.41	8.30	75.33	6.40	-1.92	0.303
35%	3.81	0.63	4.20	0.56	-0.39	**0.011**	5.84	0.96	6.30	0.80	-0.46	**0.042**	66.41	11.43	67.14	7.42	-0.73	0.763

Cross-section location	Cross-sectional property																
	Cross-sectional shape (Imax/Imin)						Polar second moment of area (J)						Polar section modulus (Zp)					
	Normal		Obese		Mean	Univar.	Normal		Obese		Mean	Univar.	Normal		Obese		Mean	Univar.
	mean	sd	mean	sd	Difference	Sig.	mean	sd	mean	sd	Difference	Sig.	mean	sd	mean	sd	Difference	Sig.
65%	1.26	0.17	1.22	0.13	0.04	0.329	0.86	0.27	0.92	0.26	-0.06	0.341	0.070	0.016	0.075	0.015	-0.005	0.281
50%	1.57	0.19	1.55	0.18	0.02	0.714	0.95	0.24	1.06	0.25	-0.11	0.068	0.075	0.016	0.081	0.014	-0.006	0.107
35%	1.30	0.16	1.31	0.20	-0.01	0.833	1.10	0.27	1.21	0.29	-0.11	**0.005**	0.077	0.017	0.090	0.015	-0.013	**0.011**

Univar. sig., univariate significance of one-way ANOVA for each bone, cross-section location, and CSG separately; significant values (p < 0.05) bolded; sd, standard deviation

Mean Difference = Normal mean – Obese mean; negative values indicate larger obese means.

Table 11. Continued

b.   Male Radius

Cross-section location	Cross-sectional property											
	Cortical Area (CA)					Total Area (TA)					%CA = CA/TA *100	
	Normal		Obese		Mean Difference	Univar. Sig.	Normal		Obese		Mean Difference	Univar. Sig.	Normal		Obese		Mean Difference	Univar. Sig.
	mean	sd	mean	sd			mean	sd	mean	sd			mean	sd	mean	sd		
65%	1.82	0.26	1.84	0.25	-0.02	0.710	2.12	0.30	2.18	0.28	-0.06	0.352	85.03	4.88	84.56	6.09	0.47	0.734
50%	1.92	0.25	1.98	0.23	-0.06	0.318	2.16	0.28	2.23	0.26	-0.07	0.251	88.46	4.10	88.58	5.07	-0.12	0.917
35%	1.88	0.27	1.92	0.23	-0.04	0.551	2.22	0.31	2.29	0.29	-0.07	0.349	84.66	4.84	84.16	6.29	0.50	0.718

Cross-section location	Cross-sectional property											
	Cross-sectional shape (Imax/Imin)					Polar second moment of area (J)					Polar section modulus (Zp)	
	Normal		Obese		Mean Difference	Univar. Sig.	Normal		Obese		Mean Difference	Univar. Sig.	Normal		Obese		Mean Difference	Univar. Sig.
	mean	sd	mean	sd			mean	sd	mean	sd			mean	sd	mean	sd		
65%	1.72	0.33	1.69	0.33	0.03	0.719	0.20	0.05	0.22	0.06	-0.02	0.311	0.023	0.004	0.024	0.005	-0.001	0.288
50%	1.62	0.27	1.61	0.23	0.01	0.797	0.22	0.05	0.23	0.06	-0.01	0.158	0.023	0.004	0.024	0.004	-0.001	0.241
35%	1.91	0.30	1.97	0.29	-0.06	0.386	0.23	0.06	0.25	0.06	-0.02	0.225	0.024	0.005	0.025	0.005	-0.001	0.464

Univar. sig., univariate significance of one-way ANOVA for each bone, cross-section location, and CSG separately; significant values (p < 0.05) bolded; sd, standard deviation

Mean Difference = Normal mean − Obese mean; negative values indicate larger obese means.

Table 11. Continued

c.   Male Femur

Cross-section location	Cross-sectional property																
	Cortical Area (CA)						Total Area (TA)						%CA = CA/TA *100					
	Normal		Obese		Mean	Univar.	Normal		Obese		Mean	Univar.	Normal		Obese		Mean	Univar.
	mean	sd	mean	sd	Difference	Sig.	mean	sd	mean	sd	Difference	Sig.	mean	sd	mean	sd	Difference	Sig.
80%	6.85	1.04	8.01	1.64	-1.16	**0.001**	12.91	2.45	13.74	2.87	-0.83	0.205	52.38	7.41	58.65	9.24	-6.27	**0.004**
65%	7.15	0.72	8.15	1.44	-1.00	**0.001**	9.24	0.90	10.23	1.80	-0.99	**0.005**	77.57	5.86	79.93	5.09	-2.36	0.085
50%	6.72	0.62	7.68	1.32	-0.96	**< 0.001**	8.83	0.85	9.70	1.64	-0.87	**0.007**	76.26	4.86	79.12	4.07	-2.86	**0.011**
35%	5.98	0.68	6.80	1.16	-0.82	**0.001**	9.52	1.08	10.31	1.78	-0.79	**0.031**	63.14	6.38	66.50	6.30	-3.36	**0.034**
20%	5.33	0.80	5.96	1.20	-0.63	**0.012**	13.48	1.87	14.61	2.86	-1.13	0.060	39.98	6.65	42.12	8.42	-2.14	0.250

Cross-section location	Cross-sectional property																
	Cross-sectional shape (Imax/Imin)						Polar second moment of area (J)						Polar section modulus (Zp)					
	Normal		Obese		Mean	Univar.	Normal		Obese		Mean	Univar.	Normal		Obese		Mean	Univar.
	mean	sd	mean	sd	Difference	Sig.	mean	sd	mean	sd	Difference	Sig.	mean	sd	mean	sd	Difference	Sig.
80%	1.51	0.30	1.55	0.25	-0.04	0.597	3.22	0.59	3.95	0.99	-0.73	**< 0.001**	0.15	0.02	0.18	0.04	-0.03	**0.001**
65%	1.31	0.15	1.24	0.14	0.07	0.056	1.90	0.30	2.44	0.58	-0.54	**< 0.001**	0.12	0.02	0.14	0.03	-0.02	**< 0.001**
50%	1.32	0.18	1.30	0.12	0.02	0.668	1.76	0.27	2.24	0.54	-0.48	**< 0.001**	0.10	0.01	0.13	0.03	-0.03	**< 0.001**
35%	1.19	0.10	1.18	0.09	0.01	0.524	1.83	0.32	2.28	0.52	-0.45	**< 0.001**	0.11	0.02	0.13	0.03	-0.02	**< 0.001**
20%	1.42	0.15	1.56	0.17	-0.14	**< 0.001**	2.70	0.53	3.43	0.91	-0.73	**< 0.001**	0.13	0.02	0.15	0.03	-0.02	**0.001**

Univar. sig., univariate significance of one-way ANOVA for each bone, cross-section location, and CSG separately; significant values (p < 0.05) bolded; sd, standard deviation

Mean Difference = Normal mean − Obese mean; negative values indicate larger obese means.

Table 11. Continued

d. Male Tibia

Cross-section location	Cross-sectional property																
	Cortical Area (CA)						Total Area (TA)						%CA = CA/TA *100				
	Normal		Obese		Mean	Univar.	Normal		Obese		Mean	Univar.	Normal		Obese		Mean	Univar.
	mean	sd	mean	sd	Difference	Sig.	mean	sd	mean	sd	Difference	Sig.	mean	sd	mean	sd	Difference	Sig.
80%	5.75	0.78	6.66	1.48	-0.91	**0.003**	13.31	1.79	14.39	1.88	-1.08	**0.023**	43.61	6.25	46.41	8.18	-2.80	0.132
65%	5.70	0.62	6.41	0.71	-0.71	**< 0.001**	8.64	0.97	9.35	0.97	-0.71	**0.006**	66.17	4.97	68.69	5.09	-2.52	0.054
50%	5.35	0.59	6.04	0.61	-0.69	**< 0.001**	6.93	0.75	7.71	0.75	-0.78	**< 0.001**	77.30	4.25	78.43	3.62	-1.13	0.271
35%	4.54	0.44	5.16	0.54	-0.62	**< 0.001**	5.82	0.62	6.59	0.86	-0.77	**< 0.001**	78.30	4.79	78.58	4.94	-0.28	0.823
20%	3.63	0.47	4.27	0.75	-0.64	**< 0.001**	6.53	0.83	7.56	1.69	-1.03	**0.003**	56.10	7.69	57.32	8.50	-1.22	0.554

Cross-section location	Cross-sectional property																
	Cross-sectional shape (Imax/Imin)						Polar second moment of area (J)						Polar section modulus (Zp)				
	Normal		Obese		Mean	Univar.	Normal		Obese		Mean	Univar.	Normal		Obese		Mean	Univar.
	mean	sd	mean	sd	Difference	Sig.	mean	sd	mean	sd	Difference	Sig.	mean	sd	mean	sd	Difference	Sig.
80%	2.48	0.34	2.38	0.48	0.10	0.370	3.71	0.80	4.54	1.06	-0.83	**0.001**	0.17	0.03	0.20	0.04	-0.03	**0.002**
65%	2.43	0.38	2.36	0.51	0.07	0.528	2.06	0.39	2.47	0.44	-0.41	**< 0.001**	0.11	0.02	0.13	0.02	-0.02	**< 0.001**
50%	2.20	0.38	2.13	0.46	0.07	0.491	1.42	0.27	1.78	0.34	-0.36	**< 0.001**	0.08	0.01	0.10	0.01	-0.02	**< 0.001**
35%	1.92	0.35	1.92	0.40	0.00	0.974	0.97	0.18	1.28	0.38	-0.31	**< 0.001**	0.07	0.01	0.08	0.02	-0.01	**< 0.001**
20%	1.29	0.11	1.33	0.26	-0.04	0.454	0.97	0.20	1.37	0.74	-0.40	**0.004**	0.07	0.01	0.09	0.03	-0.02	**0.001**

Univar. sig., univariate significance of one-way ANOVA for each bone, cross-section location, and CSG separately; significant values ($p < 0.05$) bolded; sd, standard deviation

Mean Difference = Normal mean − Obese mean; negative values indicate larger obese means.

Table 11. Continued

e.   Male Fibula

Cross-section location	Cross-sectional property																	
	Cortical Area (CA)						Total Area (TA)						%CA = CA/TA *100					
	Normal		Obese		Mean	Univar.	Normal		Obese		Mean	Univar.	Normal		Obese		Mean	Univar.
	mean	sd	mean	sd	Difference	Sig.	mean	sd	mean	sd	Difference	Sig.	mean	sd	mean	sd	Difference	Sig.
80%	1.19	0.26	1.38	0.37	-0.19	**0.019**	1.51	0.30	1.72	0.38	-0.21	**0.013**	77.97	8.26	79.54	8.85	-1.57	0.484
65%	1.47	0.26	1.66	0.36	-0.19	**0.017**	1.76	0.33	1.97	0.37	-0.21	**0.019**	84.12	6.14	84.50	6.34	-0.38	0.813
50%	1.55	0.28	1.71	0.34	-0.16	**0.044**	1.93	0.36	2.10	0.37	-0.17	0.077	80.52	6.06	81.63	5.86	-1.11	0.466
35%	1.46	0.25	1.64	0.30	-0.18	**0.017**	1.78	0.31	1.95	0.31	-0.17	**0.033**	82.84	6.99	83.50	5.56	-0.66	0.693
20%	1.26	0.21	1.41	0.37	-0.15	0.056	1.52	0.28	1.70	0.37	-0.18	**0.041**	82.47	8.70	81.22	7.98	1.25	0.582

Cross-section location	Cross-sectional property																	
	Cross-sectional shape (Imax/Imin)						Polar second moment of area (J)						Polar section modulus (Zp)					
	Normal		Obese		Mean	Univar.	Normal		Obese		Mean	Univar.	Normal		Obese		Mean	Univar.
	mean	sd	mean	sd	Difference	Sig.	mean	sd	mean	sd	Difference	Sig.	mean	sd	mean	sd	Difference	Sig.
80%	1.95	0.56	2.07	0.67	-0.12	0.428	0.07	0.02	0.09	0.04	-0.02	**0.004**	0.01	0.00	0.01	0.00	0.00	**0.007**
65%	2.31	0.94	2.36	0.83	-0.05	0.825	0.10	0.04	0.13	0.05	-0.03	**0.007**	0.01	0.00	0.01	0.00	0.00	**0.012**
50%	1.85	0.55	1.99	0.62	-0.14	0.362	0.12	0.04	0.15	0.05	-0.03	**0.009**	0.01	0.00	0.02	0.00	0.00	**0.049**
35%	1.66	0.46	1.93	0.78	-0.27	0.109	0.09	0.03	0.12	0.04	-0.03	**0.003**	0.01	0.00	0.01	0.00	0.00	**0.015**
20%	2.25	0.66	2.14	0.48	0.11	0.457	0.07	0.02	0.09	0.04	-0.02	**0.019**	0.01	0.00	0.01	0.00	0.00	**0.027**

Univar. sig., univariate significance of one-way ANOVA for each bone, cross-section location, and CSG separately; significant values ($p < 0.05$) bolded; sd, standard deviation

Mean Difference = Normal mean − Obese mean; negative values indicate larger obese means.

Table 11. Continued

f.   Female Humerus

Cross-section location	Cross-sectional property														
	Cortical Area (CA)						Total Area (TA)						%CA = CA/TA *100					
	Normal		Obese		Mean	Univar.	Normal		Obese		Mean	Univar.	Normal		Obese		Mean	Univar.
	mean	sd	mean	sd	Difference	Sig.	mean	sd	mean	sd	Difference	Sig.	mean	sd	mean	sd	Difference	Sig.
65%	2.64	0.48	2.96	0.46	-0.32	**0.026**	4.04	0.53	4.18	0.52	-0.14	0.378	65.98	13.02	71.71	13.12	-5.73	0.154
50%	2.79	0.48	3.13	0.51	-0.34	**0.029**	4.29	0.41	4.28	0.39	0.01	0.905	65.49	11.98	72.39	10.79	-6.90	0.054
35%	2.77	0.46	3.03	0.57	-0.26	0.095	4.49	0.54	4.41	0.63	0.08	0.657	62.23	10.91	68.99	10.09	-6.76	**0.039**

Cross-section location	Cross-sectional property														
	Cross-sectional shape (Imax/Imin)						Polar second moment of area (J)						Polar section modulus (Zp)					
	Normal		Obese		Mean	Univar.	Normal		Obese		Mean	Univar.	Normal		Obese		Mean	Univar.
	mean	sd	mean	sd	Difference	Sig.	mean	sd	mean	sd	Difference	Sig.	mean	sd	mean	sd	Difference	Sig.
65%	1.30	0.14	1.38	0.22	-0.08	0.156	0.44	0.11	0.53	0.12	-0.09	**0.023**	0.044	0.009	0.050	0.007	-0.006	**0.037**
50%	1.63	0.20	1.71	0.25	-0.08	0.224	0.51	0.09	0.57	0.11	-0.06	**0.049**	0.047	0.007	0.050	0.008	-0.003	**0.019**
35%	1.37	0.10	1.39	0.20	-0.02	0.778	0.53	0.12	0.58	0.18	-0.05	0.286	0.049	0.008	0.054	0.011	-0.005	0.154

Univar. sig., univariate significance of one-way ANOVA for each bone, cross-section location, and CSG separately; significant values ($p < 0.05$) bolded; sd, standard deviation

Mean Difference = Normal mean − Obese mean; negative values indicate larger obese means.

105

Table 11. Continued

g.   **Female Radius**

Cross-section location	Cross-sectional property																	
	Cortical Area (CA)						Total Area (TA)						%CA = CA/TA *100					
	Normal		Obese		Mean	Univar.	Normal		Obese		Mean	Univar.	Normal		Obese		Mean	Univar.
	mean	sd	mean	sd	Difference	Sig.	mean	sd	mean	sd	Difference	Sig.	mean	sd	mean	sd	Difference	Sig.
65%	1.34	0.24	1.48	0.21	-0.14	0.054	1.63	0.23	1.74	0.19	-0.11	0.091	82.48	10.64	82.69	9.84	-0.21	0.951
50%	1.44	0.24	1.57	0.19	-0.13	0.069	1.70	0.22	1.75	0.15	-0.05	0.428	83.15	10.25	87.64	6.66	-4.49	0.140
35%	1.46	0.25	1.51	0.26	-0.05	0.489	1.80	0.25	1.76	0.22	0.04	0.565	80.99	10.49	85.00	8.34	-4.01	0.181

Cross-section location	Cross-sectional property																	
	Cross-sectional shape (Imax/Imin)						Polar second moment of area (J)						Polar section modulus (Zp)					
	Normal		Obese		Mean	Univar.	Normal		Obese		Mean	Univar.	Normal		Obese		Mean	Univar.
	mean	sd	mean	sd	Difference	Sig.	mean	sd	mean	sd	Difference	Sig.	mean	sd	mean	sd	Difference	Sig.
65%	1.64	0.37	1.64	0.30	0.00	0.997	0.11	0.03	0.13	0.03	-0.02	**0.022**	0.016	0.003	0.018	0.003	-0.002	**0.015**
50%	1.67	0.29	1.61	0.27	0.06	0.499	0.12	0.03	0.14	0.02	-0.02	0.115	0.016	0.003	0.018	0.003	-0.002	**0.038**
35%	2.04	0.45	1.86	0.32	0.18	0.145	0.14	0.04	0.14	0.04	0.00	0.998	0.018	0.003	0.018	0.004	0.000	0.604

Univar. sig., univariate significance of one-way ANOVA for each bone, cross-section location, and CSG separately; significant values ($p < 0.05$) bolded; sd, standard deviation

Mean Difference = Normal mean − Obese mean; negative values indicate larger obese means.

Table 11. Continued

h.   Female Femur

Cross-section location	Cross-sectional property																
	Cortical Area (CA)						Total Area (TA)						%CA = CA/TA *100				
	Normal		Obese		Mean	Univar.	Normal		Obese		Mean	Univar.	Normal		Obese		Mean	Univar.
	mean	sd	mean	sd	Difference	Sig.	mean	sd	mean	sd	Difference	Sig.	mean	sd	mean	sd	Difference	Sig.
80%	5.86	1.09	7.05	1.41	-1.19	**0.004**	11.31	1.81	11.34	1.84	-0.03	0.958	50.94	8.81	62.85	11.54	-11.91	**0.001**
65%	6.21	0.86	7.24	1.13	-1.03	**0.002**	8.68	0.60	9.25	1.16	-0.57	0.050	71.53	8.60	78.33	8.05	-6.80	**0.011**
50%	5.86	0.80	6.79	1.06	-0.93	**0.002**	8.25	0.68	8.79	1.15	-0.54	0.069	71.10	8.39	77.33	7.06	-6.23	**0.012**
35%	5.20	0.91	5.97	0.91	-0.77	**0.008**	9.08	0.76	9.31	1.31	-0.23	0.480	57.50	9.71	64.79	9.26	-7.29	**0.016**
20%	4.55	0.77	5.07	0.88	-0.52	**0.044**	12.91	1.22	13.14	2.39	-0.23	0.697	35.42	6.49	40.02	10.91	-4.60	0.103

Cross-section location	Cross-sectional property																
	Cross-sectional shape (Imax/Imin)						Polar second moment of area (J)						Polar section modulus (Zp)				
	Normal		Obese		Mean	Univar.	Normal		Obese		Mean	Univar.	Normal		Obese		Mean	Univar.
	mean	sd	mean	sd	Difference	Sig.	mean	sd	mean	sd	Difference	Sig.	mean	sd	mean	sd	Difference	Sig.
80%	1.41	0.16	1.57	0.26	-0.16	**0.015**	2.23	0.47	2.62	0.74	-0.39	**0.046**	0.126	0.022	0.143	0.029	-0.017	**0.036**
65%	1.29	0.18	1.27	0.17	0.02	0.639	1.51	0.21	1.83	0.44	-0.32	**0.003**	0.104	0.013	0.121	0.022	-0.017	**0.004**
50%	1.34	0.17	1.25	0.13	0.09	0.052	1.38	0.21	1.69	0.42	-0.31	**0.005**	0.092	0.011	0.109	0.022	-0.017	**0.003**
35%	1.21	0.10	1.19	0.16	0.02	0.604	1.46	0.25	1.69	0.42	-0.23	**0.031**	0.097	0.015	0.111	0.019	-0.014	**0.014**
20%	1.61	0.28	1.63	0.20	-0.02	0.826	2.15	0.43	2.45	0.66	-0.30	0.082	0.112	0.020	0.125	0.023	-0.013	0.057

Univar. sig., univariate significance of one-way ANOVA for each bone, cross-section location, and CSG separately; significant values ($p < 0.05$) bolded; sd, standard deviation

Mean Difference = Normal mean − Obese mean; negative values indicate larger obese means.

Table 11. Continued

i.   Female Tibia

Cross-section location	Cross-sectional property																
	Cortical Area (CA)						Total Area (TA)						%CA = CA/TA *100					
	Normal		Obese		Mean	Univar.	Normal		Obese		Mean	Univar.	Normal		Obese		Mean	Univar.
	mean	sd	mean	sd	Difference	Sig.	mean	sd	mean	sd	Difference	Sig.	mean	sd	mean	sd	Difference	Sig.
80%	4.71	1.04	5.31	0.91	-0.60	**0.048**	11.43	2.35	12.17	1.65	-0.74	0.237	40.46	7.92	44.25	8.17	-3.79	0.136
65%	4.81	0.88	5.31	0.87	-0.50	0.068	7.75	0.84	8.05	1.09	-0.30	0.325	62.24	9.98	66.44	8.96	-4.20	0.153
50%	4.59	0.79	5.06	0.86	-0.47	0.070	6.41	0.64	6.65	1.00	-0.24	0.349	71.54	9.96	76.43	8.84	-4.89	0.096
35%	3.83	0.66	4.30	0.75	-0.47	**0.036**	5.62	0.78	5.75	0.88	-0.13	0.605	68.42	9.93	75.12	9.20	-6.70	**0.027**
20%	3.10	0.65	3.60	0.71	-0.50	**0.023**	6.55	1.32	6.48	0.99	0.07	0.853	48.15	10.15	56.09	10.19	-7.94	**0.014**

Cross-section location	Cross-sectional property																
	Cross-sectional shape (Imax/Imin)						Polar second moment of area (J)						Polar section modulus (Zp)					
	Normal		Obese		Mean	Univar.	Normal		Obese		Mean	Univar.	Normal		Obese		Mean	Univar.
	mean	sd	mean	sd	Difference	Sig.	mean	sd	mean	sd	Difference	Sig.	mean	sd	mean	sd	Difference	Sig.
80%	2.34	0.43	2.31	0.34	0.03	0.804	2.55	0.68	2.96	0.73	-0.41	0.066	0.132	0.031	0.150	0.030	-0.018	0.064
65%	2.28	0.32	2.29	0.39	-0.01	0.922	1.48	0.32	1.69	0.41	-0.21	0.069	0.092	0.015	0.102	0.019	-0.010	0.060
50%	2.09	0.30	2.00	0.31	0.09	0.356	1.08	0.22	1.23	0.35	-0.15	0.099	0.072	0.012	0.080	0.017	-0.008	0.083
35%	1.76	0.29	1.71	0.30	0.05	0.628	0.79	0.21	0.89	0.27	-0.10	0.170	0.061	0.013	0.066	0.014	-0.005	0.193
20%	1.24	0.21	1.30	0.16	-0.06	0.251	0.83	0.35	0.92	0.26	-0.09	0.346	0.064	0.019	0.068	0.019	-0.004	0.514

Univar. sig., univariate significance of one-way ANOVA for each bone, cross-section location, and CSG separately; significant values ($p < 0.05$) bolded; sd, standard deviation

Mean Difference = Normal mean − Obese mean; negative values indicate larger obese means.

Table 11. Continued

j.   Female Fibula

Cross-section location	Cross-sectional property																
	Cortical Area (CA)						Total Area (TA)						%CA = CA/TA *100				
	Normal		Obese		Mean	Univar.	Normal		Obese		Mean	Univar.	Normal		Obese		Mean	Univar.
	mean	sd	mean	sd	Difference	Sig.	mean	sd	mean	sd	Difference	Sig.	mean	sd	mean	sd	Difference	Sig.
80%	0.99	0.24	1.06	0.21	-0.07	0.322	1.31	0.27	1.43	0.26	-0.12	0.137	75.38	12.44	75.14	13.20	0.24	0.952
65%	1.25	0.30	1.33	0.29	-0.08	0.399	1.50	0.30	1.63	0.28	-0.13	0.177	81.25	9.92	81.13	10.27	0.12	0.969
50%	1.30	0.29	1.43	0.30	-0.13	0.169	1.62	0.30	1.78	0.31	-0.16	0.083	79.32	10.87	80.15	7.56	-0.83	0.772
35%	1.24	0.26	1.35	0.25	-0.11	0.142	1.53	0.27	1.63	0.23	-0.10	0.211	79.69	9.56	82.48	7.95	-2.79	0.314
20%	1.00	0.24	1.10	0.18	-0.10	0.122	1.30	0.24	1.38	0.21	-0.08	0.261	75.26	12.21	80.09	8.59	-4.83	0.144

Cross-section location	Cross-sectional property																
	Cross-sectional shape (Imax/Imin)						Polar second moment of area (J)						Polar section modulus (Zp)				
	Normal		Obese		Mean	Univar.	Normal		Obese		Mean	Univar.	Normal		Obese		Mean	Univar.
	mean	sd	mean	sd	Difference	Sig.	mean	sd	mean	sd	Difference	Sig.	mean	sd	mean	sd	Difference	Sig.
80%	2.12	0.67	2.39	0.76	-0.27	0.218	0.05	0.02	0.06	0.03	-0.01	0.102	0.007	0.002	0.008	0.002	-0.001	0.182
65%	2.57	0.65	2.98	0.96	-0.41	0.101	0.08	0.02	0.09	0.04	-0.02	0.101	0.009	0.002	0.010	0.003	-0.001	0.182
50%	2.20	0.51	2.42	0.74	-0.22	0.244	0.08	0.03	0.10	0.04	-0.02	0.056	0.010	0.002	0.012	0.003	-0.002	**0.048**
35%	2.00	0.47	2.34	0.69	-0.34	0.070	0.07	0.02	0.08	0.03	-0.01	0.063	0.009	0.002	0.011	0.002	-0.002	0.057
20%	2.58	0.74	2.47	0.52	0.11	0.568	0.05	0.01	0.06	0.02	-0.01	0.122	0.007	0.002	0.008	0.002	-0.001	0.112

Univar. sig., univariate significance of one-way ANOVA for each bone, cross-section location, and CSG separately; significant values ($p < 0.05$) bolded; sd, standard deviation

Mean Difference = Normal mean − Obese mean; negative values indicate larger obese means.

A MANOVA test for each bone was performed with BMI category and cross-section location (percentage of the bone) as independent variables and CA, TA, %CA, I_{max}/I_{min}, and J as dependent variables. Polar section modulus, Z_p, was analyzed separately using a two-way ANOVA because of autocorrelation with J (section moduli are calculated as second moments of area divided by moment arms; see Table 1). Results for the MANOVA tests are presented in Table 12 and show that BMI category is a significant main effect for CSG properties of the humerus, femur, tibia, and fibula. Additionally, females demonstrate significant differences for the radius; thus, females demonstrate significant differences between BMI groups for all long bones. Because the multivariate tests do not indicate which individual CSG properties differ between groups, post-hoc results were examined. The univariate post-hoc results are presented in Table 13, and show which CSG properties differ between BMI categories.

Table 12. MANOVA results for CSG properties by sex, bone, and bone location

a. males

Bone	Factor	df	F	p
Humerus	BMI category	(5, 187)	3.324	**0.007***
	Bone location	(10, 376)	19.864	**< 0.001***
	location * BMI category	(10, 376)	0.434	0.930
Radius	BMI category	(5, 187)	1.646	0.150
	Bone location	(10, 376)	7.562	**< 0.001***
	location * BMI category	(10, 376)	0.244	0.922
Femur	BMI category	(5, 312)	36.983	< 0.001*
	Bone location	(20, 1260)	44.054	< 0.001*
	location * BMI category	(20, 1260)	3.156	**< 0.001***
Tibia	BMI category	(5, 312)	16.710	< 0.001*
	Bone location	(20, 1260)	67.746	< 0.001*
	location * BMI category	(20, 1260)	1.776	**0.019***
Fibula	BMI category	(5, 312)	7.919	**< 0.001***
	Bone location	(20, 1260)	8.231	**< 0.001***
	location * BMI category	(20, 1260)	1.085	0.358

b. females

Bone	Factor	df	F	p
Humerus	BMI category	(5, 124)	7.809	**< 0.001***
	Bone location	(10, 250)	7.015	**< 0.001***
	location * BMI category	(10, 250)	0.558	0.847
Radius	BMI category	(5, 124)	2.504	**0.035***
	Bone location	(10, 250)	2.301	**0.014***
	location * BMI category	(10, 250)	0.736	0.690
Femur	BMI category	(5, 204)	11.333	**< 0.001***
	Bone location	(20, 828)	21.130	**< 0.001***
	location * BMI category	(20, 828)	1.434	0.098
Tibia	BMI category	(5, 204)	5.748	**< 0.001***
	Bone location	(20, 828)	34.668	**< 0.001***
	location * BMI category	(20, 828)	0.868	0.629
Fibula	BMI category	(5, 204)	4.272	**0.001***
	Bone location	(20, 828)	5.299	**< 0.001***
	location * BMI category	(20, 828)	0.514	0.962

*significant $p < 0.05$

Table 13. Post-hoc results of MANOVA for main effect of BMI category

a. males

CSG property	humerus p value	radius p value	femur p value	tibia p value	fibula p value
CA	**0.001***	0.580	**< 0.001***	**< 0.001***	**< 0.001***
TA	**0.078**	0.393	**< 0.001***	**< 0.001***	**< 0.001***
%CA	**0.039***	0.792	**< 0.001***	**0.019***	0.420
I_{max}/I_{min}	0.462	0.792	0.301	0.340	0.185
J	**0.004***	0.164	**< 0.001***	**< 0.001***	**< 0.001***
Z_p	**0.010***	0.143	**< 0.001***	**< 0.001***	**< 0.001***

b. females

CSG property	humerus p value	radius p value	femur p value	tibia p value	fibula p value
CA	**< 0.001***	0.062	**< 0.001***	**< 0.001***	**0.019***
TA	0.802	0.532	0.089	0.360	**0.027***
%CA	**0.001***	0.073	**< 0.001***	**< 0.001***	0.192
I_{max}/I_{min}	0.102	0.119	0.974	0.903	**0.013***
J	**0.003***	0.233	**< 0.001***	**0.003***	**0.001***
Z_p	**0.001***	**0.010***	**< 0.001***	**0.002***	**< 0.001***

CA, TA, %CA, I_{max}/I_{min}, and J entered as dependent variables and BMI category and cross-section location as independent variables. Each bone analyzed separately.

Z_p was entered as the dependent variable, with BMI category and cross-section location as independent variables. Each bone analyzed separately.

*significant p < 0.05

The results of the MANOVA also indicate a significant interaction effect for BMI category and cross-section location for male femora and tibiae. These interaction effects are meant to compare whether or not there are differences in patterns between groups, within elements; however, when analyzing the data in this manner, the fact that cross-section locations are not independent of one another (i.e., multiple cross-sections are examined within each bone of an individual) violates this assumption of MANOVA testing. The within-subjects comparisons can be better addressed using a repeated measures design where cross-section location is a within-subject factor with either 3 (35, 50, 65% for humerus and radius) or 5 levels (20, 35, 50, 65, 80% for femur, tibia, fibula) for each CSG measurement (multiple measures for the within-subjects factor) and BMI category is the between-subjects factor. This design requires one line of data for each individual, with each CSG measurement at each cross-section location represented by a separate column variable (rather than relying on categorical coding variables, as in the MANOVA), and allows for testing the variability of CSG properties within-subjects, ensuring that no assumptions have been violated.

Results of the repeated measures design are presented in Table 14, along with the univariate post-hoc results in Table 15. These tests indicate that there are differences between groups, within diaphyses for the humerus, femur, and tibia (see also fibula, Table 14) in males, and the radius and femur of females. Post-hoc univariate tests indicate that the differences between groups within the male humerus and tibia are due to differences in polar second moments of area (J), while the differences between groups for the male femur are due to differences in cross-section shape (I_{max}/I_{min}). Within the female radius, differences between groups can be attributed to CA, TA, %CA, and J, and CA, %CA, and I_{max}/I_{min} for the female femur.

113

Table 14. Multivariate repeated measures results of within-subjects effects for CSG properties by cross-section location (bone percentage) and BMI category

a. males

Bone	Within Subjects Effects	df	F	*p*
Humerus	Cross-section location	(10, 250)	34.509	< 0.001*
	Cross-section location * BMI category	(10, 250)	1.941	**0.040***
Radius	Cross-section location	(10, 238)	19.724	< 0.001*
	Cross-section location * BMI category	(10, 238)	0.693	0.731
Femur	Cross-section location	(20, 988)	55.995	< 0.001*
	Cross-section location * BMI category	(20, 988)	6.427	**< 0.001***
Tibia	Cross-section location	(20, 956)	74.535	< 0.001*
	Cross-section location * BMI category	(20, 956)	3.109	**< 0.001***
Fibula	Cross-section location	(20, 844)	16.901	< 0.001*
	Cross-section location * BMI category	(20, 844)	1.566	**0.054**

b. females

Bone	Within Subjects Effects	df	F	p
Humerus	Cross-section location	(10, 158)	11.090	< 0.001*
	Cross-section location * BMI category	(10, 158)	1.126	0.346
Radius	Cross-section location	(10, 114)	8.686	< 0.001*
	Cross-section location * BMI category	(10, 114)	2.358	**0.014***
Femur	Cross-section location	(20, 636)	29.216	< 0.001*
	Cross-section location * BMI category	(20, 636)	2.376	**0.001***
Tibia	Cross-section location	(20, 636)	42.630	< 0.001*
	Cross-section location * BMI category	(20, 636)	1.417	0.107
Fibula	Cross-section location	(20, 556)	12.217	< 0.001*
	Cross-section location * BMI category	(20, 556)	0.784	0.734

*significant p < 0.05; Bonferonni correction applied for multiple comparisons.

Table 15. Post-hoc results of repeated measures design (univariate tests)

a. males

Bone	CSG	Within-subjects (cross-section location*BMI category)			Between-subjects effects (BMI category)		
		df	F	*p*	df	F	*p*
Humerus	CA	1.537	2.543	0.097	1	4.892	**0.031***
	TA	1.209	3.456	0.059	1	2.157	0.147
	%CA	1.182	1.081	0.313	1	1.086	**0.033***
	Imax/Imin	2.00	0.335	0.716	1	0.302	0.585
	J	1.281	6.367	**0.002***	1	4.178	**0.045***
Radius	CA	1.483	0.564	0.520	1	0.351	0.556
	TA	1.358	0.114	0.813	1	0.502	0.481
	%CA	1.700	0.436	0.615	1	0.001	0.977
	Imax/Imin	1.407	0.748	0.432	1	0.088	0.768
	J	1.293	0.382	0.592	1	0.996	0.322
Femur	CA	1.943	2.339	0.102	1	11.963	**0.001***
	TA	2.098	1.465	0.234	1	5.345	**0.024***
	%CA	2.249	2.522	0.077	1	5.795	**0.019***
	Imax/Imin	2.464	3.682	**0.020***	1	0.999	0.321
	J	1.941	2.122	0.126	1	20.306	**< 0.001***
Tibia	CA	1.646	1.071	0.336	1	20.126	**< 0.001***
	TA	1.441	0.538	0.528	1	15.280	**< 0.001***
	%CA	2.404	0.930	0.412	1	1.782	0.187
	Imax/Imin	2.552	0.793	0.482	1	0.275	0.602
	J	1.302	3.439	**0.055**	1	23.908	**< 0.001***
Fibula	CA	2.817	1.032	0.377	1	3.000	**0.089**
	TA	2.490	0.612	0.578	1	2.574	0.115
	%CA	2.779	0.511	0.662	1	0.004	0.952
	Imax/Imin	2.946	0.680	0.563	1	0.447	0.507
	J	2.447	1.022	0.375	1	4.829	**0.032***

*significant p < 0.05; Bonferonni correction applied for multiple comparisons

Table 15. Continued.

b. females

Bone	CSG	Within-subjects (cross-section location*BMI category)			Between-subjects effects (BMI category)		
		df	F	*p*	df	F	*p*
Humerus	CA	1.809	1.138	0.322	1	3.531	**0.067**
	TA	1.133	1.114	0.305	1	0.012	0.912
	%CA	1.374	0.690	0.454	1	3.062	0.088
	Imax/Imin	1.910	0.364	0.686	1	2.114	0.154
	J	1.190	0.559	0.574	1	3.597	**0.065**
Radius	CA	1.210	5.855	**0.016***	1	0.447	0.509
	TA	1.162	8.740	**0.004***	1	0.006	0.939
	%CA	1.459	4.259	**0.031***	1	0.566	0.458
	Imax/Imin	1.283	2.091	0.152	1	1.388	0.248
	J	1.180	6.897	**0.010***	1	0.030	0.864
Femur	CA	2.122	3.096	**0.047***	1	8.958	**0.005***
	TA	2.080	1.758	0.177	1	0.507	0.481
	%CA	2.395	2.995	**0.046***	1	8.997	**0.005***
	Imax/Imin	2.700	3.349	**0.026***	1	0.057	0.812
	J	1.969	0.528	0.589	1	5.861	**0.020***
Tibia	CA	2.026	0.191	0.829	1	4.260	**0.046***
	TA	1.340	0.509	0.531	1	0.503	0.482
	%CA	2.347	2.532	0.076	1	3.749	**0.060**
	Imax/Imin	2.365	0.666	0.540	1	0.000	0.999
	J	1.364	1.782	0.186	1	3.639	**0.064**
Fibula	CA	2.682	0.584	0.608	1	0.593	0.446
	TA	2.923	0.185	0.902	1	0.423	0.520
	%CA	2.584	0.685	0.543	1	0.439	0.512
	Imax/Imin	3.363	0.876	0.558	1	3.828	**0.058**
	J	2.423	0.567	0.414	1	1.622	0.211

*significant p < 0.05; Bonferonni correction applied for multiple comparisons

The univariate post-hoc between-subjects results from the repeated measures design are similar to the post-hoc results of the MANOVA for males; statistical significance is noted in both cases for: CA of the humerus, femur, tibia; TA of the femur and tibia; %CA for the humerus and femur; *J* for the humerus, femur, tibia, and fibula. When the much smaller female sample is analyzed this way, power to detect some of the statistical differences is lost. Post-hoc results of the MANOVA test and repeated measures tests both indicate significance for CA of the femur and tibia (and trends toward significance for the humerus), as well as %CA and J for the femur (with trends toward significance in the tibia) for females. Power tests conducted for females indicate that total sample sizes of n=60 and n=67 would be necessary to detect significant differences (at $\alpha = 0.05$) for the humerus and tibia respectively; sample sizes as large as those available for males would be likely to present similar statistical significance.

Boxplots for each CSG property (by bone, cross-section location, sex, and BMI category) can be found in Figures 11-35 for illustrative reference. The box itself represents the first quartile, median (bold line), and the third quartile of the measurement, while the whiskers indicate the minimum and maximum values in the distribution of each variable. Statistically significant differences between obese and normal mass individuals for each CSG property can be found in Table 13 for the MANOVA and Table 15 for the repeated measures design. Where significant results for these two methods of comparison agree (i.e., a CSG property is significantly different between BMI groups for a particular bone), an asterisk (*) is placed along the x-axis under the sex label, indicating significance ($\alpha = 0.05$); an open circle (○) is placed along the x-axis where trends are apparent ($\alpha = 0.10$). Subsequently, univariate ANOVA significance values are consulted (Table 11) to elucidate which specific cross-sections are different; recall that these actual significance values are subject to Type I error, which is why

117

they are not interpreted alone. Furthermore, the plots are presented by cross-sectional property (in the following order CA, TA, %CA, J, and Z_p), from proximal to distal element (humerus, radius, femur, tibia, and fibula) with male results on the left panel and females on the right panel. Note that values of CA and TA are scaled by estimated body mass, and J and Z_p are scaled by the product of estimated body mass and bone length.
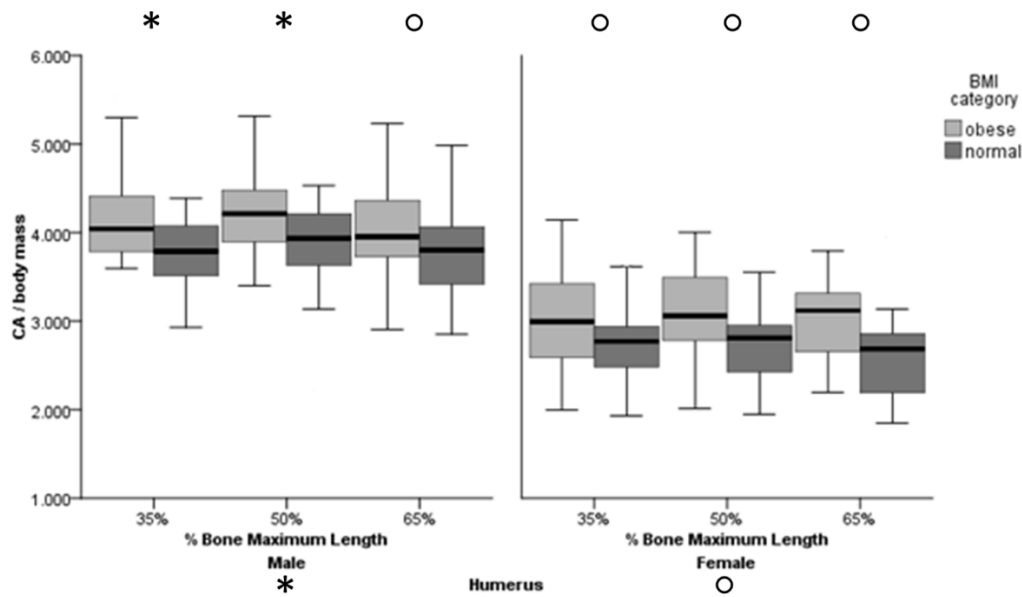
Figure 10. Standardized CA for Humerus by sex and BMI category
* indicates significance (p < 0.05); ○ indicates trends (p < 0.10)
Symbols along the x-axis labels reflect post-hoc results from the repeated measures design; when this CSG property is of interest for a particular sex, symbols along the superior margin of the figure reflect univariate significance for the particular cross-section location (% bone maximum length).
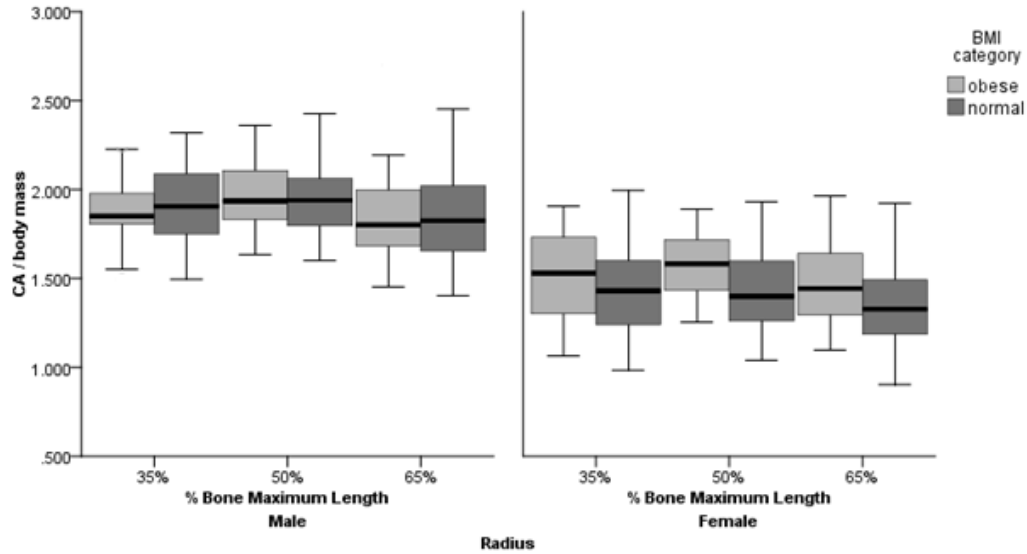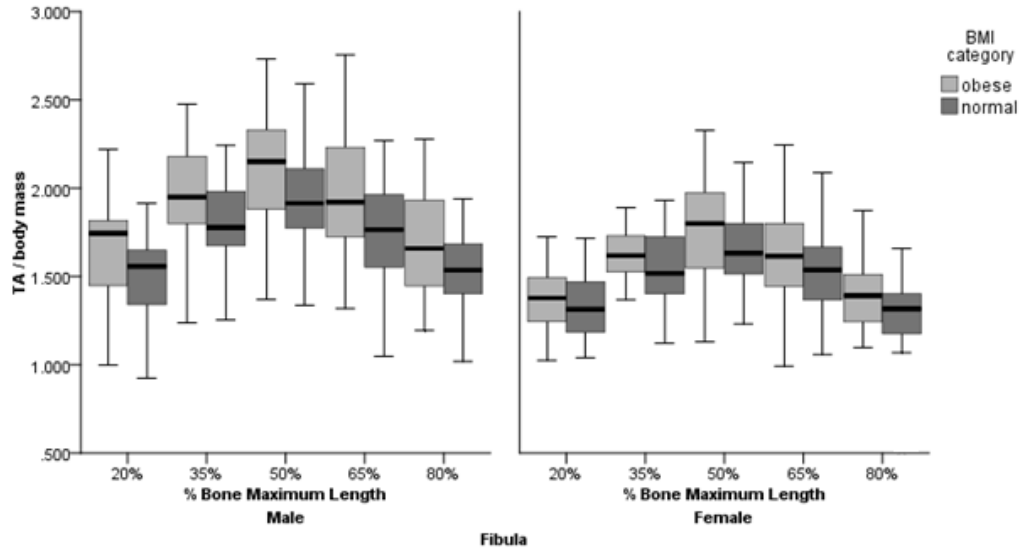
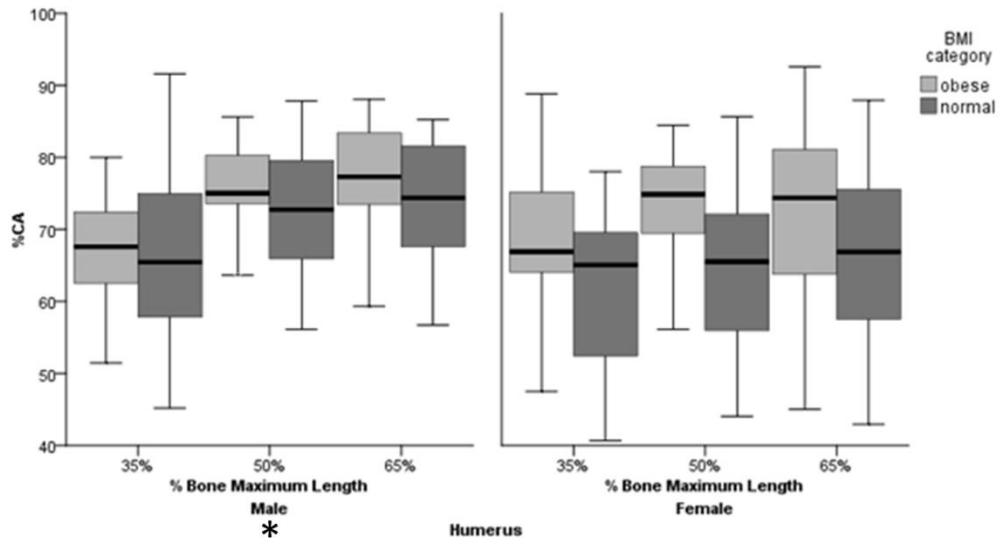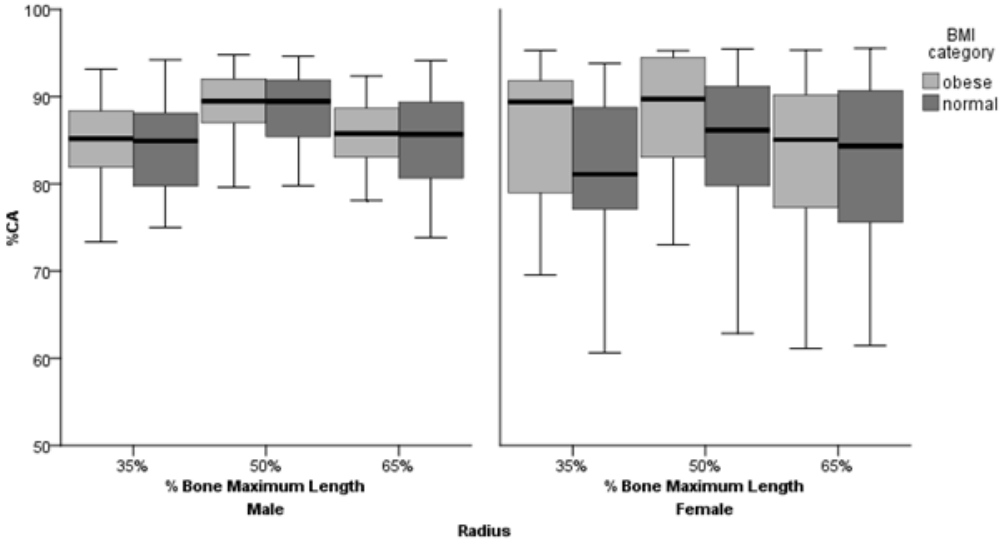**Figure 11. Standardized CA for Radius by sex and BMI category**
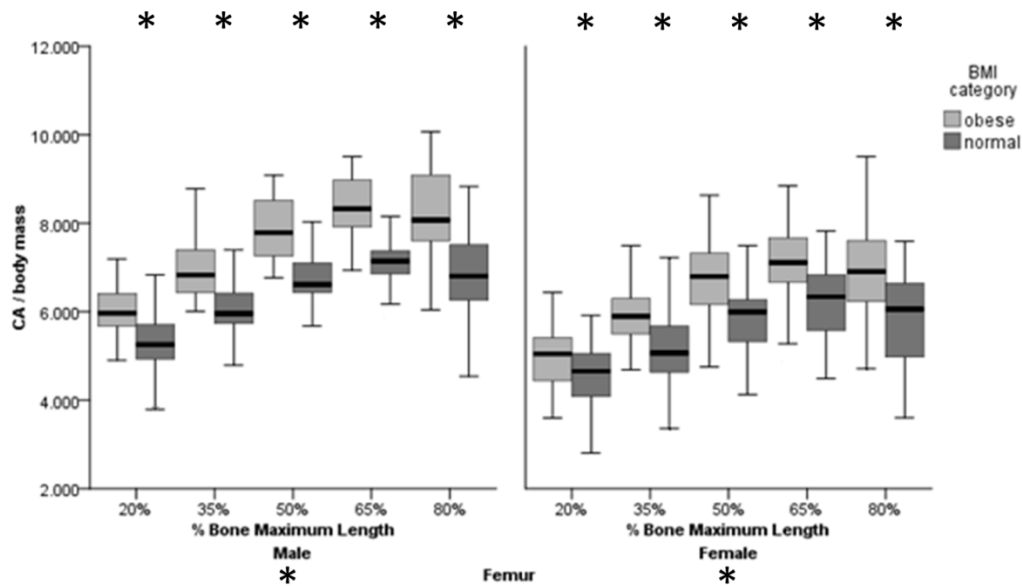
Figure 12. Standardized CA for Femur by sex and BMI category
* indicates significance (p < 0.05); ○ indicates trends (p < 0.10)
Symbols along the x-axis labels reflect post-hoc results from the repeated measures design; when this CSG property is of interest for a particular sex, symbols along the superior margin of the figure reflect univariate significance for the particular cross-section location (% bone maximum length).

119
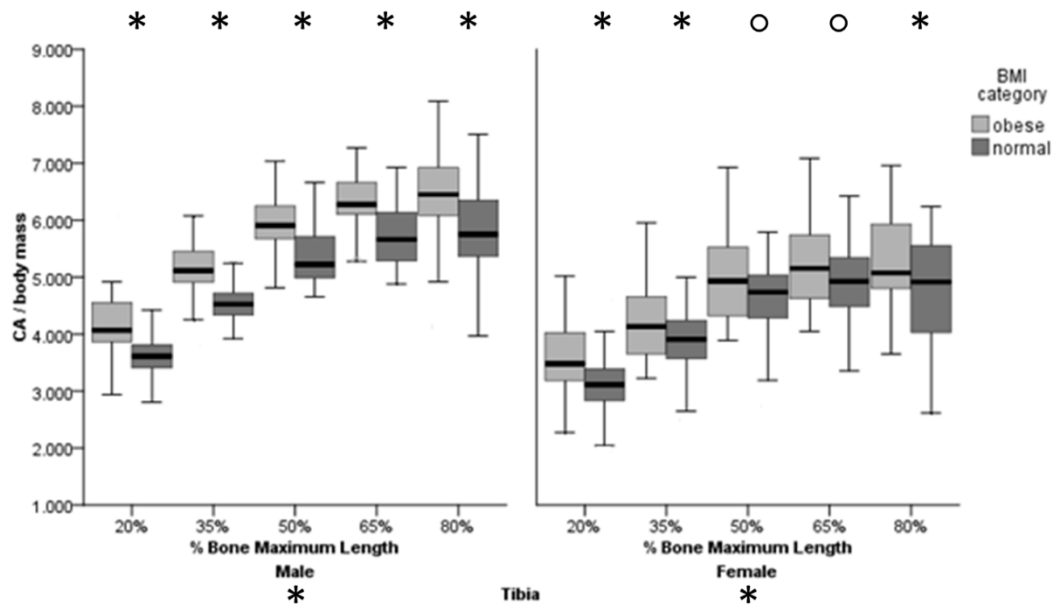
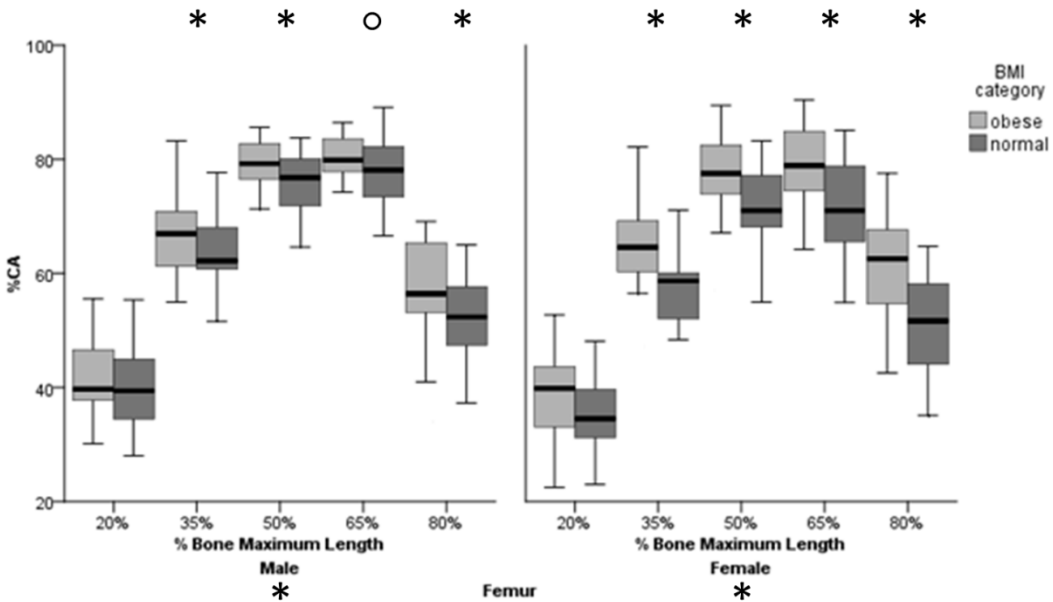**Figure 13. Standardized CA for Tibia by sex and BMI category**
* indicates significance (p < 0.05); ○ indicates trends (p < 0.10)
Symbols along the x-axis labels reflect post-hoc results from the repeated measures design; when this CSG property is of interest for a particular sex, symbols along the superior margin of the figure reflect univariate significance for the particular cross-section location (% bone maximum length).
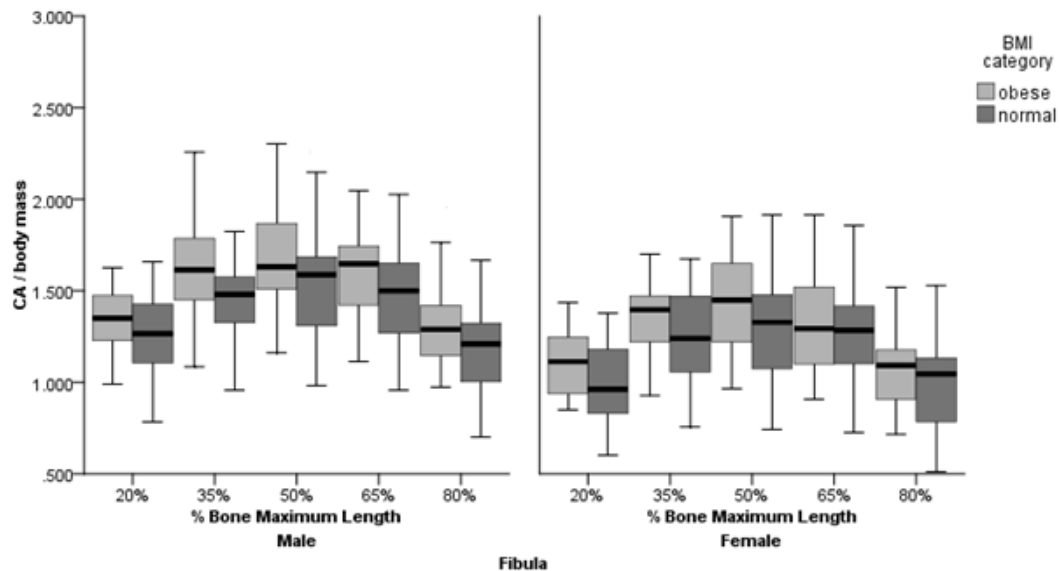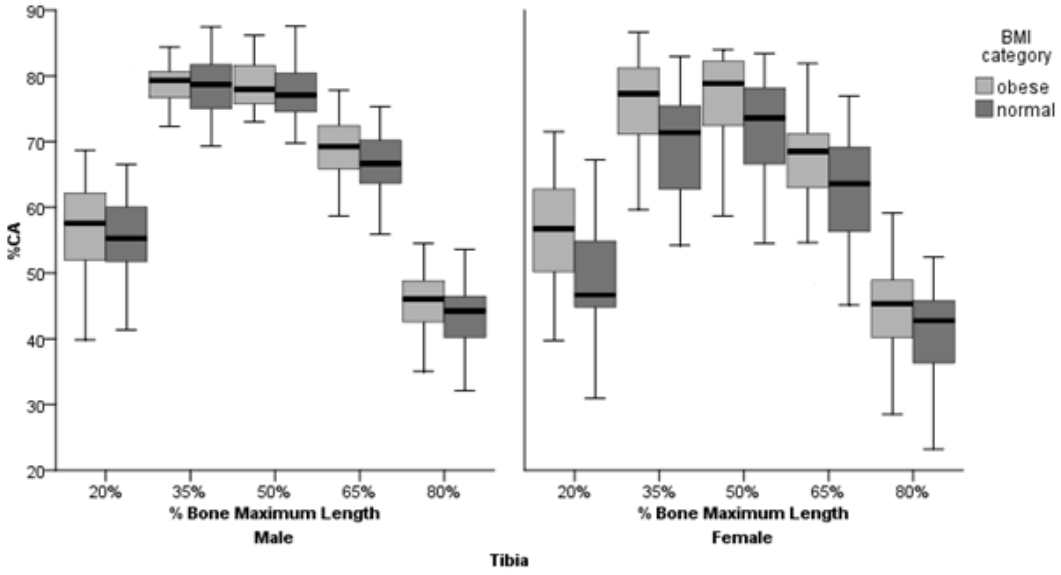

Figure 14. Standardized CA for Fibula by sex and BMI category
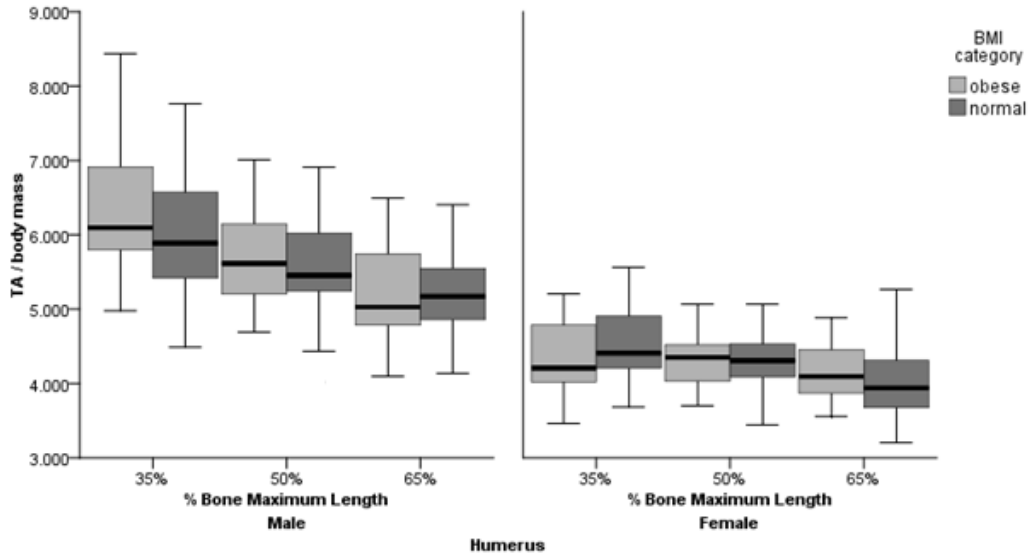
Figure 15. Standardized TA for Humerus by sex and BMI category
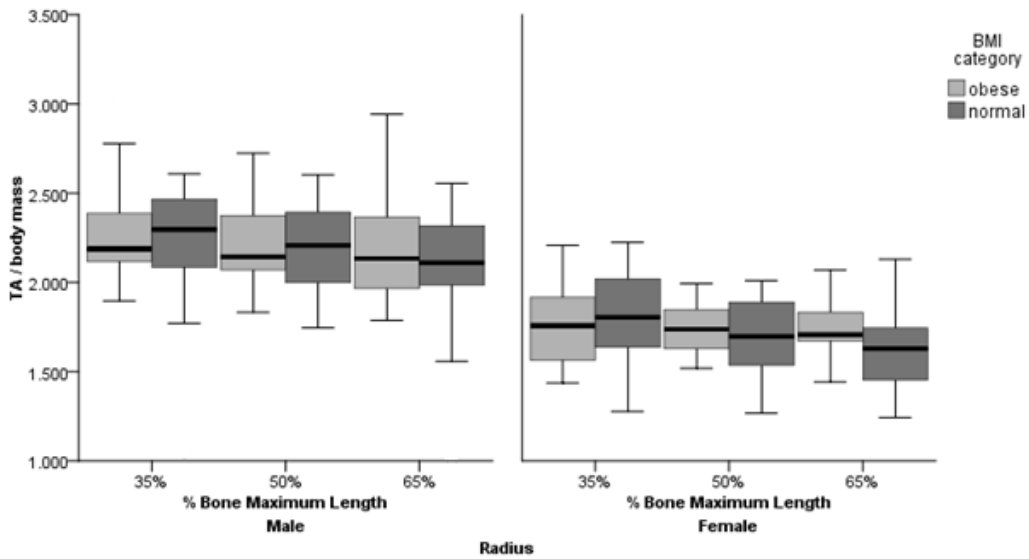
Figure 16. Standardized TA for Radius by sex and BMI category
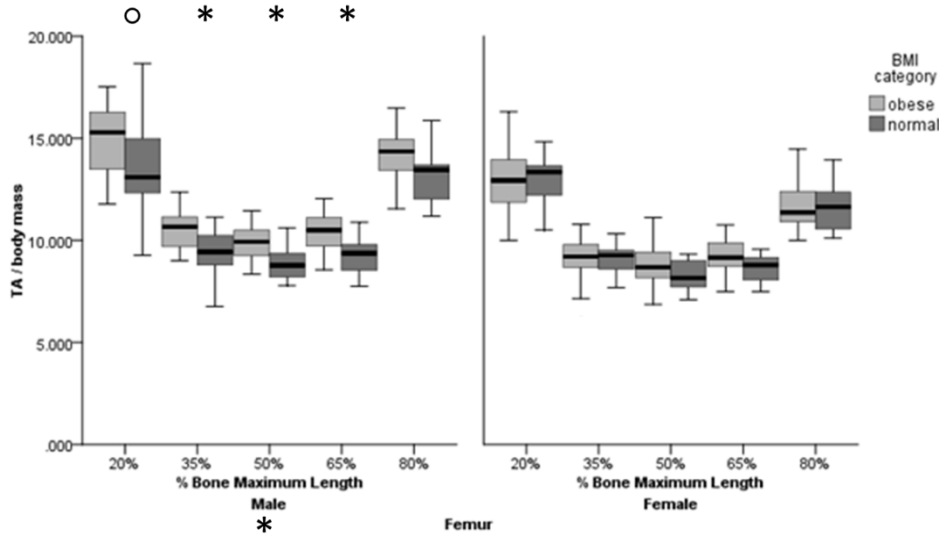
Figure 17. Standardized TA for Femur by sex and BMI category
* indicates significance (p < 0.05); ○ indicates trends (p < 0.10)
Symbols along the x-axis labels reflect post-hoc results from the repeated measures design; when this CSG property is of interest for a particular sex, symbols along the superior margin of the figure reflect univariate significance for the particular cross-section location (% bone maximum length).
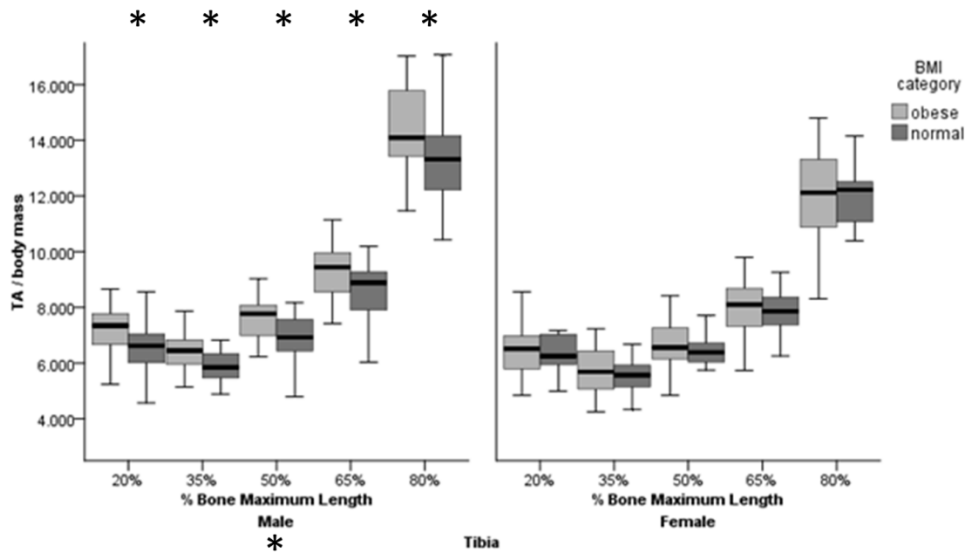
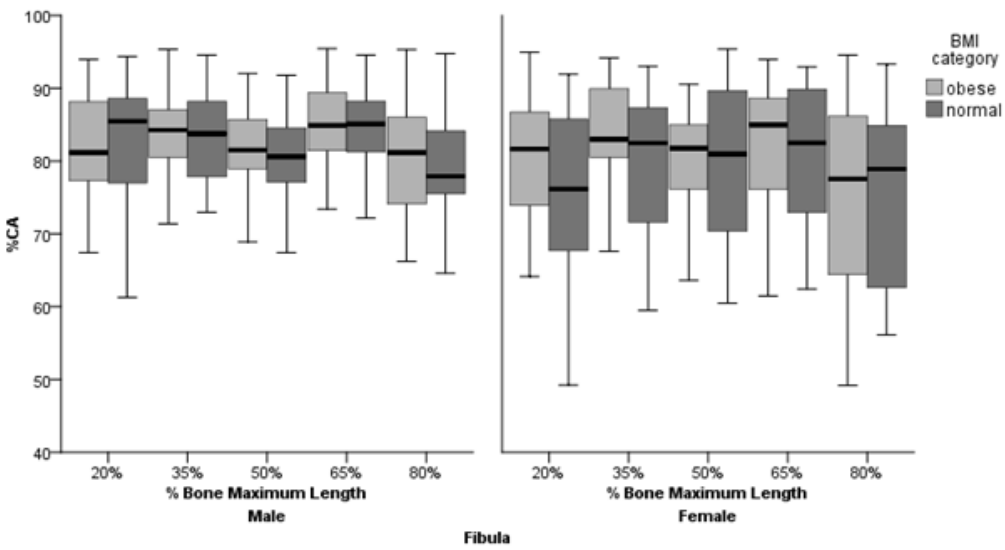**Figure 18. Standardized TA for Tibia by sex and BMI category**
* indicates significance (p < 0.05); ○ indicates trends (p < 0.10)
Symbols along the x-axis labels reflect post-hoc results from the repeated measures design; when this CSG property is of interest for a particular sex, symbols along the superior margin of the figure reflect univariate significance for the particular cross-section location (% bone maximum length).
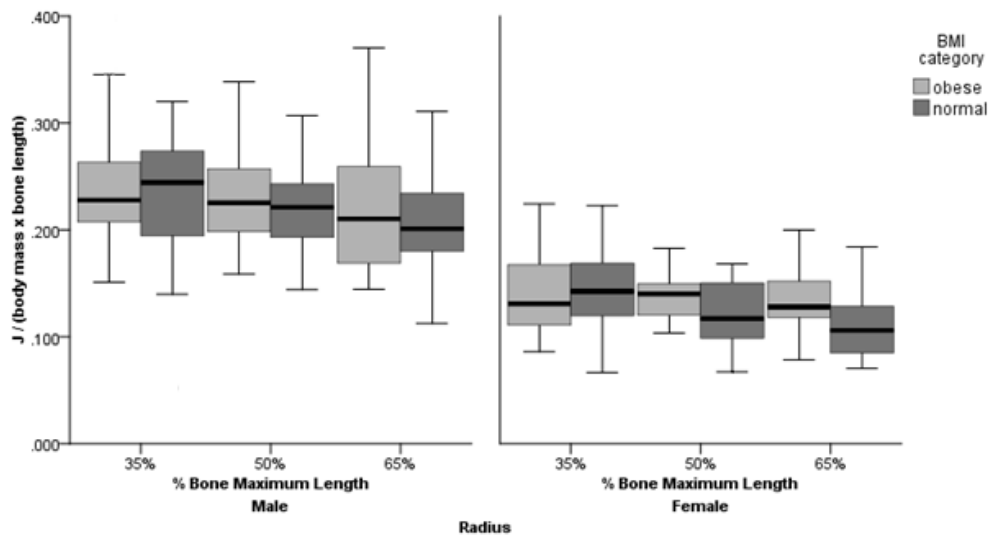
Figure 19. Standardized TA for Fibula by sex and BMI category

Figure 20. %CA for Humerus by sex and BMI category

Figure 21. %CA for Radius by sex and BMI category

Figure 22. %CA for Femur by sex and BMI category
* indicates significance ($p < 0.05$); ○ indicates trends ($p < 0.10$)
Symbols along the x-axis labels reflect post-hoc results from the repeated measures design; when this CSG property is of interest for a particular sex, symbols along the superior margin of the figure reflect univariate significance for the particular cross-section location (% bone maximum length).

Figure 23. %CA for Tibia by sex and BMI category

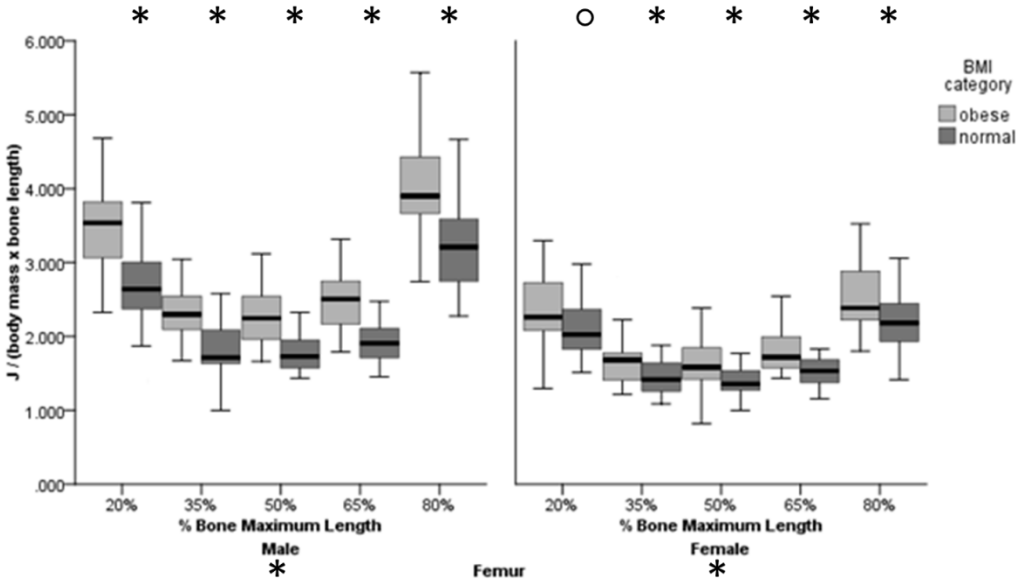**Figure 24. %CA for Fibula by sex and BMI category**
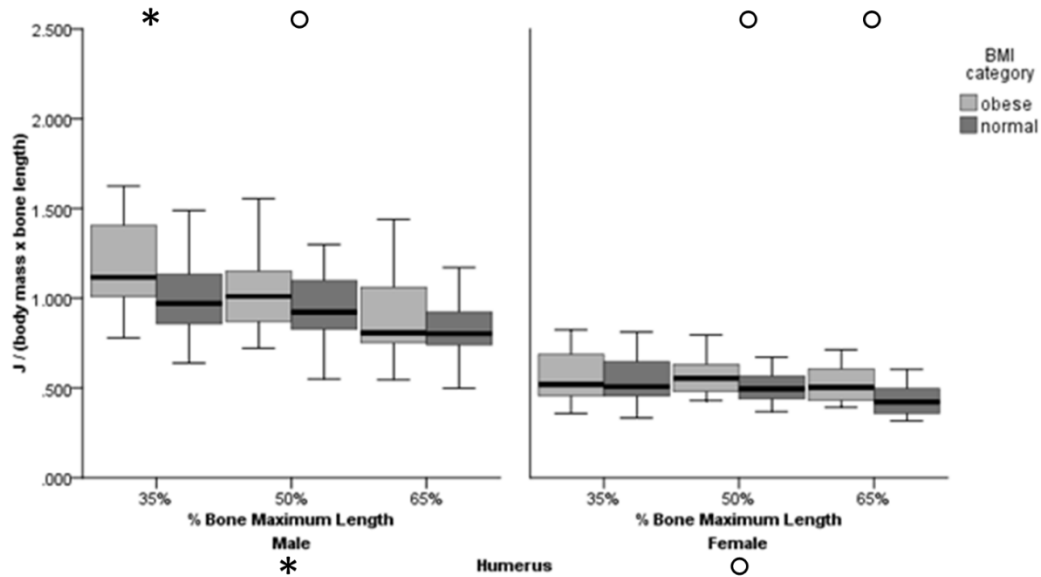
Figure 25. Standardized Polar Second Moment of Area (*J*) for Humerus by sex and BMI category

* indicates significance (p < 0.05); ○ indicates trends (p < 0.10)

Symbols along the x-axis labels reflect post-hoc results from the repeated measures design; when this CSG property is of interest for a particular sex, symbols along the superior margin of the figure reflect univariate significance for the particular cross-section location (% bone maximum length).
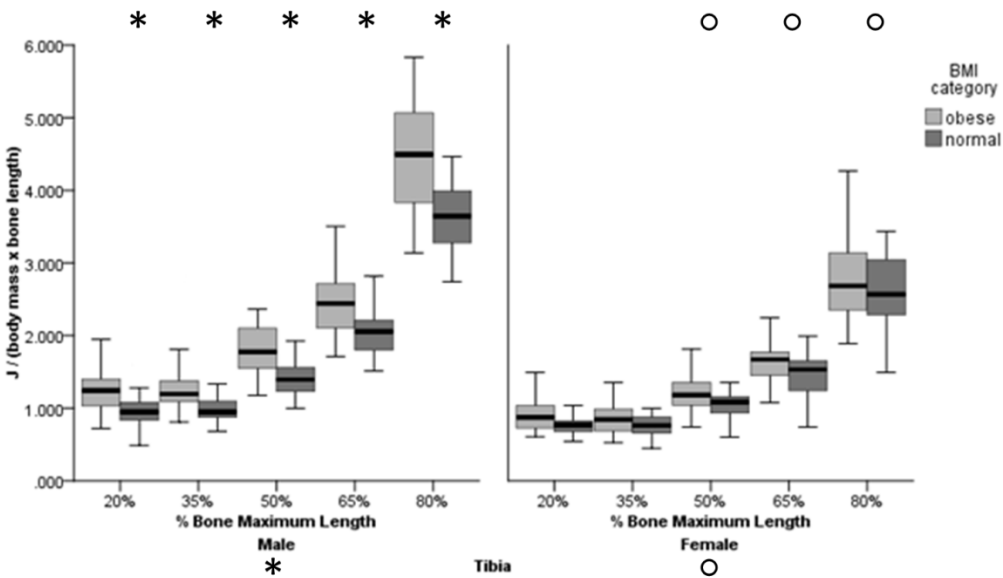

Figure 26. Standardized Polar Second Moment of Area (*J*) for Radius by sex and BMI category

Figure 27. Standardized Polar Second Moment of Area (*J*) for Femur by sex and BMI category

* indicates significance (p < 0.05); ○ indicates trends (p < 0.10)

Symbols along the x-axis labels reflect post-hoc results from the repeated measures design; when this CSG property is of interest for a particular sex, symbols along the superior margin of the figure reflect univariate significance for the particular cross-section location (% bone maximum length).
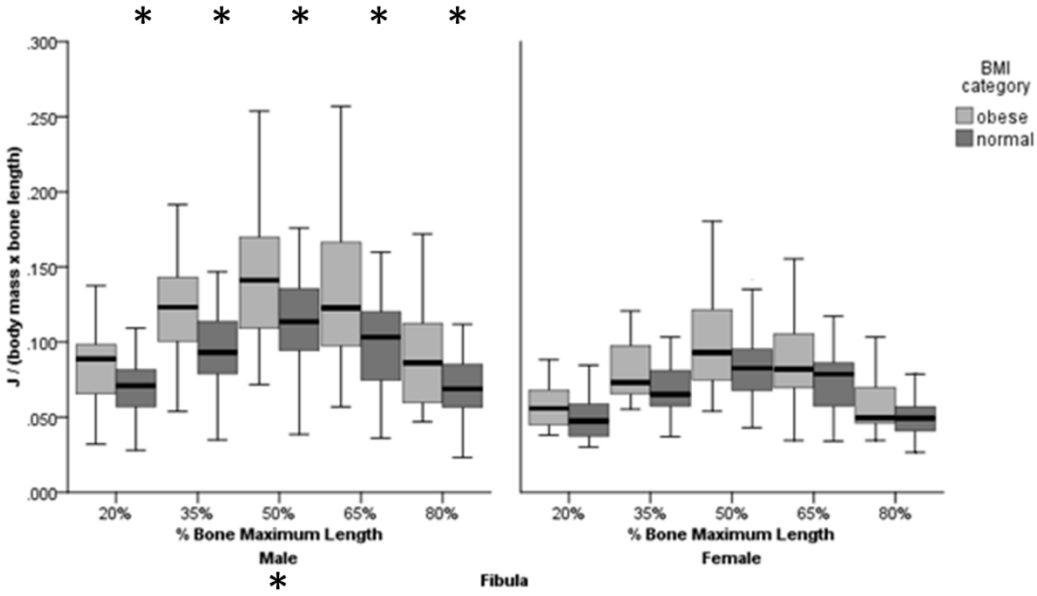

Figure 28. Standardized Polar Second Moment of Area (*J*) for Tibia by sex and BMI category

* indicates significance (p < 0.05); ○ indicates trends (p < 0.10)

Symbols along the x-axis labels reflect post-hoc results from the repeated measures design; when this CSG property is of interest for a particular sex, symbols along the superior margin of the figure reflect univariate significance for the particular cross-section location (% bone maximum length).

Figure 29. Standardized Polar Second Moment of Area (*J*) for Fibula by sex and BMI category

* indicates significance (p < 0.05); ○ indicates trends (p < 0.10)

Symbols along the x-axis labels reflect post-hoc results from the repeated measures design; when this CSG property is of interest for a particular sex, symbols along the superior margin of the figure reflect univariate significance for the particular cross-section location (% bone maximum length).
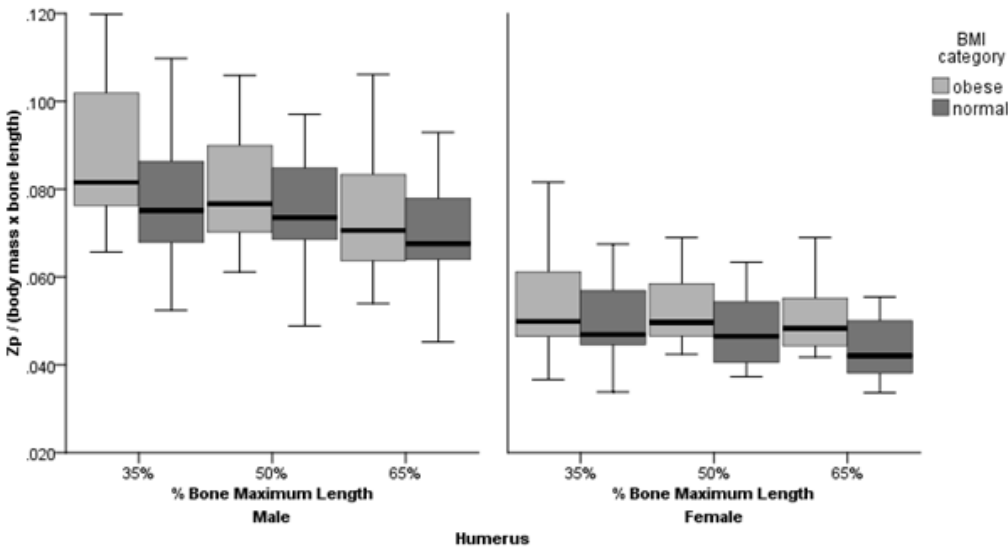
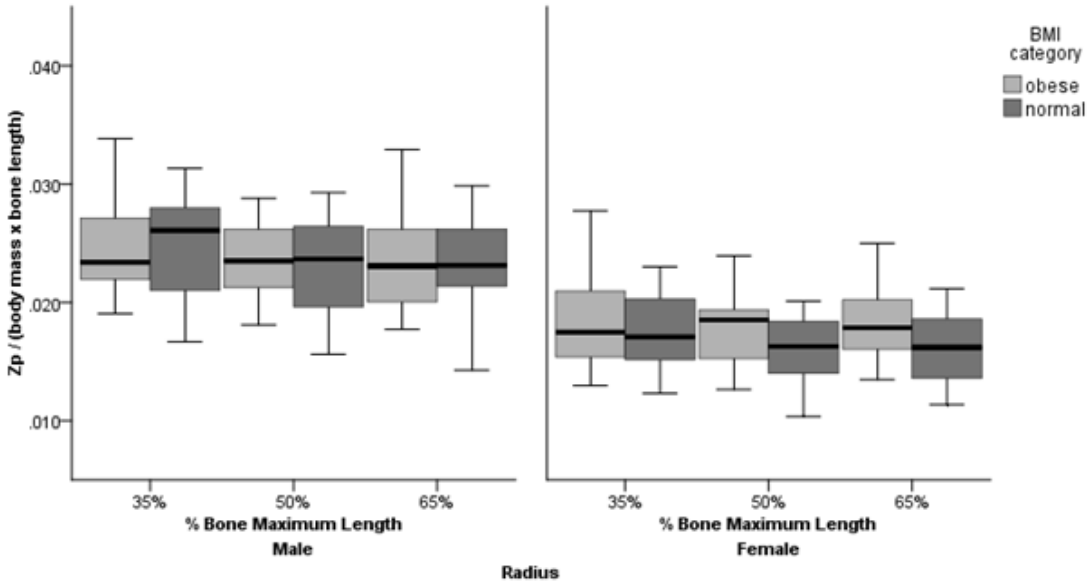**Figure 30. Standardized Polar Section Modulus (*Z_p*) for Humerus by sex and BMI category**

128

Figure 31. Standardized Polar Section Modulus (Z_p) for Radius by sex and BMI category
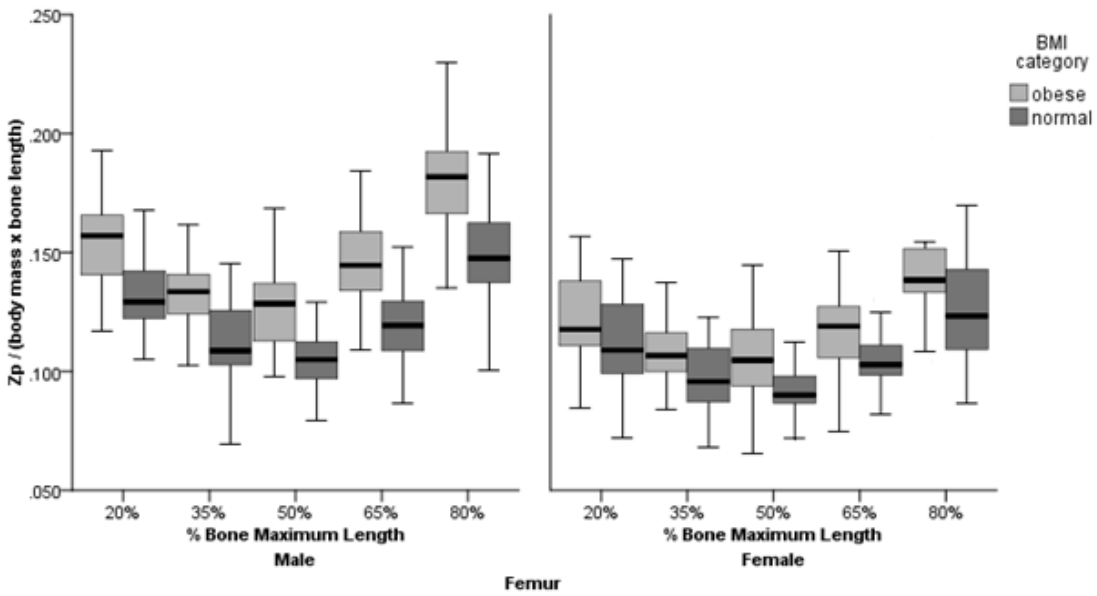

Figure 32. Standardized Polar Section Modulus (Z_p) for Femur by sex and BMI category
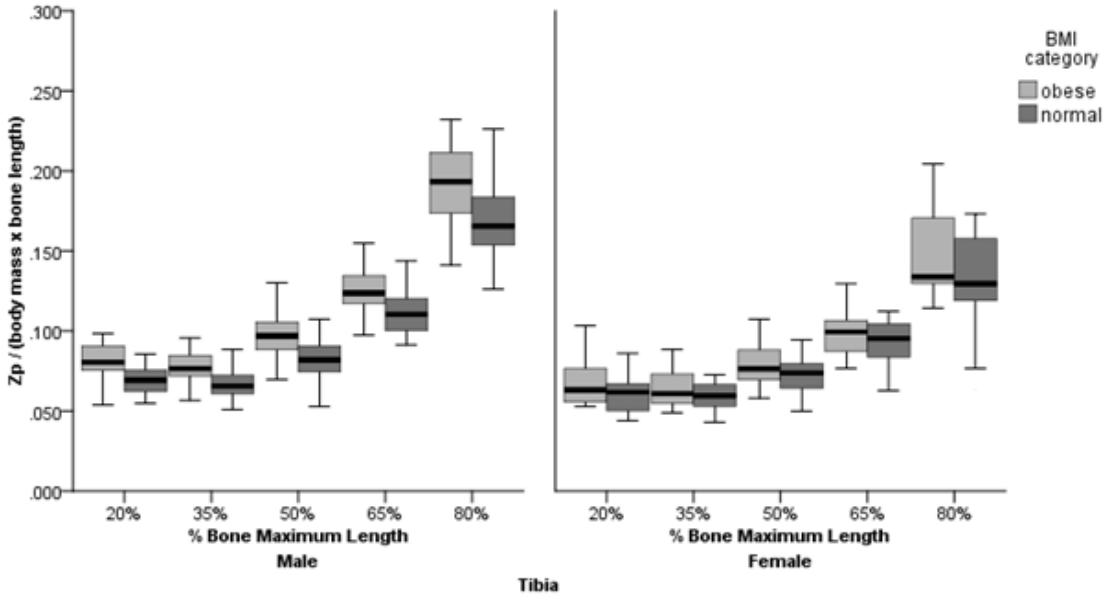
Figure 33. Standardized Polar Section Modulus (Z_p) for Tibia by sex and BMI category
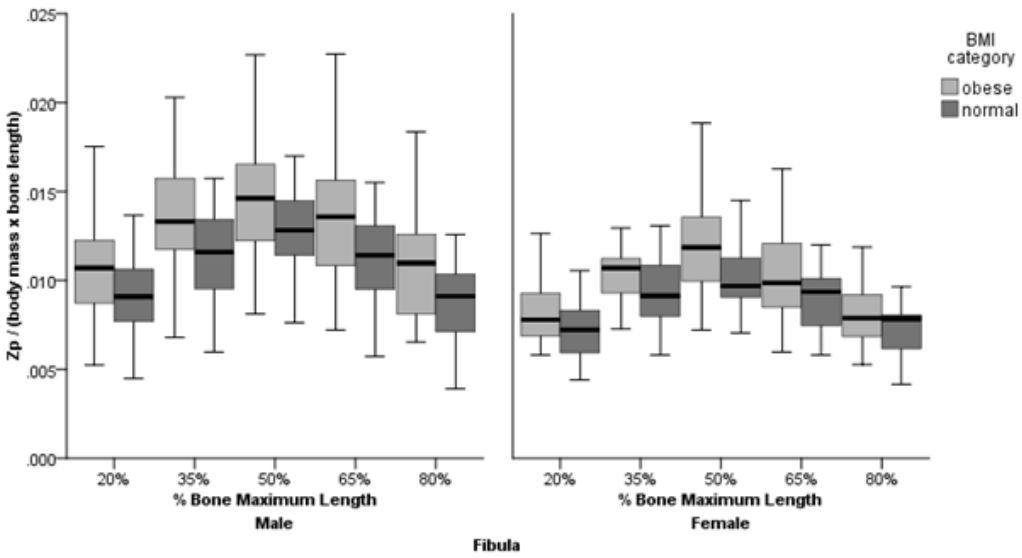

Figure 34. Standardized Polar Section Modulus (Z_p) for Fibula by sex and BMI category

For males, CA is significantly different between BMI categories for the humerus, femur, and tibia, with obese individuals consistently exhibiting greater values. The same is true for females, although a larger sample size (n=60) is necessary to reach statistical significance at α = 0.05. Patterns of %CA are also similar between the sexes. Obese individuals show significantly greater amounts cortical area relative to cross-section area for the femora and tibia when compared to normal mass individuals. Furthermore, the boxplots for cortical areas and total areas highlight sexual dimorphic differences in the sample, with males demonstrating consistently larger cortical areas throughout the skeleton, when compared to females, even after standardizing for size.

Perhaps the most informative result is that demonstrated for polar second moment of area, *J*. As reviewed in Chapter 3, this property is one of the most accurate and mechanically meaningful for estimation of bone strength (Lieberman et al. 2004). For males and females, this strength property is significantly different between obese and normal mass categories with respect to the humerus, femur, and tibia (as well as the fibula in males). These results indicate that the obese sample has greater strength properties than the normal mass group, and not only for weight bearing bones, as differences are detected for the humerus as well. The polar section modulus Z_p shows a similar pattern to J, where again, the obese group consistently has greater values. For both of these strength properties, sexual dimorphic characteristics can also be noted; in particular, diaphyseal torsional strength properties nearest to the knee joint (i.e., the distal 20% femur and proximal 80% tibia) for these CSG properties are especially disparate between sexes.

Articular Dimensions

A multivariate ANOVA was used to test whether or not there were differences in articular dimensions between sexes, age categories, and BMI categories. A significant main effect for sex ($p < 0.001$) indicates that the sexes should be treated separately with regards to the articular dimensions, just as for the diaphyseal measurements. Futher investigation of the articular dimensions reveals that age is a significant factor for all linear articular dimensions (humeral head diameter, femoral head diameter, tibial plateau breadth), with articular dimensions increasing with age for males only.

Next, an ANOVA was perfomed for each linear articular dimension, with BMI category and age category as factors. Results for each articular dimension show significant age effects only for males (Table 16). BMI category is only significant in the female tibial plateau measurement (Table 16; Figures 36-38). Curiously, the age effect shows an increase in articular dimensions with increasing age, in all three dimensions among males (though also in tibial plateau in females). This pattern will be considered further in the Discussion.

Table 16. ANOVA results for articular measurements representing the shoulder, hip, and knee

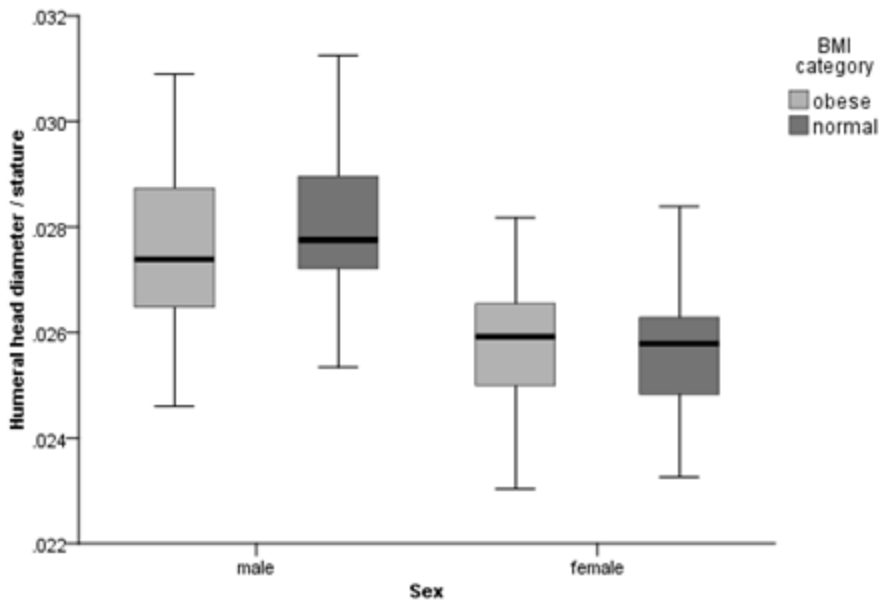|		Humeral head diameter			Femoral head diameter			Breadth of Tibial Plateau		
Sex	**Factor**	**df**	**F**	***p***	**df**	**F**	***p***	**df**	**F**	***p***
Male	Age	1	10.655	**0.002***	1	6.362	**0.014***	1	6.813	**0.011***
	BMI category	1	1.647	0.204	1	0.511	0.478	1	0.166	0.685
Female	Age	1	1.566	0.218	1	0.036	0.851	1	1.286	0.264
	BMI category	1	0.687	0.412	1	0.985	0.327	1	8.749	**0.005***

* significant $p < 0.05$

Figure 35. Boxplots between BMI category and sex for humeral head
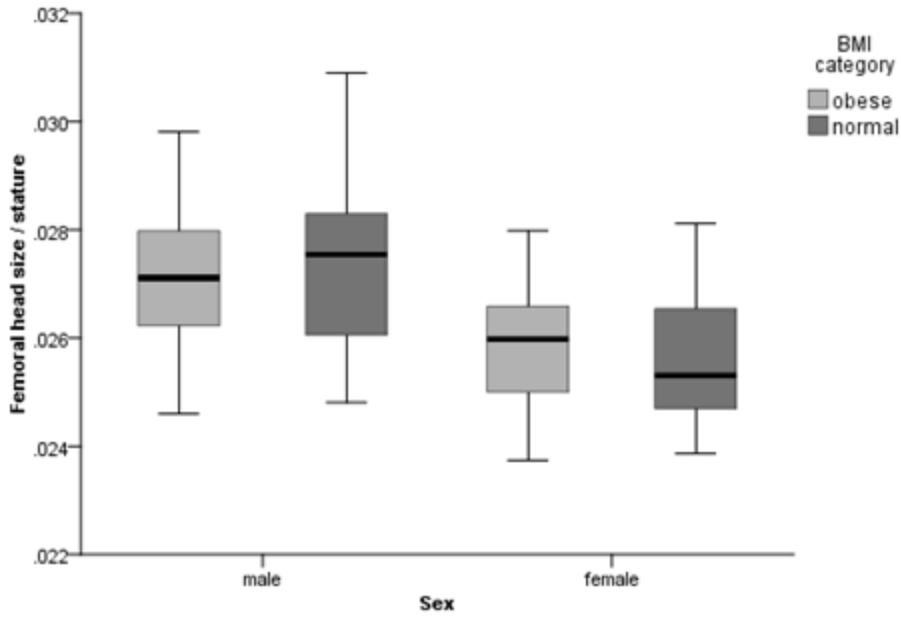
133

Figure 36. Boxplots between BMI category and sex for femoral head diameter

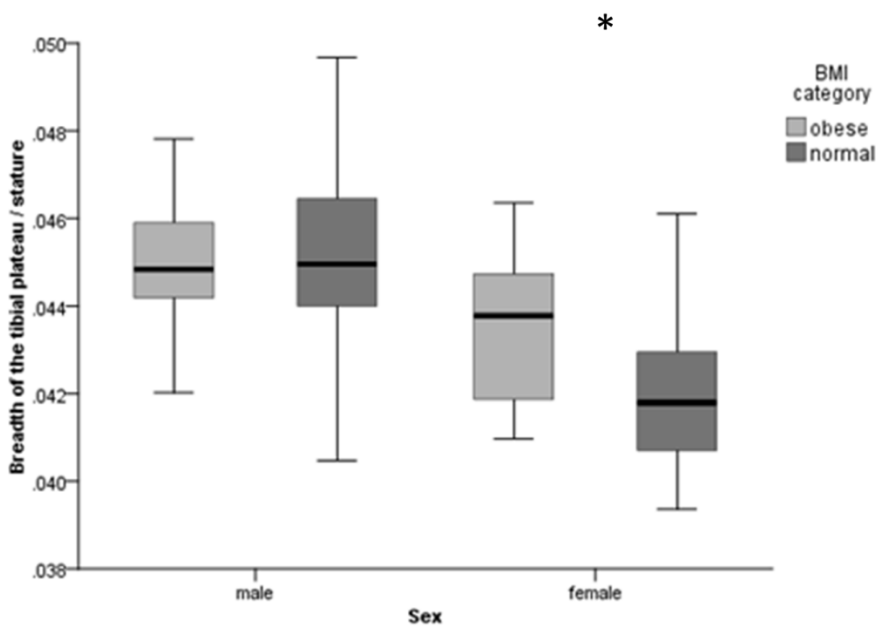**Figure 37. Boxplots between BMI category and sex for breadth of the tibial plateau**
* indicates significance (p < 0.05); ○ indicates trends (p < 0.10)

134

Cranial Vault Thickness

A series of ANOVA tests, with BMI category as the independent variable, and CA, TA, %CA, max 2D thickness, and mean 2D thickness separately as dependent variables were used to test for differences between groups. The max and mean 2D thicknesses were investigated as they would be the closest to thickness measurements taken with calipers. Descriptive statistics for the measurements (CA, TA, %CA, max 2D thickness, and mean 2D thickness) are presented in Table 17. Values for the pooled sample are included for a general idea of the overall group means. Results of the ANOVA tests for males and females are presented in Table 18, and the corresponding boxplots illustrate the differences in Figures 39-42. For males, the mean 2D thickness of the vault is statistically significant, and the max 2D thickness and TA of the vault trend toward significance. The thickness values, while significant, or nearly so, represent 1 mm mean difference between BMI groups; obese males present with higher values and a wider range of thickness values. As for TA, while the differences between BMI categories did not reach statistical significance, the difference in means between the groups for this CSG property is on the order of 100 mm. This measurement likely represents the accumulation of subtle thickness differences in vault thickness. These findings indicate that point selection (i.e. measuring vault thickness at a single point) may or may not capture the subtle differences between groups that can be detected when analyzing points along an arc (i.e., maximum or mean thicknesses). Computer software allowing for collection of information along an arc could be more informative than sampling grid points.

Table 17. Descriptive statistics for cranial vault measurements – Males and Females

Sex	CSG property	Normal		Obese		Pooled Sample	
		mean	sd	mean	sd	mean	sd
Male	CA (mm)	697	165	718	159	707	161
	TA (mm)	841	179	926	211	881	198
	%CA	84	13	79	16	82	15
	Max 2D Thickness (mm)	8.06	1.49	8.87	2.05	8.44	1.81
	Mean 2D Thickness (mm)	6.38	1.24	7.08	1.56	6.71	1.43
Female	CA (mm)	689	145	727	137	714	154
	TA (mm)	872	199	870	177	870	195
	%CA	81	15	85	13	84	14
	Max 2D Thickness (mm)	8.46	1.61	8.61	1.53	8.65	1.79
	Mean 2D Thickness (mm)	7.05	1.52	7.07	1.20	6.87	1.46

Table 18. Results of ANOVA tests for male and female cranial measurements

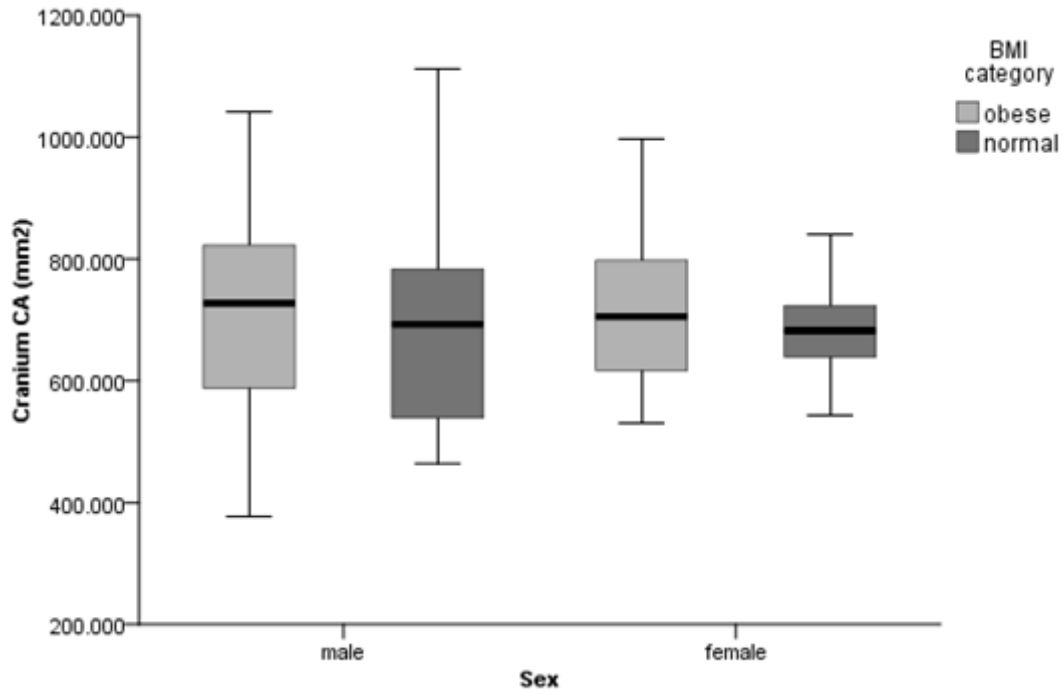| Factor	Males			Females		
	df	F	p	df	F	p
CA	1	0.247	0.603	1	0.756	0.390
TA	1	3.149	**0.081**	1	0.002	0.962
%CA	1	1.423	0.237	1	0.947	0.336
Max 2D Thickness	1	3.350	**0.072**	1	0.101	0.753
Mean 2D Thickness	1	4.015	**0.049***	1	0.002	0.963

*statistical significance $p < 0.05$

Figure 38. Cranial vault CA by sex and BMI category
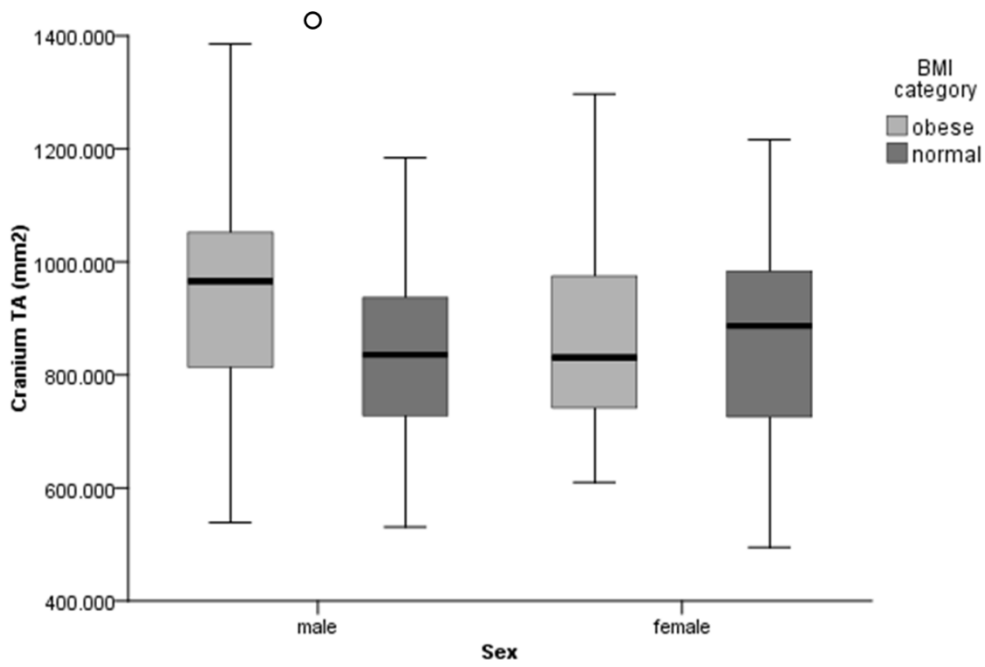
Figure 39. Cranial vault TA by sex and BMI category
* indicates significance (p < 0.05); ○ indicates trends (p < 0.10)

137
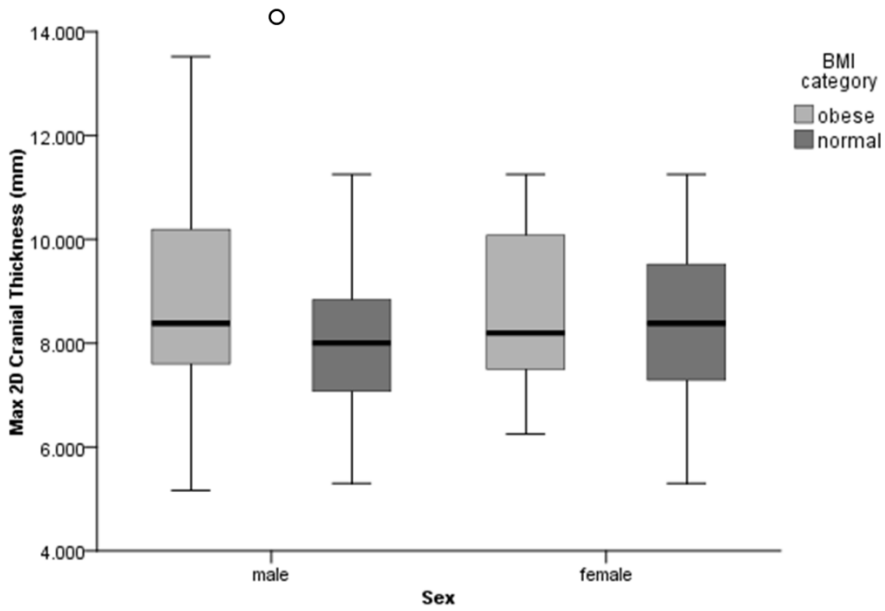
Figure 40. Cranial vault max 2D thickness by sex and BMI category
* indicates significance (p < 0.05); ○ indicates trends (p < 0.10)

Figure 41. Cranial vault mean 2D thickness by sex and BMI category
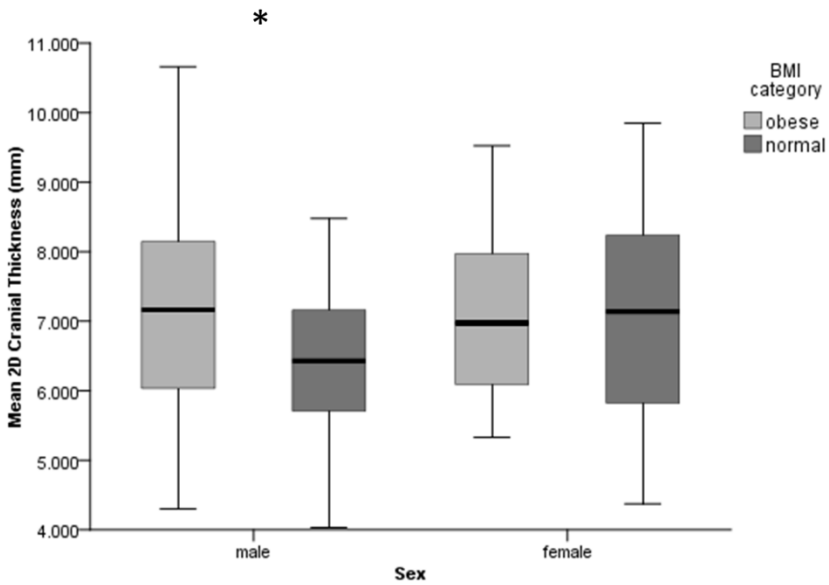* indicates significance (p < 0.05); ○ indicates trends (p < 0.10)

138

CHAPTER 8

DISCUSSION AND CONCLUSIONS

As shown in the results, there are notable differences in the morphology and mechanical properties of cortical bone between individuals classified into the normal and obese BMI categories. This chapter reviews these patterns of variation in relation to the background and hypotheses provided in chapters 2 through 5. As this study is one of the first to consider the interaction of mechanical and metabolic factors on bone and limb joint morphology throughout the skeleton, these patterns are a novel contribution, which will set the foundation for future studies of osteological responses to both mechanical and physiological factors associated with high-mass obesity.

The results of this study inform the existing literature concerning the relative influence of biomechanical and systemic neuroendocrine-metabolic factors on bone mass and shape throughout the skeleton. It is also acknowledged that the relationships between obesity and the significantly different morphologies should not be interpreted as causal, as that relationship cannot be drawn directly from this data. The findings presented here are intended as a first step in applying conclusions from the experimental literature, which often examines biomechanical or metabolic stimuli in isolation (despite the fact that both affect bone tissues in known capacities) to a human skeletal sample with known demographics.

Reviewing the Hypotheses, Aims, and Limitations of the Study

Before discussing the results, the hypotheses and aims of this study should be reviewed. The central question addressed by this research is whether there are differences in bone morphology associated with individuals classified as obese by their BMI, and if so, whether these differences are specific to certain limbs or generalized throughout the skeleton. The analyses were performed to investigate these effects on a macroscopic scale through comparisons of cross-sectional geometric properties and joint articular dimensions. Considering the available literature detailing biomechanical and neuroendocrine-metabolic effects on bone mass and shape, in general, obese individuals were expected to demonstrate greater CSG properties, especially in the lower limb (as it mechanically supports body weight) but not differences in joint size, relative to normal mass individuals.

More specifically, the hypotheses present a pair of expectations given what is known about the responses of bone to mechanical loading: 1) cortical bone is expected to have increased strength properties in limb long bones, but not the cranium, and 2) articular dimensions will not be significantly different. Central to these hypotheses is the inherent difference established in the literature about cortical bone response in the diaphysis of long bones versus the external articular dimensions; Lieberman et al. established much of this in 2001, wherein they demonstrated that articular dimensions do not change under variable experimental loading regimes, which do cause functional adaptation in the cross-sections of long bones. Ruff (1991) and Auerbach and Ruff (2006), among others (e.g., Reeves et al., in review), have also lent support to this pattern. The results of this study, as explored below, reinforce this separation in cortical bone response to mechanical loads. Furthermore, the study also examined the unique but unverified difference in cranial vault thickness observed by Lieberman and colleagues (1996) between exercised and

non-exercised model animals, where the former developed thicker cortical bone in the cranium independent of direct mechanical loading.

As with any non-experimental study, there are caveats and limitations to the current research that must be considered. The inherent complexity associated with the number of factors and their interactions that *could* affect bone tissue adaptation (see Chapters 3 and 4, and Figure 4) limits the scope and conclusions of the presented research. While it is acknowledged that *specific* mechanical (e.g. *in vivo* strains, detailed loading history) and systemic influences (e.g. genetics, levels of circulating hormones) cannot be assessed with this project, the suite of characteristics known to be linked with the obese phenotype provide the basis for a more general test: whether obesity is associated with differences in bone mass and/or shape in the form of localized and/or tissue-level adaptation. Although causal relationships cannot be established from the cross-sectional properties, associations between body mass and characteristics of the skeleton can be demonstrated. The examination of six skeletal elements from three biomechanically disparate regions, at the very least, provides a first step toward understanding the relative influence of these two broad factors: mechanics and metabolism.

After considering the known limitations of the research, exploration of the hypotheses yielded the following summary results:

1) Obesity is associated with greater macroscopic bone mass and strength properties for bones of the appendicular skeleton, in absolute terms. The only notable exception is for the cross-section shape index (I_{max}/I_{min}), where the group means for normal individuals are often greater, indicating greater AP elongation.

2) The larger CSG properties observed for obese individuals are greatest in magnitude, and statistically significant, especially for the femur and tibia. This is logical given the role of these bones in supporting body mass.

3) Strength properties were also significantly different between BMI categories for the humerus (as well as the fibula for males), as evidenced by measures of CA, J, and Z_p.

4) There is evidence for the differential effect of factors both between and within elements. Variation of CSG properties is greater in more proximal elements, relative to their distal counterparts (i.e., the humerus relative to the radius). Furthermore, distal segments within a diaphysis are often more constrained; the tibia is the best example of this generalization.

5) Even after size-standardization, there are notable sex differences with respect to cross-section geometry and strength properties.

6) Obese and normal mass individuals, overall, do not differ in linear dimensions of the joints. The only exception is the female tibial plateau, where statistical significance indicates obese females have wider tibial plateaus.

7) While significantly different in their recorded body masses, obese and normal mass individuals do not differ in their estimated body mass from femoral head size. This lends support to the test (see item five above) that indicates no significant increased external articular bone apposition or expansion in obese individuals relative to the normal weight individuals.

8) Despite the lack of differences between the BMI groups, older males exhibit larger articular dimensions than younger males.

9) Obese and normal mass individuals do not differ in cross-sectional areas of the cranial vault. Thickness values for males, however, indicate statistically significant differences on the order of 0.5 to 1 millimeter greater in the obese sample. TA of the male cranial vault also demonstrates a trend toward significant differences between the BMI groups.

The subsequent sections discuss these results in detail. Special consideration is first given to the effects of using femoral head-derived body mass estimates, rather than recorded body mass, in the scaling factors for the CSG properties. Age and sex effects are also revisited, followed by a section relating the results directly to the hypotheses. Finally, an explanation of how the results generally inform (and are informed by) the broader theory provided in Chapters 2 through 4 is presented.

Synthesizing the Results

The Effect of Body Mass Choice on Scaling

As shown in Chapter 7 (Table 9), there were no significant differences between BMI groups in the estimated body masses (i.e., their femoral head diameters were not significantly different), despite significant differences in their recorded body masses. This result was used to argue that, as femoral head size is apparently not affected by increased body mass, its use—or body masses derived from it—provides a scaling factor that is independent from the effects of increased body weight, thus avoiding a tautology. It is interesting, though not unexpected (see Hypothesis Set 2), that femoral head size does not track with changes in body mass. Thus, this

study lends support to the hypothesis that the femoral head predicts something more like "lean mass" or, possibly, genetically programmed mass at skeletal maturity (see Ruff 2007). The findings regarding standardization of cross-sections by estimates from the femoral head also indicate differences noted between BMI groups can be attributed to effects associated with the non-lean (fat) mass, and also inform Hypothesis Set 2. These implications will be discussed in more detail in the sections to follow.

An ontogenetic, longitudinal study would be necessary to assess whether femoral head size adapts to the increased loading in juveniles with early onset obesity. Anecdotal evidence, as provided in Figure 3 of Ruff's 2007 paper, seems to indicate integration in the development of femoral length and femoral head breadth to the exclusion of variation in body mass (so, for a period, juveniles may have disproportionately large femoral heads for their body masses). Generally, though, an increase in articular surface area (and the linear articular dimensions, by proxy) would help distribute greater loads, although to what extent the size of the femoral head is predetermined is unknown. It is possible that it is more adaptable at a younger age.

Age and Sex Effects

After standardizing the cross-sectional geometric properties of each element using estimated body mass and following the protocols explained in Chapter 6, it was necessary to determine how age and sex might be affecting the sample. BMI and age did not covary in the sample; this did not mean that individuals' body masses did not increase or decrease with age, but that there was no systematic bias in the sample for the magnitude of BMIs among ages; that is, BMI did not change with age. Differences between the sexes were predicted based on previous study results, but a test for the midshaft femur confirmed that sex is a significant factor

differentiating the CSG property measurements between BMI groups. Thus, support for separating the sexes was validated. This effect is likely due to sexual dimorphism in bone strength and rigidity properties, even when they are scaled for body size; males tend to have greater measures of these CSG properties than females, despite reduced sexual dimorphism in postindustrial populations (Ruff et al. 1993). Whether obesity has additional sexually dimorphic effects on the CSG properties of the skeleton may be ascertained by comparing the results of tests conducted for Hypothesis Set 1.

Synthesizing Hypothesis Set 1

Limb bone cross-sectional geometric properties

Obese individuals can generally be characterized as having increased strength in resistance to compression, bending, and torsion, as evidenced by greater strength properties (e.g. CA, J, and Z_p) throughout the skeleton, when compared to individuals of normal mass. Boxplots presented in the previous chapter provide a quick visual illustrating the differences discussed hereafter. The mean values for cortical area (CA), polar moment of area (J), and polar section modulus (Z_p) are absolutely greater at 19 out of 21 cross-sections throughout the skeleton (the exceptions being the proximal and distal radius). These findings suggest that obese individuals adapt stronger bones throughout the appendicular skeleton, not exclusively in the load bearing bones of the lower limb; significant differences for strength properties between groups are found in the humerus and male fibula as well.

The results for cross-section properties measuring bone strength in multiple planes (axial compression: CA; bending and torsion: J, Z_p) also highlight the expectation that bones experiencing different loading regimes will demonstrate different magnitudes of strength

properties. As predicted, the femur (followed by the tibia) of obese individuals adapted the strongest cross-sectional properties, and greatest magnitude of difference between BMI groups. When further examining magnitudes of difference, sexually dimorphic results are also found throughout the skeleton. In general, the patterns between males and females are similar (i.e., the boxplots demonstrate the same overall shape); however, the magnitudes of CSG properties for males are consistently greater than those for females, even after standardizing for size. These findings are especially pronounced in the measures of CA, J, and Z_p, as well as TA of the upper limb. Overall, when examining the lower limb, it is clear that the significant differences between BMI groups can be attributed to obesity, but the findings here do not inform whether the effects of obesity are mechanic or metabolic (or both).

In absolute terms, strength properties of the humerus and fibula of obese individuals also demonstrate greater values for cross-section strength properties. The results for the humeri of both sexes indicate significant differences between BMI categories for CA, J, and Z_p (as well as %CA for males). The differences are distinct, but they are less in magnitude than those reported for the femur. These results for the humeri indicate that there are effects of obesity that can be detected in regions of the skeleton beyond body weight-bearing bones. At present, the significant differences discovered for the humerus are known to be associated with obesity, but again, the mechanic and/or metabolic effects cannot be teased apart. Findings for the humerus could be the result of three possibilities: 1) increased fat mass of the arm, and therefore loading of the arm, have resulted in the differential CSG properties; 2) the increased adipose tissue in the upper limb as well as throughout the body has resulted in secretion of circulating hormones signaling for increased bone remodeling; 3) a combination of these two sets of factors.

Findings for the male fibula reveal similar difficulties for interpretation. The torsional strength indicators, J and Z_p were significantly different between BMI categories, again with the obese group demonstrating larger values. Greater magnitudes were found primarily in the distal fibula (20-50%). These results seem to suggest a greater role for weight bearing of the fibula in obese males; however, hormonal effects cannot be ruled out. Gait analysis of the fibula should be assessed to see if, and by what magnitude, the fibula functions in increased load bearing capacities for obese versus control groups. Results of such a study would reveal whether or not the biomechanics of obesity are primarily responsible for the differences noted for strength properties.

Because the largest physiologic loads placed on bones are from muscle contraction, muscle forces scale to muscle cross-sectional area, and lean mass is predominantly muscle (Janz et al. 2007), it follows that, controlling (standardizing measurements) for lean mass leaves differences between groups to be explained by physical activity levels (moderate to vigorous in intensity) and/or a combination of mechanical/systemic effects associated with the remaining non-lean mass (fat mass). Studies of physical activity and obesity have noted that as BMI increases, average daily steps taken decrease (Vincent et al. 2012a). Yamakawa et al. (2004), for example, demonstrate that obese individuals (characterized by BMI in excess of 30 kg/m^2) take an average of 55% fewer steps per day than non-obese individuals. With evidence from the literature suggesting an obese BMI is associated with reduced physical activity, muscle weakening, and increased joint stiffness and pain (O'Keefe et al. 2011; Sherwood et al. 2013; Vincent et al. 2012b), it can be inferred that the obese individuals in the current sample are likely less active than the normal mass group. If this is the case, and even if obese individuals have weaker muscle (less lean tissue mass), standardizing the cross-sections by a proxy for lean body

mass, should, if anything, reduce the magnitude of differences between BMI groups. Furthermore, the increased strength properties noted for males and females for the humerus, femur, and tibia can be wholly attributed to effects associated with obesity, either biomechanical (excess mass) or systemic (neuroendocrine-metabolic).

The whole-diaphyses data for proximal and distal skeletal elements presented here further inform the theory that variability in bone robusticity decreases along a proximal-to-distal gradient, likely as a result of energetic trade-off between bone strength and weight (Stock 2006). In general, the results support this idea, as the radius and tibia demonstrate particularly constrained ranges of values, relative to their proximal counterparts (humerus and femur, respectively). Furthermore, distal segments within the diaphysis, especially of the lower limb, demonstrate less variation, evidenced by the shorter whiskers of the boxplots for these cross-sections; the proximal to distal gradient noted for the tibia is the most obvious example. These findings support the differential effect of factors both between and within elements.

Cranial vault geometry

Cross-sectional areas of the cranial vault arc were not statistically significantly different between obese and normal mass individuals. These findings indicate that there are no macroscopically detectable systemic differences between groups with regards to mass of the cranial vault at the specified arc. This finding was expected, as the vault reflects minimal mechanical loading; thus, any changes associated with increased mass due to obesity should have no mechanical affect that would impact bone formation or resorption in the vault. However, mean two-dimensional thickness and maximum two-dimensional thickness values for obese males were statistically significantly different from the normal BMI males. The magnitude of

148

these differences is on the order of 0.5 to 1 millimeter. This result could have two interpretations: 1) although statistically significant, this difference between groups is not biologically significant—there are no meaningful systemic hormonal effects resulting in thickness differences in the cranial vault; or, 2) when viewing the cranial vault at the macroscopic level, the differences between the BMI groups are so small in magnitude that they would be better analyzed microscopically. The low (but not significant) *p*-values in the male total area comparison may indicate that a series of minute differences between groups add up along the arc, as this trend is of a greater magnitude, around 100 millimeters difference between groups.

Taken together, the results of the cranial assessment suggest that further inquiry into the use of cranial arc data should be undertaken. It appears that measures procured when viewing the whole arc may be more informative of differences between groups, rather than particular point selections. That is, a single point selection, or even a series of point selections, on the vault may miss the important differences between groups. CT technology provides a way to analyze all points along an arc, which could better elucidate systemic differences between BMI groups.

While additional cranial vault arcs, as well as microscopic study, should be considered in the future, current results suggest that known neuroendocrine-metabolic stimuli are not responsible for biologically significant differences in amounts of bone deposition between BMI categories, at the macroscopic level. Taken one step further, the findings suggest that biomechanical stimuli have a greater relative influence on macroscopic bone properties than systemic factors (considered as a whole) typically associated with obesity. Once again, the individuals incorporated into the study sample had no known metabolic or chronic illness, although unreported or undiagnosed conditions remain a possibility within the sample.

Synthesizing Hypothesis Set 2

The results partially support hypothesis set 2, as only one of the linear articular dimensions varied significantly between the BMI categories (tibial plateau breadth in females). Obese females demonstrate plateau breadths that are, on average, one millimeter wider. This finding is unexpected, and should be explored further. It could be that pathological bone growth associated with obesity as well as osteoarthritis is incorporated into the breadth measurement, as clear delineation of the articular surface becomes obscured, or that the statistical significance is not biologically significant, or would not be significant in a larger female sample. As discussed in detail above, femoral head diameter is not significantly different between BMI categories. Coincidentally, body mass estimates from these measurements are not significantly different either, though this simply indicates that the obese and normal BMI individuals likely come from the same general source population. For this study, the advantage for using the estimated body masses was that they would provide a standardizing measure that preserved the effect of interest, the effect of obesity. Overall, the lack of significance between BMI groups and articular dimensions are in line with previous research that indicates that articular dimensions are less susceptible to environmental factors (including mechanics) than diaphyseal breadths (Auerbach and Ruff 2006; Reeves et al. in review).

The significant age effects for male articular dimensions was unexpected, especially the finding that older males tended toward greater articular dimensions; however, the differences between the means of the older and younger groups are nominal. This could be an artifact of disparate sample sizes between the two groups, as the mean differences are very close, and the younger sample is approximately half the size of the older category. When the males are divided further into decadal groups (30-39, 40-49, 50-59, 60+) the age effect disappears. This finding

150

could also be explained by secular changes. Males born more recently could be experiencing earlier maturation, resulting in smaller articular dimensions. An increased sample of younger male individuals would be necessary to assess the significance of an age effect, if there still appears to be one.

Results in Light of Prior Understanding of Mechanical and Metabolic Effects on Bone

This project provides evidence for an interaction between biomechanics and metabolic effects, with the biomechanical effects being relatively more influential at the macroscopic level. The greatest differences in strength properties between BMI categories are found in the two bones resisting the greatest loads in the lower limb (the femur and tibia), reinforcing expectations from the biomechanics literature, while the significant differences between BMI categories for the humerus and, to a lesser degree, the fibula appear to reflect systemic responses, perhaps from factors like leptin and related hormones. As a whole, though, the mechanical effects of obesity throughout the skeleton are important on their own. As expected, load bearing bones of the lower limb exhibit differences between BMI categories, and the magnitude of these differences is significantly greater (stronger) in resistance to compressive, bending, and torsional loads. Greater strength properties, representing resistance to compressive, bending, and torsional loads, support the conclusion that obese individuals functionally adapt stronger bones to support the increased body mass, when compared to normal mass individuals.

These findings would be supplemented by subadult data or known age of onset of obesity; however, the results support reasonable inference that the current sample was not

151

collectively obese as pre-adolescents. As indicated, many of the differences between BMI groups for both males and females are largely in measures of CA, rather than TA (i.e., in %CA); the obese sample represented here appear to have increased CSG properties as a result of endosteal bone deposition. Individuals who were obese as children should present with increased TA of the cross-sections, and not necessarily CA. Because the subadult skeleton is more adaptable than the adult skeleton (after primary growth), these findings indicate that the population sampled here were not obese as children. Additionally, the non-significant differences in articular dimensions suggest that the obese and normal mass samples were comparable prior to cessation of primary growth; these samples originate from the same general population. Larger articular dimensions may be expected as well, if the individuals were obese at a very young age. However, given the apparent canalization and developmental stability argued to exist in the limb articular dimensions discussed in Chapter 3, the lack of larger articular sizes in obese individuals may be further evidence of restricted morphological change in these dimensions in response to environmental variables.

Cortical thicknesses and CSG properties have clearly been shown to be important factors in determining bone strength, and they follow the same general patterns within diaphyses, after controlling for bone length and body mass. In general, the tissue responds in a similar pattern within a diaphysis (regardless of BMI group), keeping bone and muscle stresses relatively constant and likely serving as a compromise between optimal stiffness and minimal weight; limb bones must be grown and maintained in addition to functioning during locomotion (Biewener 1989). The consistent patterning of cross-sectional structure after scaling indicates that cortical bone adaptation is tracking to a particular range of variance as a result of pre-programmed limitations. The skeleton, as a system, seems to adapt on a tissue level in response to functional

locomotor demands, as well as systemic pre-adapted demands. This finding is demonstrated by the overall lack of significant within-subjects interaction effects between BMI category and cross-section location; one exception being the cross-section shape index of the femur, which indicates obese individuals have more circular shaped cross-sections throughout the femur. Distal segments of the limb, especially the lower limb in humans, must be light enough to reduce forces of inertia needed to accelerate the limb during gait. Therefore, the pattern of reduced variability of CSG properties proximal to distal (again, regardless of BMI category) may also be the result of pre-programmed morphological integration.

In addition, the present study supports existing research regarding morphological integration of different types of limb bone measurements. The diaphyseal measurements exhibited more phenotypic plasticity, as evidenced by significantly CSG properties different between BMI groups, relative to articular dimensions. As expected, articular dimensions appear to be more genetically canalized, and less susceptible to adaptation after skeletal maturity, relative to diaphyseal measures.

Sexually dimorphic responses to factors known to affect bone and adipose tissues are exemplified by the differences in measures, even after size-standardization of the cross-sections. These differences are likely due to systemic factors. For example, sex differences of the cranial vault could be due to the differential effects of estrogen in the sample, or a lack of loading-induced signaling. The small sample of females, coupled with the small number of females under the age of fifty, indicates that post-menopausal estrogen reduction is likely affecting the bone strength properties of older females. Males, in contrast, would demonstrate estrogen decline but at a slower pace compared to females (Chapter 4). This could be one reason for the sexual dimorphism of the cranial vault thicknesses, as well as the small magnitude of difference noted

for obese males. The cranial vault findings are of particular interest, and further assessment and the addition of a younger sample.

It is also important to consider that the cranial vault has an intramembranous origin, unlike the endochondral origins of much of the rest of the skeleton, and could be responding to mechanical factors or systemic factors differently. The cranial vault may be more genetically canalized, more similar to bone maximum lengths or articular dimensions. The research presented here lends support to the effectiveness of studying the skeleton as a system, rather than focusing on just the cranium or the postcrania. The cranium could be an important contributor to future research in teasing apart systemic versus mechanical adaptations of bone.

When the whole study is examined together, it is important to remember that mechanical and systemic factors are truly interactive. Many of the endocrine responses known to elicit bone formation or resorption can be partially mediated by the same signaling pathways induced by dynamic loading (Figure 4). When viewed this way, mechanical effects are exogenous factors that serve as the impetus for signaling cascades, produced, initiated, and mediated by endogenous circulating factors/pathways; these signals can involve many body systems (e.g., the endocrine, immune, nervous, reproductive, skeletal, circulatory systems in particular).

Future Directions

This study serves as the first in a series of steps toward investigating potential systemic effects in a human skeletal sample. Ideally the relationships explored through this research should be tested using experimental models. In addition, more direct comparisons of experimental findings using murine models to conclusions from human samples with known demographics would be useful for validating the experimental models (e.g., mice, sheep, etc.)

154

widely used for obesity research. Comparing a known obese sample with various athletic samples would also be of interest to elucidate systemic differences in skeletal dimensions throughout the body.

A larger sample size (especially for females and younger individuals) coupled with the inclusion of individuals in the underweight and overweight BMI categories are also obvious next steps for expanding the scope of the current hypotheses. Additionally, subadult data would greatly enhance this study, as much of adult bone morphology is set by the age of skeletal maturity.

Conclusions

In sum, this research should be accepted as an initial investigation into the relative impacts of biomechanical and systemic factors on cortical areas and cross-sectional properties throughout the skeleton. While direct causal impact on bone morphology cannot be delineated herein, several trends and patterns of bone mass and shape differences between obese and normal mass phenotypes have been presented, allowing for three general conclusions:

1) Biomechanical effects on the human skeleton are relatively greater in magnitude than systemic effects, but are not the only influence on skeletal morphology. Obese individuals functionally adapt greater strength properties, which can be seen throughout the skeleton, especially in the humerus, femur, tibia, and fibula. As would be expected from biomechanical studies, load bearing bones of the lower limb display the highest levels of diaphyseal strength properties relative to bones of the upper limb and fibula. The small increases in cranial vault thicknesses for obese males suggests that cranial arc data should be further explored, perhaps with micro CT imaging.

155

2) The skeleton, as a system, seems to adapt on a tissue level in response to functional locomotor demands, as well as systemic pre-adapted demands. Distal segments of the limb, especially the lower limb in humans, must be light enough to reduce forces of inertia needed to accelerate the limb during gait. Therefore, the pattern of reduced variability of CSG properties proximal to distal may be the result of pre-programmed morphological integration.

3) Articular dimensions appear to be highly constrained, relative to diaphyseal measures, and less susceptible to adaptation after skeletal maturity.

Applications of Conclusions

As the obesity epidemic continues to expand in the United States and worldwide, a thorough understanding of its etiology and effects on the human body are essential. While the effects of obesity on bone mechanics in humans is still being established, studies such as this one, aimed at assessing the relative influence of the factors known to affect bone tissue, will benefit practitioners and researchers spanning many disciplines. Clinicians, physical therapists, biomedical researchers, and the like, will need to be informed on how obesity alters the skeleton, as they treat patients to manage or reduce their excess body mass, through solutions such as exercise. Findings of this research will also be important to biomedical engineers and orthopedists in the effective design and construction of prostheses and joint replacements for obese individuals.

Within the field of anthropology, this study also has broad impact, informing the literature with regard to the relative influence of biomechanic and systemic adaptations of bone. These findings add to the breadth of knowledge with respect to interpretations of body size,

156

behavior, and adaptation from skeletal remains, which would be useful in both archaeological and forensic contexts. The conclusions presented here also provide supporting evidence for the utility of diaphyseal strength and shape properties of the lower limbs for interpretations of loading history. More generally, the current research helps in understanding the complex interactions of factors known to influence bone morphology.

LIST OF REFERENCES

Ackermann RR. 2009. Morphological Integration and the Interpretation of Fossil Hominin
Diversity. Evolutionary Biology 36(1):149-156.

Agostini GM, and Ross AH. 2011. The effect of weight on the femur: a cross-sectional analysis.
Journal of forensic sciences 56(2):339-343.

Alemany M. 2013. Relationship between energy dense diets and white adipose tissue
inflammation in metabolic syndrome. Nutrition Research 33(1):1-11.

Algire C, Medrikova D, and Herzig S. 2013. White and brown adipose stem cells: from signaling
to clinical implications. Biochimica et biophysica acta 1831(5):896-904.

Anderson PH, Atkins GJ, Turner AG, Kogawa M, Findlay DM, and Morris HA. 2011. Vitamin
D metabolism within bone cells: effects on bone structure and strength. Mol Cell
Endocrinol 347(1-2):42-47.

Anderson PH, Lam NN, Turner AG, Davey RA, Kogawa M, Atkins GJ, and Morris HA. 2013.
The pleiotropic effects of vitamin D in bone. J Steroid Biochem Mol Biol 136:190-194.

Antuna-Puente B, Feve B, Fellahi S, and Bastard JP. 2008. Adipokines: The missing link
between insulin resistance and obesity. Diabetes & Metabolism 34(1):2-11.

Aoki A, Muneyuki T, Yoshida M, Munakata H, Ishikawa SE, Sugawara H, Kawakami M, and
Kakei M. 2011. Circulating osteocalcin is increased in early-stage diabetes. Diabetes
research and clinical practice 92(2):181-186.

Aspden RM. 2008. Osteoarthritis: a problem of growth not decay? Rheumatology (Oxford)
47:1452-1460.

Aspden RM. 2011. Obesity punches above its weight in osteoarthritis. Nature Reviews
Rheumatology 7(1):65-68.

Auerbach BM, and Raxter MH. 2008. Patterns of clavicular bilateral asymmetry in relation to the

    humerus: variation among humans. Journal of human evolution 54(5):663-674.

Auerbach BM, and Ruff CB. 2004. Human body mass estimation: a comparison of

    "morphometric" and "mechanical" methods. American journal of physical anthropology

    125(4):331-342.

Auerbach BM, and Ruff CB. 2006. Limb bone bilateral asymmetry: variability and commonality

    among modern humans. Journal of human evolution 50(2):203-218.

Auerbach BM, and Sylvester AD. 2011. Allometry and apparent paradoxes in human limb

    proportions: implications for scaling factors. American journal of physical anthropology

    144:382-391.

Barneda D, Frontini A, Cinti S, and Christian M. 2013. Dynamic changes in lipid droplet-

    associated proteins in the "browning" of white adipose tissues. Biochimica et biophysica

    acta 1831(5):924-933.

Beck T, Ruff CB, Scott W, Plato C, Tobin J, and Quan C. 1992. Sex differences in geometry of

    the femoral neck with aging: a structural analysis of bone mineral data. Calcified tissue

    international 50:24-29.

Bell CG, Walley AJ, and Froguel P. 2005. The genetics of human obesity. Nature Reviews

    Genetics 6(3):221-234.

Bellido T, and Hill Gallant KM. 2014. Chapter 15 - Hormonal Effects on Bone Cells. In: David

    BB, and Matthew RA, editors. Basic and Applied Bone Biology. San Diego: Academic

    Press. p 299-314.

Bellido T, Saini V, and Pajevic PD. 2013. Effects of PTH on osteocyte function. Bone

    54(2):250-257.

Bennell KL, and Hinman RS. 2011. A review of the clinical evidence for exercise in osteoarthritis of the hip and knee. Journal of Science and Medicine in Sport 14(1):4-9.

Beranger GE, Karbiener M, Barquissau V, Pisani DF, Scheideler M, Langin D, and Amri EZ. 2013. In vitro brown and "brite"/"beige" adipogenesis: human cellular models and molecular aspects. Biochimica et biophysica acta 1831(5):905-914.

Berryman DE, Glad CA, List EO, and Johannsson G. 2013. The GH/IGF-1 axis in obesity: pathophysiology and therapeutic considerations. Nat Rev Endochrinol 9:346-356.

Biewener A. 1989. Scaling body support in mammals: limb posture and muscle mechanics. Science 245:45-48.

Blum WF, Englaro P, Hanitsch S, Juul A, Hertel NT, Muller J, Skakkebaek NE, Heiman ML, Birkett M, Attanasio AM et al. . 1997. Plasma letptin levels in healthy children and adolescents: dependence on body mass index, body fat mass, gender, pubertal stage, and testosterone. Clin Endocrinol Metab 82:2904-2910.

Bohler H, Jr., Mokshagundam S, and Winters SJ. 2010. Adipose tissue and reproduction in women. Fertil Steril 94(3):795-825.

Bolamperti S, Mrak E, Moro G, Sirtori P, Fraschini G, Guidobono F, Rubinacci A, and Villa I. 2013. 17beta-estradiol positively modulates growth hormone signaling through the reduction of SOCS2 negative feedback in human osteoblasts. Bone 55(1):84-92.

Brahmabhatt V, Rho J, Bernardis L, Gillespie R, and Ziv I. 1998. The effects of dietary-induced obesity on the biomechanical properties of femora in male rats. Int J Obes 22:813-818.

Bredella MA, Torriani M, Ghomi RH, Thomas BJ, Brick DJ, Gerweck AV, Harrington LM, Breggia A, Rosen CJ, and Miller KK. 2011. Determinants of bone mineral density in obese premenopausal women. Bone 48(4):748-754.

Brickley M, and Ives R. 2008. The bioarchaeology of metabolic bone disease. San Diego, CA: Elsevier.

Bridges PS. 1995. Skeletal biology and behavior in ancient humans. Evolutionary anthropology 4:112-120.

Brunner AM, Henn CM, Drewniak EI, Lesieur-Brooks A, Machan J, Crisco JJ, and Ehrlich MG. 2012. High dietary fat and the development of osteoarthritis in a rabbit model. Osteoarthritis and cartilage / OARS, Osteoarthritis Research Society 20(6):584-592.

Burr DB. 1997. Muscle strength, bone mass, and age-related bone loss. Journal of bone and Mineral Research 12(10):1547-1551.

Burr DB, Robling AG, and Turner CH. 2002. Effects of biomechanical stress on bones in animals. Bone 30(5):781-786.

Burr DB, Turner CH, Naick P, Forwood MR, Ambrosius W, Sayeed Hasan M, and Pidaparti R. 1998. Does microdamage accumulation affect the mechanical properties of bone? Journal of biomechanics 31(4):337-345.

Butcher MT, White BJ, Hudzik NB, Gosnell WC, Parrish JH, and Blob RW. 2011. In vivo strains in the femur of the Virginia opossum (*Didelphis virginiana*) during terrestrial locomotion: testing hypotheses of evolutionary shifts in mammalian bone loading and design. J Exp Biol 214(2631-2640).

Caluwaerts S, Lambin S, van Bree R, Peeters H, Vergote I, and Verhaeghe J. 2007. Diet-induced obesity in gravid rats engenders early hyperadiposity in the offspring. Metabolism 56(10):1431-1438.

Cannon B, and Nedergaard J. 2003. Brown adipose tissue: function and physiological significance. Physiol Rev 84:277-359.

Capurso C, and Capurso A. 2012. From excess adiposity to insulin resistance: The role of free fatty acids. Vascular Pharmacology 57(2–4):91-97.

Carey AL, and Kingwell BA. 2013. Brown adipose tissue in humans: Therapeutic potential to combat obesity. Pharmacology & therapeutics 140(1):26-33.

Carlton ED, Demas GE, and French SS. 2012. Leptin, a neuroendocrine mediator of immune responses, inflammation, and sickness behaviors. Hormones and Behavior 62(3):272-279.

Carson EA, Kenney-Hunt JP, Pavlicev M, Bouckaert KA, Chinn AJ, Silva MJ, and Cheverud JM. 2012. Weak genetic relationship between trabecular bone morphology and obesity in mice. Bone 51(1):46-53.

Carter DR, Beaupre GS, Wong M, Smith RL, Andriacchi TP, and Schurman DJ. 2004. The mechanobiology of articular cartilage development and degeneration. Clinical Orthopaedics and Related Research(427):S69-S77.

Carter DR, and Orr TE. 1992. Skeletal development and bone functional adaptation. Journal of Bone and Mineral Research 7:S389-S395.

CDC. The history of state obesity prevalence. Division of Nutrition, Physical Activity, and Obesity, National Center for Chronic Disease Prevention and Health Promotion.

Chandra A, Lan S, Zhu J, Lin T, Zhang X, Siclari VA, Altman AR, Cengel KA, Liu XS, and Qin L. 2013. PTH prevents the adverse effects of focal radiation on bone architecture in young rats. Bone 55(2):449-457.

Chechi K, Carpentier AC, and Richard D. 2013. Understanding the brown adipocyte as a contributor to energy homeostasis. Trends in Endocrinology & Metabolism 24(8):408-420.

Cheverud JM. 1982. Phenotypic, genetic, and environmental morphological integration in the cranium. Evolution 36(3):499-516.

Cheverud JM, Lawson HA, Fawcett GL, Wang B, Pletscher LS, A RF, Maxwell TJ, Ehrich TH, Kenney-Hunt JP, Wolf JB et al. . 2011. Diet-dependent genetic and genomic imprinting effects on obesity in mice. Obesity 19(1):160-170.

Cheverud JM, Pletscher LS, Vaughn TT, and Marshall B. 1999. Differential response to dietary fat in large (LG/J) and small (SM/J) inbred mouse strains. Physiol Genomics 1:33-39.

Chim SM, Tickner J, Chow ST, Kuek V, Guo B, Zhang G, Rosen V, Erber W, and Xu J. 2013. Angiogenic factors in bone local environment. Cytokine & Growth Factor Reviews 24(3):297-310.

Cole HA, Yuasa M, Hawley G, Cates JM, Nyman JS, and Schoenecker JG. 2013. Differential development of the distal and proximal femoral epiphysis and physis in mice. Bone 52(1):337-346.

Currey JD. 2002. Bones: Structure and Mechanics. Princeton, NJ: Princeton University Press.

Currey JD. 2003. The many adaptations of bone. Journal of biomechanics 36(10):1487-1495.

Currey JD, Landete-Castillejos T, Estevez JA, Olgiun A, Garcia AJ, and Gallego L. 2009. The Young's Modulus and impact energy absorption of wet and dry deer cortical bone. The Open Bone Journal 1:38-45.

Darcy A, Meltzer M, Miller J, Lee S, Chappell S, Ver Donck K, and Montano M. 2012. A novel library screen identifies immunosuppressors that promote osteoblast differentiation. Bone 50(6):1294-1303.

Devlin MJ. 2011. Estrogen, exercise, and the skeleton. Evolutionary anthropology 20(2):54-61.

Dinsa GD, Goryakin Y, Fumagalli E, and Suhrcke M. 2012. Obesity and socioeconomic status in developing countries: a systematic review. Obes Rev 13(11):1067-1079.

Doube M, Klosowski MM, Arganda-Carreras I, Cordelieres FP, Dougherty RP, Jackson JS, Schmid B, Hutchinson JR, and Shefelbine SJ. 2010. BoneJ: Free and extensible bone image analysis in ImageJ. Bone 47(6):1076-1079.

Dowthwaite JN, Rosenbaum PF, and Scerpella TA. 2011. Mechanical loading during growth is associated with plane-specific differences in vertebral geometry: A cross-sectional analysis comparing artistic gymnasts vs. non-gymnasts. Bone 49(5):1046-1054.

Dowthwaite JN, Rosenbaum PF, and Scerpella TA. 2012. Site-specific advantages in skeletal geometry and strength at the proximal femur and forearm in young female gymnasts. Bone 50(5):1173-1183.

Dubern B, and Clement K. 2012. Leptin and leptin receptor-related monogenic obesity. Biochimie 94(10):2111-2115.

Ducy P, Amling M, Takeda S, Priemel M, Schilling A, Beil F, Shen J, Vinson C, Rueger J, and Karsenty G. 2000. Leptin inhibits bone formation through a hypothalamic relay: a central control of bone mass. Cell 100:197-207.

Durmaz E, Zou M, Al-Rijjal RA, Baitei EY, Hammami S, Bircan I, Akcurin S, Meyer B, and Shi Y. 2013. Novel and de novo PHEX mutations in patients with hypophosphatemic rickets. Bone 52(1):286-291.

Eastell R. 2005. Role of oestrogen in the regulation of bone turnover at the menarche. The Journal of endocrinology 185(2):223-234.

Eckstein F, Faber S, Muhlbauer R, Hohe J, Englmeier KH, Reiser M, and Putz R. 2002. Functional adaptation of human joints to mechanical stimuli. Osteoarthritis and cartilage / OARS, Osteoarthritis Research Society 10(1):44-50.

Eleazer CD. 2013. The interaction of mechanical loading and metabolic stress on human cortical bone: testing anthropological assumptions using cross-sectional geometry and histomorphology: University of Tennessee.

Eringa EC, Bakker W, and van Hinsbergh VW. 2012. Paracrine regulation of vascular tone, inflammation and insulin sensitivity by perivascular adipose tissue. Vascul Pharmacol 56(5-6):204-209.

Falcao-Pires I, Castro-Chaves P, Miranda-Silva D, Lourenco AP, and Leite-Moreira AF. 2012. Physiological, pathological and potential therapeutic roles of adipokines. Drug Discov Today 17(15-16):880-889.

Felber K, Croucher P, and Roehl HH. 2011. Hedgehog signalling is required for perichondral osteoblast differentiation in zebrafish. Mechanisms of development 128(1-2):141-152.

Felson DT. 2013. Osteoarthritis as a disease of mechanics. Osteoarthritis and Cartilage 21(1):10-15.

Ferry B, Lespessailles E, Rochcongar P, Duclos M, and Courteix D. 2013. Bone health during late adolescence: effects of an 8-month training program on bone geometry in female athletes. Joint Bone Spine 80(1):57-63.

Flegal KM. 2005. Epidemiologic aspects of overweight and obesity in the United States. Physiology & behavior 86(5):599-602.

Flegal KM, Carroll MD, Ogden CL, and Curtin LR. 2010. Prevalence and trends in obesity among US adults, 1999-2008. JAMA 303(3):235-241.

Forwood MR, and Turner CH. 1995. Skeletal adaptations to mehcanical usage: results from tibial loading studies in rats Bone 17(4):197S-205S.

Frost H. 1997. Obesity and Bone Strength and "Mass": A tutorial based on insights from a new paradigm. Bone 3:211-214.

Frost H. 2000. The Utah paradigm of skeletal physiology: an overview of its insights for bone, cartilage and collagenous tissue organs. Journal of Bone and Mineral Metabolism 18(6):305-316.

Fulzele K, and Clemens TL. 2012. Novel functions for insulin in bone. Bone 50(2):452-456.

Fuqua JS, and Rogol AD. 2013. Neuroendocrine alterations in the exercising human: implications for energy homeostasis. Metabolism 62(7):911-921.

Gale SM, Castracane VD, and Mantzoros CS. 2004. Energy homeostasis, obesity and eating disorders: recent advances in endocrinology. J Nutr 134(2):295-298.

Galic S, Oakhill JS, and Steinberg GR. 2010. Adipose tissue as an endocrine organ. Molecular and Cellular Endocrinology 316(2):129-139.

Gallagher D, Visser M, Sepulveda D, Pierson RN, Harris T, and Heymsfield SB. 1996. How useful is Body Mass Index for comparison of body fatness across age, sex, and ethnic groups? Am J Epidemiol 143(3):228-239.

Gallagher JC, and Sai AJ. 2010. Molecular biology of bone remodeling: Implications for new therapeutic targets for osteoporosis. Maturitas 65(4):301-307.

Gangwisch JE, Malaspina D, and Boden-Albala B. 2005. Inadequate sleep as a risk factor for obesity: analyses of the NHANES I. Sleep 28(10):1289-1296.

García-Martín A, Reyes-García R, Ávila-Rubio V, and Muñoz-Torres M. 2013. Osteocalcin: A link between bone homeostasis and energy metabolism. Endocrinología y Nutrición (English Edition) 60(5):260-263.

Goh JC, Mech AM, Lee EH, Ang EJ, Bayon P, and Pho RW. 1992. Biomechanical study on the load-bearing characteristics of the fibula and the effects of fibular resection. Clinical Orthopaedics and Related Research 279:223-228.

Greene DA, Naughton GA, Briody JN, Kemp A, and Woodhead H. 2006. Assessment of bone strength at differentially-loaded skeletal regions in adolescent middle-distance runners. Journal of science and medicine in sport / Sports Medicine Australia 9(3):221-230.

Griffin TM, Huebner JL, Kraus VB, and Guilak F. 2009. Extreme obesity due to impaired leptin signaling in mice does not cause knee osteoarthritis. Arthritis Rheum 60:2935-2944.

Hallgrimsson B, Miyake T, Wilmore K, and Hall BK. 2003. Embryological origins of developmental stability: Size, shape and fluctuating asymmetry in prenatal random bred mice. Journal of Experimental Zoology Part B-Molecular and Developmental Evolution 296B(1):40-57.

Hallgrímsson B, Willmore K, and Hall BK. 2002. Canalization, developmental stability, and morphological integration in primate limbs. American journal of physical anthropology 119(S35):131-158.

Hamrick MW, Della-Fera M, Choi Y, Pennington C, and Baile C. 2005. Leptin treatment induces loss of bone marrow adipocytes and increases bone formation in leptin-deficient ob/ob mice. Journal of bone and mineral research : the official journal of the American Society for Bone and Mineral Research 20:994-1001.

Harada S, and Rodan GA. 2003. Control of osteoblast function and regulation of bone mass. Nature 426:349-355.

Harwood HJ, Jr. 2012. The adipocyte as an endocrine organ in the regulation of metabolic homeostasis. Neuropharmacology 63(1):57-75.

Heaney RP. 2003. How does bone support calcium homeostasis? Bone 33(3):264-268.

Heinonen A, Oja P, Kannus P, Sievanen H, Haapsalo H, Manttari A, and Vuori I. 1995. Bone mineral density in female athletes representing sports with different loading characteristics of the skeleton. Bone 17(3):197-203.

Henneicke H, Herrmann M, Kalak R, Brennan-Speranza TC, Heinevetter U, Bertollo N, Day RE, Huscher D, Buttgereit F, Dunstan CR et al. . 2011. Corticosterone selectively targets endo-cortical surfaces by an osteoblast-dependent mechanism. Bone 49(4):733-742.

Henriksen K, Neutzsky-Wulff AV, Bonewald LF, and Karsdal MA. 2009. Local communication on and within bone controls bone remodeling. Bone 44(6):1026-1033.

Heymsfield S, Gallagher D, Mayer L, Beetsch J, and Pietrobelli A. 2007. Scaling of human body composition to stature: new insights into body mass index. Am J Clin Nutr 86:82-91.

Hillman JB, Dorn LD, Loucks TL, and Berga SL. 2012. Obesity and the hypothalamic-pituitary-adrenal axis in adolescent girls. Metabolism 61(3):341-348.

Hollo G, Szathmary L, Marcsik A, and Barta Z. 2010. Linear measurements of the neurocranium are better indicators of population differences than those of the facial skeleton: comparative study of 1,961 skulls. Hum Biol 82(1):29-46.

Hsieh YF, and Turner CH. 2001. Effects of offloading frequency on mechanically induced bone formation. Journal of Bone and Mineral Research 16:918-924.

Janz KF, Gilmore JM, Levy SM, Letuchy EM, Burns TL, and Beck TJ. 2007. Physical activity and femoral neck bone strength during childhood: the Iowa Bone Development Study. Bone 41(2):216-222.

Järvinen TLN, Kannus P, Pajamäki I, Vuohelainen T, Tuukkanen J, Järvinen M, and Sievänen H. 2003. Estrogen deposits extra mineral into bones of female rats in puberty, but simultaneously seems to suppress the responsiveness of female skeleton to mechanical loading. Bone 32(6):642-651.

Kang J-H, Kim C-S, Han I-S, Kawada T, and Yu R. 2007. Capsaicin, a spicy component of hot peppers, modulates adipokine gene expression and protein release from obese-mouse adipose tissues and isolated adipocytes, and suppresses the inflammatory responses of adipose tissue macrophages. FEBS Letters 581(23):4389-4396.

Kanter R, and Caballero B. 2012. Global Gender Disparities in Obesity: A Review. Adv Nutr 3(4):491-498.

Kapur JN, Sahoo P, and Wong A. 1985. A new method for gray-level picture thresholding using the entropy of the histogram. Graphical Models and Image Processing 29(3):273-285.

Karsenty G. 2006. Convergence between bone and energy homeostases: Leptin regulation of bone mass. Cell Metab 4(5):341-348.

Karsenty G. 2011. Bone endocrine regulation of energy metabolism and male reproduction. C R Biol 334(10):720-724.

Khosla S, Oursler MJ, and Monroe DG. 2012. Estrogen and the skeleton. Trends in endocrinology and metabolism: TEM 23(11):576-581.

Kim S, and Moustaid-Moussa N. 2000. Secretory, endocrine and autocrine/paracrine function of the adipocyte. J Nutr 130:3110S-3115S.

Kimmel DB. 1993. A paradigm for skeletal strength homeostasis. Journal of bone and mineral research : the official journal of the American Society for Bone and Mineral Research 8:S515-S522.

Klein-Nulend J, Bakker AD, Bacabac RG, Vatsa A, and Weinbaum S. 2013. Mechanosensation and transduction in osteocytes. Bone 54(2):182-190.

Klingenberg CP. 2008. Morphological Integration and Developmental Modularity. Annual Review of Ecology Evolution and Systematics 39:115-132.

Kontulainen S, Sievanen H, Kannus P, Pasanen M, and Vuori I. 2003. Effect of long-term impact-loading on mass, size, and estimated strength of humerus and radius of female racquet-sports players: A peripheral quantitative computed tomogrpahy study between young and old starters and controls. Journal of bone and mineral research : the official journal of the American Society for Bone and Mineral Research 18:352-359.

Korostishevsky M, Malkin I, Trofimov S, Pei Y, Deng HW, and Livshits G. 2012. Significant association between body composition phenotypes and the osteocalcin genomic region in normative human population. Bone 51(4):688-694.

Kozak LP. 2013. Genetic variation in brown fat activity and body weight regulation in mice: Lessons for human studies. Biochimica et biophysica acta.

Krings A, Rahman S, Huang S, Lu Y, Czernik PJ, and Lecka-Czernik B. 2012. Bone marrow fat has brown adipose tissue characteristics, which are attenuated with aging and diabetes. Bone 50(2):546-552.

Krishnakanth P, Schmutz B, Steck R, Mishra S, Schutz MA, and Epari DR. 2011. Can the contra-lateral limb be used as a control with respect to analyses of bone remodelling? Med Eng Phys 33(8):987-992.

Lago F, Gomez R, Gomez-Reino JJ, Dieguez C, and Gualillo O. 2009. Adipokines as novel
modulators of lipid metabolism. Trends Biochem Sci 34(10):500-510.

Lago R, Gomez R, Lago F, Gomez-Reino JJ, and Gualillo O. 2008. Leptin beyond body weight
regulation--current concepts concerning its role in immune function and inflammation.
Cell Immunol 252(1-2):139-145.

Lasar D, Julius A, Fromme T, and Klingenspor M. 2013. Browning attenuates murine white
adipose tissue expansion during postnatal development. Biochimica et biophysica acta
1831(5):960-968.

Lazenby RA, Angus S, Cooper DM, and Hallgrimsson B. 2008a. A three-dimensional
microcomputed tomographic study of site-specific variation in trabecular
microarchitecture in the human second metacarpal. Journal of anatomy 213(6):698-705.

Lazenby RA, Cooper DM, Angus S, and Hallgrimsson B. 2008b. Articular constraint,
handedness, and directional asymmetry in the human second metacarpal. Journal of
human evolution 54(6):875-885.

Leal Vde O, and Mafra D. 2013. Adipokines in obesity. Clinica chimica acta; international
journal of clinical chemistry 419:87-94.

Lecka-Czernik B. 2012. Marrow fat metabolism is linked to the systemic energy metabolism.
Bone 50(2):534-539.

Leder BZ. 2010. Chapter 26 - Androgens and the Skeleton – Humans. In: Eric SO, John PB, Dirk
VanderschuerenA2 - Eric S. Orwoll JPB, and Dirk V, editors. Osteoporosis in Men
(Second Edition). San Diego: Academic Press. p 319-334.

Lee NK, Sowa H, Hinoi E, Ferron M, Ahn JD, Confavreux C, Dacquin R, Mee PJ, McKee MD, Jung DY et al. . 2007a. Endocrine regulation of energy metabolism by the skeleton. Cell 130(3):456-469.

Lee NK, Sowa H, Hinoi E, Ferron M, Ahn JD, Confavreux C, Dacquin R, Mee PJ, McKee MD, Jung DY et al. . 2007b. Endocrine Regulation of Energy Metabolism by the Skeleton. Cell 130(3):456-469.

Lee YH, Mottillo EP, and Granneman JG. 2013. Adipose tissue plasticity from WAT to BAT and in between. Biochimica et biophysica acta.

Lieben L, and Carmeliet G. 2013. Vitamin D signaling in osteocytes: effects on bone and mineral homeostasis. Bone 54(2):237-243.

Lieberman DE. 1996. How and why humans grow thin skulls: Experimental evidence for systemic cortical robusticity. American journal of physical anthropology 101:217-236.

Lieberman DE, Devlin MJ, and Pearson OM. 2001. Articular area responses to mechanical loading: effects of exercise, age, and skeletal location. American journal of physical anthropology 116:266-277.

Lieberman DE, Pearson OM, Polk JD, Demes B, and Crompton AW. 2003. Optimization of bone growth and remodeling in response to loading in tapered mammalian limbs. J Exp Biol 206:3125-3138.

Lieberman DE, Polk JD, and Demes B. 2004. Predicting long bone loading from cross-sectional geometry. American journal of physical anthropology 123(2):156-171.

Lim AYN, and Doherty M. 2011. What of guidelines for osteoarthritis? Int J Rheumatic Diseases 14:136-144.

Lu C, Wan Y, Cao J, Zhu X, Yu J, Zhou R, Yao Y, Zhang L, Zhao H, Li H et al. . 2013. Wnt-mediated reciprocal regulation between cartilage and bone development during endochondral ossification. Bone 53(2):566-574.

Lumeng CN. 2013. Innate immune activation in obesity. Molecular Aspects of Medicine 34(1):12-29.

Ma H, Turpeinen T, Silvennoinen M, Torvinen S, Rinnankoski-Tuikka R, Kainulainen H, Timonen J, Kujala UM, Rahkila P, and Suominen H. 2011. Effects of diet-induced obesity and voluntary wheel running on the microstructure of the murine distal femur. Nutrition & metabolism 8(1):1.

Macintosh AA, Davies TG, Ryan TM, Shaw CN, and Stock JT. 2013. Periosteal versus true cross-sectional geometry: a comparison along humeral, femoral, and tibial diaphyses. American journal of physical anthropology 150(3):442-452.

Mackie EJ, Ahmed YA, Tatarczuch L, Chen KS, and Mirams M. 2008. Endochondral ossification: how cartilage is converted into bone in the developing skeleton. The international journal of biochemistry & cell biology 40(1):46-62.

Macsai CE, Hopwood B, Chung R, Foster BK, and Xian CJ. 2011. Structural and molecular analyses of bone bridge formation within the growth plate injury site and cartilage degeneration at the adjacent uninjured area. Bone 49(4):904-912.

Manolagas SC, and Parfitt AM. 2013. For whom the bell tolls: distress signals from long-lived osteocytes and the pathogenesis of metabolic bone diseases. Bone 54(2):272-278.

Marchi D, and Shaw CN. 2011. Variation in fibular robusticity reflects variation in mobility patterns. Journal of human evolution 61(5):609-616.

Martin BR, Burr DB, and Sharkey NA. 1998. Skeletal Tissue Mechanics. New York: Springer-Verlag

Martin R. 1928. Lehrbuch der Anthropologie in Systematischer Darstellung mit Besonderer Berucksichtigung der Anthropologischen Methoden fur Studierende, Artze und Forschungsreisende. Zweiter Band: Kraniologie, Osteologie. Second Edition. Jena: Gustav Fischer.

Martin R, and Burr DB. 1989. Structure, function and adaptation of compact bone. New York: Raven Press.

McCulloch RG, Bailey D, Whalen R, Houston C, Faulkner R, and Craven B. 1992. Bone density and bone mineral content of adolescent soccer athletes and competitive swimmers. Pediatric Exercise Sci 4:319-330.

Meijering E, Niessen W, and Viergever M. 2001. Quantitative Evaluation of Convolution-Based Methods for Medical Image Interpolation. Medical Image Analysis 5(2):111-126.

Messier SP. 2010. Diet and Exercise for Obese Adults with Knee Osteoarthritis. Clinics in Geriatric Medicine 26(3):461-477.

Michalakis K, Mintziori G, Kaprara A, Tarlatzis BC, and Goulis DG. 2013. The complex interaction between obesity, metabolic syndrome and reproductive axis: A narrative review. Metabolism 62(4):457-478.

Mitteroecker P, and Bookstein F. 2008. The evolutionary role of modularity and integration in the hominoid cranium. Evolution 62(4):943-958.

Modica S, and Wolfrum C. 2013. Bone morphogenic proteins signaling in adipogenesis and energy homeostasis. Biochimica et biophysica acta 1831(5):915-923.

Monroe DG, McGee-Lawrence ME, Oursler MJ, and Westendorf JJ. 2012. Update on Wnt
signaling in bone cell biology and bone disease. Gene 492(1):1-18.

Moore MK. 2008. Body mass estimation from the human skeleton [Dissertation]: University of
Tennessee.

Moore MK. 2013. Chapter 14 - Functional Morphology and Medical Imaging. Research
Methods in Human Skeletal Biology: Academic Press. p 397-424.

Motyl KJ, and Rosen CJ. 2012. Understanding leptin-dependent regulation of skeletal
homeostasis. Biochimie 94(10):2089-2096.

Muller MJ, Bosy-Westphal A, and Krawczak M. 2010. Genetic studies of common types of
obesity: a critique of the current use of phenotypes. Obesity reviews : an official journal
of the International Association for the Study of Obesity 11(8):612-618.

Nelson LR, and Bulun SE. 2001. Estrogen production and action. J Am Acad Dermatol 45:S116-
S124.

Nilsson O, Marino R, De Luca F, Phillip M, and Baron J. 2005. Endocrine regulation of the
growth plate. Horm Res 64:157-165.

Nyman JS, Reyes M, and Wang X. 2005. Effect of ultrastructural changes on the toughness of
bone. Micron 36(7–8):566-582.

O'Brien CA, Nakashima T, and Takayanagi H. 2013. Osteocyte control of osteoclastogenesis.
Bone 54(2):258-263.

O'Keefe JH, Vogel R, Lavie CJ, and Cordain L. 2011. Exercise Like a Hunter-Gatherer: A
Prescription for Organic Physical Fitness. Progress in Cardiovascular Diseases 53(6):471-
479.

O'Neill MC, and Ruff CB. 2004. Estimating human long bone cross-sectional geometric properties: a comparison of noninvasive methods. Journal of human evolution 47:221-235.

Oliveros E, Somers VK, Sochor O, Goel K, and Lopez-Jimenez F. 2013. The Concept of Normal Weight Obesity. Progress in Cardiovascular Diseases.

Pacifici R. 2010. T cells: critical bone regulators in health and disease. Bone 47(3):461-471.

Pavalko FM, Norvell SM, Burr DB, Turner CH, Duncan RL, and Bidwell JP. 2003. A model for mechanotransduction in bone cells: the load-bearing mechanosomes. Journal of cellular biochemistry 88(1):104-112.

Pearson OM, and Lieberman DE. 2004. The aging of Wolff's "law": ontogeny and responses to mechanical loading in cortical bone. American journal of physical anthropology Suppl 39:63-99.

Pereira D, Peleteiro B, Araujo J, Branco J, Santos RA, and Ramos E. 2011. The effect of osteoarthritis definition on prevalence and incidence estimates: a systematic review. Osteoarthritis and cartilage / OARS, Osteoarthritis Research Society 19(11):1270-1285.

Peterson J, and Dechow PC. 2003. Material properties of the human cranial vault and zygoma. The anatomical record Part A, Discoveries in molecular, cellular, and evolutionary biology 274(1):785-797.

Pettway GJ, Meganck JA, Koh AJ, Keller ET, Goldstein SA, and McCauley LK. 2008. Parathyroid hormone mediates bone growth through the regulation of osteoblast proliferation and differentiation. Bone 42(4):806-818.

Pinhas-Hamiel O, and Sabin M. 2013. Chapter 6 - Obesity in Developing Countries. In: Margaret Z, editor. Practical Pediatric Endocrinology in a Limited Resource Setting. San Diego: Academic Press. p 135-158.

Pivonka P, Zimak J, Smith DW, Gardiner BS, Dunstan CR, Sims NA, Martin TJ, and Mundy GR. 2008. Model structure and control of bone remodeling: a theoretical study. Bone 43(2):249-263.

Poulos SP, Hausman DB, and Hausman GJ. 2010. The development and endocrine functions of adipose tissue. Molecular and Cellular Endocrinology 323(1):20-34.

Prentice AM. 2005a. Early influences on human energy regulation: thrifty genotypes and thrifty phenotypes. Physiology & behavior 86(5):640-645.

Prentice AM. 2005b. Starvation in humans: evolutionary background and contemporary implications. Mechanisms of ageing and development 126(9):976-981.

Prentice AM, Hennig BJ, and Fulford AJ. 2008. Evolutionary origins of the obesity epidemic: natural selection of thrifty genes or genetic drift following predation release? International journal of obesity 32(11):1607-1610.

Provot S, Schipani E, Wu JY, and Kronenberg H. 2013. Chapter 6 - Development of the Skeleton. In: Robert M, David F, David WD, Marjorie L, Jane A. CauleyA2 - Robert Marcus DFDWDML, and Jane AC, editors. Osteoporosis (Fourth Edition). San Diego: Academic Press. p 97-126.

Rasband W. ImageJ. National Institute of Health.

Raucci R, Rusolo F, Sharma A, Colonna G, Castello G, and Costantini S. 2013. Functional and structural features of adipokine family. Cytokine 61(1):1-14.

Rauch F, and Shoenau E. 2001. The developing bone: Slave or master of its cells and molecules? Pediatr Res 50(3):309-314.

Reeves NM, Auerbach BM, and Sylvester AD. in review. Directional and non-directional asymmetry in tamarin (*Saguinus oedipus*) limb bones: implications for generalized patterns among primates. American journal of physical anthropology.

Reid IR. 2010. Fat and bone. Archives of Biochemistry and Biophysics 503(1):20-27.

Reid IR, Cornish J, and Baldock PA. 2006. Nutrition-related peptides and bone homeostasis. Journal of bone and mineral research : the official journal of the American Society for Bone and Mineral Research 21(4):495-500.

Reilly GC, and Currey JD. 2000. The effects of damage and microcracking on the impact strength of bone. Journal of biomechanics 33(3):337-343.

Reinehr T, and Roth CL. 2010. A new link between skeleton, obesity and insulin resistance: relationships between osteocalcin, leptin and insulin resistance in obese children before and after weight loss. International journal of obesity 34(5):852-858.

Reznikov N, Shahar R, and Weiner S. 2013. Three-dimensional structure of human lamellar bone: the presence of two different materials and new insights into the hierarchical organization. Bone.

Riggs BL, Khosla S, and Melton III LJ. 2002. Sex steroids and the construction and conservation of the adult skeleton. Endocr Rev 23(3):279-302.

Robling AG. 2010. Muscle loss and bone loss: master and slave? Bone 46(2):272-273.

Robling AG. 2013. The expanding role of Wnt signaling in bone metabolism. Bone 55:256-257.

Robling AG, Castillo AB, and Turner CH. 2006. Biomechanical and molecular regulation of bone remodeling. Annual Review of Biomedical Engineering. p 455-498.

Robling AG, Niziolek PJ, Baldridge LA, Condon KW, Allen MR, Alam I, Mantila SM, Gluhak-Heinrich J, Bellido TM, Harris SE et al. . 2008. Mechanical stimulation of bone in vivo reduces osteocyte expression of Sost/sclerostin. Journal of Biological Chemistry 283(9):5866-5875.

Romero-Corral A, Somers VK, Sierra-Johnson J, Thomas RJ, Collazo-Clavell ML, Korinek J, Allison TG, Batsis JA, Sert-Kuniyoshi FH, and Lopez-Jimenez F. 2008. Accuracy of body mass index in diagnosing obesity in the adult general population. International journal of obesity 32(6):959-966.

Rose AJ, and Herzig S. 2013. Metabolic control through glucocorticoid hormones: An update. Mol Cell Endocrinol 380(1-2):65-78.

Ruff C. 2003a. Ontogenetic adaptation to bipedalism: age changes in femoral to humeral length and strength proportions in humans, with a comparison to baboons. Journal of human evolution 45(4):317-349.

Ruff C. 2007. Body size prediction from juvenile skeletal remains. American journal of physical anthropology 133(1):698-716.

Ruff CB. 1994. Morphological adaptation to climate in modern and fossil hominids. Ybk Phys Anthropol 37:65-107.

Ruff CB. 2000. Body size, body shape, and long bone strength in modern humans. Journal of human evolution 38(2):269-290.

Ruff CB. 2002a. Long bone articular and diaphyseal structure in old world monkeys and apes. I: locomotor effects. American journal of physical anthropology 119(4):305-342.

Ruff CB. 2002b. Variation in human body size and shape. Annual Review of Anthropology 31(1):211-232.

Ruff CB. 2003b. Growth in bone strength, body size, and muscle size in a juvenile longitudinal sample. Bone 33(3):317-329.

Ruff CB. 2003c. Ontogenetic adaptation to bipedalism: age changes in femoral to humeral length and strength proportions in humans, with a comparison to baboons. Journal of human evolution 45:317-349.

Ruff CB. 2008a. Biomechanical analyses of archaeological human skeletons. In: Katzenberg MA, and Saunders SR, editors. Biological anthropology of the human skeleton. New York: John Wiley & Sons, Inc. p 71-102.

Ruff CB. 2008b. Femoral/humeral strength in early African Homo erectus. Journal of human evolution 54(3):383-390.

Ruff CB, and Hayes WC. 1982. Subperiosteal expansion and cortical remodeling of the human femur and tibia with aging. Science 217(4563):945-948.

Ruff CB, and Hayes WC. 1983. Cross-sectional geometry of Pecos Pueblo femora and tibiae - a biomechanical investigation. I. Method and general patterns of variations. American journal of physical anthropology 60:359-381.

Ruff CB, Holt B, and Trinkaus E. 2006. Who's afraid of the big bad Wolff?: "Wolff's law" and bone functional adaptation. American journal of physical anthropology 129:484-498.

Ruff CB, and Leo F. 1986. Use of computed tomography in skeletal structure research. Ybk Phys Anthropol 29:181-196.

Ruff CB, Scott W, and Liu AY-C. 1991. Articular and diaphyseal remodeling of the proximal femur with changes in body mass in adults. American journal of physical anthropology 86:397-413.

Ruff CB, Trinkaus E, and Holliday TW. 1997. Body mass and encephalization in Pleistocene *Homo*. Nature 387:173-176.

Ruff CB, Trinkaus E, Walker A, and Larsen CS. 1993. Postcranial robusticity in *Homo*. I. Temporal trends and mechanical interpretation. American journal of physical anthropology 91:21-53.

Ruff CB, Walker A, and Trinkaus E. 1994. Postcranial robusticity in *Homo*. III: Ontogeny. American journal of physical anthropology 93:35-54.

Runhaar J, Koes BW, Clockaerts S, and Bierma-Zeinstra SM. 2011. A systematic review on changed biomechanics of lower extremities in obese individuals: a possible role in development of osteoarthritis. Obesity reviews : an official journal of the International Association for the Study of Obesity 12(12):1071-1082.

Sadie-Van Gijsen H, Hough FS, and Ferris WF. 2013. Determinants of bone marrow adiposity: The modulation of peroxisome proliferator-activated receptor-gamma2 activity as a central mechanism. Bone 56(2):255-265.

Saito M. 2013. Brown adipose tissue as a therapeutic target for human obesity. Obesity Research & Clinical Practice.

Schaffler A, Scholmerich J, and Salzberger B. 2007. Adipose tissue as an immunological organ: Toll-like receptors, C1q/TNFs and CTRPs. Trends Immunol 28(9):393-399.

Seeman E, and Martin JT. 1989. Non-invasive techniques for the measurement of bone mineral. Baillière's Clinical Endocrinology and Metabolism 3(1):1-33.

Sezgin M, and Sankur B. 2004. Survey over image thresholding techniques and quantitative performance evaluation. Journal of Electronic Imaging 13(1):146-165.

Shaw C. 2010. 'Putting flesh back onto the bones?' Can we predict soft tissue properties from skeletal and fossil remains? Journal of human evolution 59(5):484-492.

Shaw CN. 2008. The influence of habitual athletic activity on diaphyseal morphology in modern humans, and its impact on interpretations of hominin activity patterns. Cambridge, UK: University of Cambridge.

Shaw CN. 2011. Is 'hand preference' coded in the hominin skeleton? An in-vivo study of bilateral morphological variation. Journal of human evolution 61(4):480-487.

Shaw CN, Hofmann CL, Petraglia MD, Stock JT, and Gottschall JS. 2012. Neandertal humeri may reflect adaptation to scraping tasks, but not spear thrusting. PloS one 7(7):e40349.

Shaw CN, and Stock JT. 2009a. Habitual throwing and swimming correspond with upper limb diaphyseal strength and shape in modern human athletes. American journal of physical anthropology 140(1):160-172.

Shaw CN, and Stock JT. 2009b. Intensity, repetitiveness, and directionality of habitual adolescent mobility patterns influence the tibial diaphysis morphology of athletes. American journal of physical anthropology 140(1):149-159.

Shaw CN, and Stock JT. 2013. Extreme mobility in the Late Pleistocene? Comparing limb biomechanics among fossil Homo, varsity athletes and Holocene foragers. Journal of human evolution 64(4):242-249.

Sherwood NE, Senso MM, Fleming CK, and Roeder AM. 2013. Behavioral Risk Factors for Overweight and Obesity.479-499.

Sigurdsson G, Aspelund T, Chang M, Jonsdottir B, Sigurdsson S, Eiriksdottir G, Gudmundsson A, Harris TB, Gudnason V, and Lang TF. 2006. Increasing sex difference in bone

strength in old age: The Age, Gene/Environment Susceptibility-Reykjavik study (AGES-REYKJAVIK). Bone 39(3):644-651.

Silvernail JF, Milner CE, Thompson D, Zhang S, and Zhao X. 2013. The influence of body mass index and velocity on knee biomechanics during walking. Gait & Posture 37(4):575-579.

Sisask G, Silfversward CJ, Bjurholm A, and Nilsson O. 2013. Ontogeny of sensory and autonomic nerves in the developing mouse skeleton. Autonomic neuroscience : basic & clinical 177(2):237-243.

Skedros JG, Sorenson SM, and Jenson NH. 2007. Are distributions of secondary osteon variants useful for interpreting load history in mammalian bones? Cells Tissues Organs 185:285-307.

Skraba JS. 1982. Weight bearing role of the human fibula. Foot Ankle 2:345-346.

Smith EP, Specker B, and Korach KS. 2010. Recent experimental and clinical findings in the skeleton associated with loss of estrogen hormone or estrogen receptor activity. J Steroid Biochem Mol Biol 118(4-5):264-272.

Sniekers YH, van Osch GJ, Ederveen AG, Inzunza J, Gustafsson JA, van Leeuwen JP, and Weinans H. 2009. Development of osteoarthritic features in estrogen receptor knockout mice. Osteoarthritis and cartilage / OARS, Osteoarthritis Research Society 17(10):1356-1361.

Soucek O, Lebl J, Snajderova M, Kolouskova S, Rocek M, Hlavka Z, Cinek O, Rittweger J, and Sumnik Z. 2011. Bone geometry and volumetric bone mineral density in girls with Turner syndrome of different pubertal stages. Clinical endocrinology 74(4):445-452.

Stock JT. 2006. Hunter-gatherer postcranial robusticity relative to patterns of mobility, climatic
adaptation, and selection for tissue economy. American journal of physical anthropology
131:194-204.

Stock JT, and Pfeiffer S. 2001. Linking structural variability in long bone diaphyses to habitual
behaviors: foragers from the southern African Later Stone Age and the Adaman Islands.
American journal of physical anthropology 115:337-348.

Stock JT, and Pfeiffer SK. 2004. Long bone robusticity and subsistence behavior among Later
Stone Age foragers of the forest and fynbos biomes of South Africa. J Archaeol Sci
31:999-1013.

Stock JT, and Shaw CN. 2007. Which measures of diaphyseal robusticity are robust? A
comparison of external methods of quantifying the strength of long bone diaphyses to
cross-sectional geometric properties. American journal of physical anthropology
134(3):412-423.

Sumner DR, and Andriacchi TP. 1996. Adaptation to differential loading: comparison of growth-
related changes in cross-sectional properties of the human femur and humerus. Bone
19(121-126).

Sylvester AD, Christensen AM, and Kramer PA. 2006. Factors influencing osteological changes
in the hands and fingers of rock climbers. Journal of anatomy 209(5):597-609.

Tanaka H, Mine T, Ogasa H, Taguchi T, and Liang CT. 2011. Expression of RANKL/OPG
during bone remodeling in vivo. Biochem Biophys Res Commun 411(4):690-694.

Tat SK, Pelletier JP, Lajeunesse D, Fahmi H, Duval N, and Martel-Pelletier J. 2008. Differential
modulation of RANKL isoforms by human osteoarthritic subchondral bone osteoblasts:
influence of osteotropic factors. Bone 43(2):284-291.

Teitelbaum SL, and Ross FP. 2003. Genetic regulation of osteoclast development and function. Nature reviews Genetics 4(8):638-649.

Thomas T, Burguera B, Melton Iii LJ, Atkinson EJ, O'Fallon WM, Riggs BL, and Khosla S. 2001. Role of serum leptin, insulin, and estrogen levels as potential mediators of the relationship between fat mass and bone mineral density in men versus women. Bone 29(2):114-120.

Torrance AG, Mosley JR, Suswillo RF, and Lanyon LE. 1994. Noninvasive loading of the rat ulna in vivo induces a strain-related modeling response uncomplicated by trauma or periosteal pressure. Calcified tissue international 54(241-247).

Tripuwabhrut P, Mustafa M, Gjerde CG, Brudvik P, and Mustafa K. 2013. Effect of compressive force on human osteoblast-like cells and bone remodelling: an in vitro study. Archives of oral biology 58(7):826-836.

Turner CH. 2002. Biomechanics of bone: determinants of skeletal fragility and bone quality. Osteoporosis international : a journal established as result of cooperation between the European Foundation for Osteoporosis and the National Osteoporosis Foundation of the USA 13:97-104.

Turner CH, Warden SJ, Bellido T, Plotkin LI, Kumar N, Jasiuk I, Danzig J, and Robling AG. 2009. Mechanobiology of the skeleton. Science signaling 2(68):pt3.

Valassi E, Scacchi M, and Cavagnini F. 2008. Neuroendocrine control of food intake. Nutrition, Metabolism and Cardiovascular Diseases 18(2):158-168.

van der Spek R, Kreier F, Fliers E, and Kalsbeek A. 2012. Chapter 11 - Circadian rhythms in white adipose tissue. In: Andries Kalsbeek MMTR, and Russell GF, editors. Progress in Brain Research: Elsevier. p 183-201.

van Gerven DP, Hummert J, and Burr DB. 1985. Cortical bone maintenance and geometry of the tibia in prehistoric children from Nubia's Batn el Hajar. American journal of physical anthropology 66(3):275-280.

Vazquez-Vela ME, Torres N, and Tovar AR. 2008. White adipose tissue as endocrine organ and its role in obesity. Arch Med Res 39(8):715-728.

Vigliotti A, and Pasini D. 2013. Mechanical properties of hierarchical lattices. Mechanics of Materials 62:32-43.

Vignon E, Valat JP, Rossignol M, Avouac B, Rozenberg S, Thoumie P, Avouac J, Nordin M, and Hilliquin P. 2006. Osteoarthritis of the knee and hip and activity: a systematic international review and synthesis (OASIS). Joint Bone Spine 73(4):442-455.

Villarroya J, Cereigo R, and Villarroya F. 2013. An endocrine role for brown adipose tissue? Am J Physiol 305:E567-E572.

Villemure I, and Stokes IA. 2009. Growth plate mechanics and mechanobiology. A survey of present understanding. Journal of biomechanics 42(12):1793-1803.

Vincent HK, Heywood K, Connelly J, and Hurley RW. 2012a. Obesity and weight loss in the treatment and prevention of osteoarthritis. PM & R : the journal of injury, function, and rehabilitation 4(5 Suppl):S59-67.

Vincent HK, Raiser SN, and Vincent KR. 2012b. The aging musculoskeletal system and obesity-related considerations with exercise. Ageing research reviews 11(3):361-373.

Virtanen KA, van Marken Lichtenbelt WD, and Nuutila P. 2013. Brown adipose tissue functions in humans. Biochimica et Biophysica Acta (BBA) - Molecular and Cell Biology of Lipids 1831(5):1004-1008.

Vosselman MJ, van Marken Lichtenbelt WD, and Schrauwen P. 2013. Energy dissipation in brown adipose tissue: From mice to men. Mol Cell Endocrinol 379(1-2):43-50.

Wagner GP, Booth G, and Bagheri-Chaichian H. 1997. A population genetic theory of canalization. Evolution 51:329-347.

Wallace BA, and Cumming RG. 2000. Systematic review of randomized trials of the effect of exercise on bone mass in pre- and postmenopausal women. Calcified tissue international 67(1):10-18.

Wang L, Shao YY, and Ballock RT. 2011. Leptin synergizes with thyroid hormone signaling in promoting growth plate chondrocyte proliferation and terminal differentiation in vitro. Bone 48(5):1022-1027.

Warden SJ, and Turner CH. 2004. Mechanotransduction in the cortical bone is most efficient at loading frequencies of 5-10 Hz. Bone 34(2):261-270.

Weisner RL, Hunter GR, Heini AF, Goran MI, and Sell SM. 1998. The etiology of obesity: relative contribution of metabolic factors, diet, and physical activity. Am J Med 105:145-150.

Weiss E. 2003. The effects of rowing on humeral strength. American journal of physical anthropology 121:293-302.

Welldon KJ, Findlay DM, Evdokiou A, Ormsby RT, and Atkins GJ. 2013. Calcium induces pro-anabolic effects on human primary osteoblasts associated with acquisition of mature osteocyte markers. Mol Cell Endocrinol 376(1-2):85-92.

Wells JC. 2006. The evolution of human fatness and susceptibility to obesity: an ethological approach. Biological reviews of the Cambridge Philosophical Society 81(2):183-205.

Wells JCK, Marphatia AA, Cole TJ, and McCoy D. 2012. Associations of economic and gender inequality with global obesity prevalence: Understanding the female excess. Soc Sci Med 75(3):482-490.

Wescott DJ. 2006. Effect of mobility on femur midshaft external shape and robusticity. American journal of physical anthropology 130(2):201-213.

Wesseling-Perry K, and Juppner H. 2013. The osteocyte in CKD: new concepts regarding the role of FGF23 in mineral metabolism and systemic complications. Bone 54(2):222-229.

West DB, Boozer CN, Moody DL, and Atkinson RL. 1992. Dietary obesity in nine inbred mouse strains. Am J Physiol 262(6):R1025-R1032.

West DB, and York B. 1998. Dietary fat, genetic predisposition, and obesity: lessons from animal models. Am J Clin Nutr 67(suppl):505S-512S.

Wiren KM, Semirale AA, Zhang XW, Woo A, Tommasini SM, Price C, Schaffler MB, and Jepsen KJ. 2008. Targeting of androgen receptor in bone reveals a lack of androgen anabolic action and inhibition of osteogenesis: a model for compartment-specific androgen action in the skeleton. Bone 43(3):440-451.

Wiren KM, Zhang XW, Olson DA, Turner RT, and Iwaniec UT. 2012. Androgen prevents hypogonadal bone loss via inhibition of resorption mediated by mature osteoblasts/osteocytes. Bone 51(5):835-846.

Wojcicka A, Bassett JH, and Williams GR. 2013. Mechanisms of action of thyroid hormones in the skeleton. Biochimica et biophysica acta 1830(7):3979-3986.

Xie X, Yang S, Zou Y, Cheng S, Wang Y, Jiang Z, Xiao J, Wang Z, and Liu Y. 2013. Influence of the core circadian gene "Clock" on obesity and leptin resistance in mice. Brain Research 1491(0):147-155.

Yakar S, and Adamo ML. 2012. Insulin-like growth factor 1 physiology: lessons from mouse models. Endocrinol Metab Clin North Am 41(2):231-247, v.

Yamakawa K, Tsai CK, Haig AJ, Miner JA, and Harris MJ. 2004. Relationship between ambulation and obesity in older persons with and without low back pain. Int J Obes 28:137-143.

Yamanouchi K, Yada E, Hozumi H, Ueno C, and Nishihara M. 2004. Analyses of hind leg skeletons in human growth hormone transgenic rats. Experimental Gerontology 39(8):1179-1188.

Yang X, Teoh SH, DasDe S, and Lee T. 2013. Administration of PTH and ibandronate increases ovariectomized rat compact bone viscoelasticity. J Mech Behav Biomed Mater 22:51-58.

Young NM, Wagner GP, and Hallgrimsson B. 2010. Development and the evolvability of human limbs. Proceedings of the National Academy of Sciences of the United States of America 107(8):3400-3405.

Zhang HH, Kumar S, Barnett AH, and Eggo MC. 1999. Intrinsic site-specific differences in the expression of leptin in human adipocytes and its autocrine effects on glucose uptake. J Clin Endocrinol Metab 84(7):2550-2556.

Zhang YY, Proenca R, Maffei M, Barone M, Leopold L, and Friedman JM. 1994. Positional cloning of the mouse obese gene and its human homologue. Nature 372:425-432.

Zhao LJ, Liu YJ, Liu PY, Hamilton J, Recker RR, and Deng HW. 2007. Relationship of obesity with osteoporosis. J Clin Endocrinol Metab 92(5):1640-1646.

Zhuang XF, Zhao MM, Weng CL, and Sun NL. 2009. Adipocytokines: a bridge connecting obesity and insulin resistance. Med Hypotheses 73(6):981-985.

VITA

Nicole Reeves was born in Dallas, Texas to parents George (Rocky) and Kathy Reeves. She studied at Purdue University her freshman year of college and completed the remainder of her undergraduate education at the University of Texas at Austin, graduating with a B.A. in 2005. To pursue interests in biological anthropology, she then attended Texas State University – San Marcos, receiving her M.A. degree in 2008. Continuing her graduate education, Nicole attended the University of Tennessee, earning her Ph.D. in May 2014. During her tenure in graduate school, Nicole was a graduate teaching assistant for many classes including human origins, osteology, human anatomy, and introductory forensic anthropology. She was also a graduate teaching associate for Principles of Biological Anthropology before taking on an NIJ-funded research assistant position. Nicole continues to pursue both teaching and research opportunities.